Energy

SOLAR

DOE/JPL/1060-82
(DE85014494)

ACTIVITY AND ACCOMPLISHMENTS IN DISH/STIRLING ELECTRIC POWER SYSTEM DEVELOPMENT

By
F. R. Livingston

February 15, 1985

Work Performed Under Contract No. AM04-80AL13137

Jet Propulsion Laboratory
Pasadena, California

Technical Information Center
Office of Scientific and Technical Information
United States Department of Energy

DOE/JPL/1060-82
(JPL-PUB-85-8)
(DE85014494)
Distribution Category UC-62

Activity and Accomplishments in Dish/Stirling Electric Power System Development

F.R. Livingston

February 15, 1985

Prepared for
U.S. Department of Energy
Through an Agreement with
National Aeronautics and Space Administration
by
Jet Propulsion Laboratory
California Institute of Technology
Pasadena, California

JPL Publication 85-8

DISCLAIMER

Available from the National Technical Information Service, U. S. Department of Commerce, Springfield, Virginia 22161.

Price: Printed Copy A07
Microfiche A01

Codes are used for pricing all publications. The code is determined by the number of pages in the publication. Information pertaining to the pricing codes can be found in the current issues of the following publications, which are generally available in most libraries: *Energy Research Abstracts (ERA); Government Reports Announcements* and Index *(GRA* and I); *Scientific and Technical Abstract Reports (STAR);* and publication NTIS-PR-360 available from NTIS at the above address.

ABSTRACT

Development of a modular, sun-heated, 25-kWe Stirling-engine generating plant that began in late 1977 has now been achieved. The U.S. Department of Energy Solar Thermal Technology Division sponsored the development of this solar parabolic-dish/Stirling-engine electricity generating plant known as the dish/Stirling electric power system. As of late 1984, the dish/Stirling electric power system converts sunlight to electricity more efficiently than any known existing solar electric power system. Further product development is ongoing.

The report also covers the fabrication and characterization of the test bed concentrators that were used for Stirling module testing and of the development of Parabolic Dish Concentrator No. 2, an advanced solar concentrator unit considered for use with the Stirling power conversion unit.

ACKNOWLEDGMENTS

The author wishes to thank the following people for their contributions to this report: M.E. Alper, J.W. Lucas, R.E. Morgan, P.L. Panda, J.M. Spiegel, and J.W. Stearns.

The dish/Stirling development effort led by the Jet Propulsion Laboratory was implemented with the assistance of the Lewis Research Center and seven industrial contractors, i.e., General Electric Company; Fairchild Industries, Stratos Division; Mechanical Technology, Incorporated; Acurex Corporation; United Stirling AB of Sweden; E-Systems; and Advanco Corporation.

The work described herein was conducted by the Jet Propulsion Laboratory, California Institute of Technology, for the U.S. Department of Energy through an agreement with the National Aeronautics and Space Administration (NASA Task RE-152, Amendment 327; DOE/ALO/NASA Interagency Agreement No. DE-AM04-80AL13137).

PREFACE

An executive summary highlights the accomplishments of the dish/Stirling effort. The main body of the report presents all aspects of the development program, with cited references containing further information.

ACRONYMS AND INITIALISMS

ACTF	DOE Advanced Components Test Facility
ALO	DOE Albuquerque Operations Office
CWCC	Cold-Water Cavity Calorimeter
DOE	U.S. Department of Energy
DSSR	Dish/Stirling Solar Receiver
EAFB	Edwards Air Force Base
EPRI	Electric Power Research Institute
ERG	Energy Research and Generation, Inc.
ESO	Elevation Offset
ESOR	Experimental Solar-Only Receiver
ETS	JPL Edwards Test Station
FSD	Fairchild Industries, Stratos Division
FY	U.S. Government Fiscal Year
GE	General Electric Company
GRI	Gas Research Institute
GRP	Glass Reinforced Polyester
GTRI	Georgia Tech Research Institute
HPSR	Heat Pipe Solar Receiver
JPL	Jet Propulsion Laboratory
LeRC	Lewis Research Center
MTI	Mechanical Technology, Inc.
NASA	National Aeronautics and Space Administration
PCU	Power Conversion Unit
PDTS	JPL Parabolic Dish Test Site
PID	Proportional-Integral-Differential

R&D	Research and Development
RCA	Radio Corporation of America
RFPSE	Resonant Free-Piston Stirling Engine
rms	root mean square
SNLA	Sandia National Laboratories-Albuquerque
STI	Solar Turbines International
STT	DOE Solar Thermal Technology Division
TBC	Test Bed Concentrator
TES	Thermal Energy Storage
USAB	KB United Stirling (Sweden) AB & Company

CONTENTS

I. EXECUTIVE SUMMARY 1-1

A. DISH/STIRLING ELECTRIC POWER SYSTEM 1-2

B. ACTIVITY OBJECTIVES 1-2

C. DEVELOPMENT REQUIREMENTS IDENTIFICATION 1-2

D. SYSTEM CONCEPT DEFINITION 1-3

E. SYSTEM REQUIREMENTS 1-4

F. DEVELOPMENT OF A YEAR 1985 SYSTEM 1-5

G. FIRST DISH/STIRLING POWER SUBSYSTEM MODULE DEVELOPMENT . 1-7

H. DEVELOPMENT OF AN IMPROVED DISH/STIRLING POWER CONVERSION UNIT 1-10

I. TECHNOLOGY TRANSFER 1-13

J. FUTURE DISH/STIRLING ELECTRIC POWER SUBSYSTEM DEVELOPMENT 1-13

II. INTRODUCTION 2-1

III. OBJECTIVES OF THE DISH/STIRLING ELECTRIC POWER SYSTEM DEVELOPMENT ACTIVITY 3-1

A. OBJECTIVE 1: IDENTIFICATION OF SUBSYSTEMS DEVELOPMENT REQUIREMENTS THROUGH ANALYSES OF ADVANCED DISH/STIRLING ELECTRIC POWER SYSTEMS . . . 3-1

B. OBJECTIVE 2: IMPLEMENT WITH INDUSTRY THE DESIGN, CONSTRUCTION AND FACTORY TEST OF ADVANCED SUBSYSTEMS 3-1

C. OBJECTIVE 3: OPERATIONALLY TEST AND EVALUATE ADVANCED SUBSYSTEMS 3-1

IV. IDENTIFICATION OF SUBSYSTEMS DEVELOPMENT REQUIREMENTS 4-1

A. PROJECTING ECONOMICS FOR DISTRIBUTED COLLECTOR ELECTRIC POWER SYSTEMS 4-1

1. Accounting for Inflation in Economic Projections . 4-1

2. Projections of Solar Thermal Power Plant Economics 4-2

B. TECHNO-ECONOMIC PROJECTIONS OF POWER SYSTEM CHARACTERISTICS 4-3

C. EFFECT OF SITING ON ADVANCED SOLAR THERMAL ELECTRIC POWER SYSTEM PERFORMANCE AND ENERGY COSTS . . . 4-5

V. DISH/STIRLING ELECTRIC POWER SYSTEM CONCEPT DEFINITION 5-1

A. APPROACH TO SYSTEM CONCEPT DEFINITION 5-1

B. DISH/STIRLING ELECTRIC POWER SYSTEM CONCEPT DESCRIPTION . 5-1

1. Operational Environment 5-1

2. System Functions 5-1

3. System Functional Block Diagram 5-2

VI. DISH/STIRLING ELECTRIC POWER SYSTEM REQUIREMENTS 6-1

A. GENERAL REQUIREMENTS 6-1

B. SYSTEM DESIGN CRITERIA 6-1

1. Lifetime 6-1

2. Size 6-1

3. Availability 6-1

C. SYSTEM FUNCTIONS AND FEATURES 6-2

1. Electrical Generation Functions 6-2

2. Maintenance Functions 6-2

D. SYSTEM PERFORMANCE REQUIREMENTS 6-2

VII. DEVELOPMENT OF A PROJECTED YEAR 1985 DISH/STIRLING ELECTRIC POWER SYSTEM 7-1

A. APPROACH 7-1

B. SYSTEM CONCEPT 7-1

1. Advanced Solar Concentrator Unit (Parabolic Dish Concentrator No. 2) 7-3

2. Advanced Power Conversion Unit 7-12

VIII. FIRST DISH/STIRLING POWER SUBSYSTEM MODULE DEVELOPMENT 8-1

A. SELECTION OF FIRST DISH/STIRLING POWER SUBSYSTEM MODULE FOR DEMONSTRATION 8-1

B. TEST BED CONCENTRATOR 8-2

1. Design Requirements 8-2

2. Design Characteristics 8-2

3. Installation 8-6

4. Reflector Surface Alignment 8-8

5. Test and Evaluation 8-9

C. POWER CONVERSION UNIT DEVELOPMENT 8-21

1. Design Modification of the USAB Model 4-95 (P-40) Stirling Engine 8-21

2. Assembly and Factory Testing of the USAB Model 4-95 (P-40) Stirling Engine 8-25

3. Design, Construction, and Factory Test of the Solar/Gas-Fired Receiver Assembly 8-29

4. Integration and Test of the USAB Model 4-95 (P-40) Stirling Engine with the FSD Solar/Gas-Fired Receiver 8-37

D. TECHNOLOGY ASSESSMENT 8-38

1. Test Bed Concentrator 8-38

2. Power Conversion Unit 8-39

IX. IMPROVED DISH/STIRLING POWER CONVERSION UNIT DEVELOPMENT . . . 9-1

A. DESIGN ACTIVITY 9-1

B. INTEGRATION AND TEST OF THE IMPROVED DISH/STIRLING POWER CONVERSION UNIT 9-5

1. United Stirling Testing at Georgia Tech Research Institute. 9-8

2. Testing the Experimental Solar-Only Receivers on the First Dish/Stirling Power Subsystem Module 9-10

3. Testing the Improved Dish/Stirling Power Conversion Unit on Test Bed Concentrator No. 2 9-12

C. TECHNOLOGY ASSESSMENT 9-19

X. TECHNOLOGY TRANSFER 10-1

A. REDESIGN AND TESTING THE USAB MODEL 4-95 MK II SOLAR STIRLING ENGINE FOR THE DOE/ADVANCO VANGUARD PROJECT . . 10-1

B. UNITED STIRLING POWER CONVERSION UNIT INCORPORATED INTO THE McDONNELL DOUGLAS DISH/STIRLING SOLAR ELECTRIC GENERATING SYSTEM 10-1

XI. FUTURE DISH/STIRLING ELECTRIC POWER SUBSYSTEM DEVELOPMENT . . . 11-1

A. FUTURE SOLAR CONCENTRATOR UNIT DEVELOPMENT 11-1

B. FUTURE POWER CONVERSION UNIT DEVELOPMENT 11-2

XII. REFERENCES 12-1

Figures

4-1 Comparative Energy Costs for 100-MWe Plants 4-2

4-2 Study Plan Flow Diagram 4-4

4-3 Projected Solar Thermal and Conventional Power Plant Energy Costs at Selected Sites 4-6

5-1 Dish/Stirling Electric Power System Functional Block Diagram 5-3

5-2 Dish/Stirling Electric Power System: Hardware Hierarchy 5-4

7-1 Dish/Stirling System Concept 7-2

7-2 Deep-Dish Point-Focusing Concentrator 7-3

7-3 Concentrator Design Description 7-5

7-4 Advanced Concentrator (Parabolic Dish Concentrator No. 2) 7-8

7-5 Outer Gore Cross Section 7-9

7-6 Cellular Glass Contouring Apparatus 7-11

7-7 25-ft Space Simulator Data 7-13

7-8 Projected Concentrator Performance 7-14

7-9 Flow Chart for Solar Stirling Engine Development 7-16

7-10 15-kWe Free-Piston Stirling Engine/Alternator Conceptual Design 7-19

7-11 Advanced Kinematic Stirling Engine 7-21

7-12 Stirling Hydraulic System Schematic 7-22

7-13 Schematic Diagram of Heat Flow in the HPSR 7-24

7-14 Heat Pipe Solar Receiver with Flame Impingement Fossil-Fuel Combustor 7-24

7-15 Cost of Electricity versus TES Storage Time for Systems with Combustors 7-26

7-16 Heat Pipe Test Facility 7-26

7-17 Operating Characteristics of Heat Pipe No. 1 at a 10-deg Inclination 7-27

7-18 TES Modular Experiment Components 7-28

7-19 Typical TES Charging Curve for the Modular Experiment . . 7-28

7-20 25-kWe Prototype HPSR/Engine/Generator System 7-29

7-21 Secondary Heat Pipe Wicking 7-30

8-1 Two Test Bed Concentrator Units with PCUs Mounted at the Focus 8-5

8-2 Close-Up of Flux Mapper from Outer End 8-10

8-3 Solar Flux Measurements on Test Bed Concentrators 8-11

8-4 Superimposed Focal Plane Flux Distribution Based on Flux Mapper Data 8-12

8-5 Aperture Plane Flux Profiles 8-14

8-6 Accumulative Energy Distribution 8-15

8-7 Intercept Factor Distribution 8-16

8-8 Equal Intensity Contour in X_T-Z_T Plane 8-17

8-9 CWCC Radiation Shield and Aperture Mounting Assembly . . 8-18

8-10 CWCC Graphite 10.16-cm-Diameter Insert Retainment 8-19

8-11 CWCC Flow Instrumentation Diagram 8-20

8-12 TBC Mirror Configurations 8-22

8-13 Engine Electronic Control Unit Input and Output Signals 8-26

8-14 4-95 Engine Inverted with Combustor and TBC Mounting Ring 8-28

8-15 First Dish/Stirling Power Conversion Unit Being Mounted on TBC-2 8-30

8-16 DSSR and P-40 Engine/Alternator 8-31

8-17 P-40 Cylinder and Regenerator Arrangement 8-32

8-18 Dish/Stirling Solar Receiver 8-32

8-19 Refractory Combustion Chamber 8-34

8-20 Combustion Air Preheater 8-34

8-21 Hybrid Receiver, External Configuration 8-36

9-1 Heater Design for Direct Heating -- Top View, Modified P-40 Engine Heater Design 9-1

9-2 Heater Design for Direct Heating -- Cross Section 9-2

9-3 Power Conversion Unit Model 4-95 No. 2 9-4

9-4 ESOR-IIA 9-4

9-5 ESOR-IIB 9-5

9-6 Calculated Performance of ESOR-IIA and ESOR-IIB, Power Output versus Maximum Working Gas Pressure 9-6

9-7 Calculated Performance of ESOR-IIA and ESOR-IIB, Efficiency versus Maximum Working Gas Pressure 9-7

9-8 4-95 Standard Involute Heat Exchanger 9-9

9-9 Variation of Output Power with Time 9-9

9-10 Electric Output As a Function of Thermal Input to Cavity for Three Different Experimental Solar-Only Receivers . . 9-11

9-11 TBC-2 Flux Maps 9-13

9-12 Variation of PCU Output Power with Receiver Location . . 9-15

9-13 ESOR-III 9-16

9-14 ESOR-IV Quadrant, Including Cylinder and Regenerator Housings 9-17

9-15 Stirling Module with Radiator System 9-18

9-16 Insolation and Power from a Full-Day Test 9-20

9-17 Mean Daily Output 9-20

10-1 Vanguard Dish/Stirling Module 10-2

Tables

7-1 Dish/Stirling Electric Power System Component Efficiency and Power Level Projections 7-2

7-2 Key Characteristics of the HPSR System 7-31

8-1 Key TBC Design Requirements 8-3

8-2 TBC Structure Weight Summary 8-6

8-3 Results of Pointing Angular Error Analysis 8-7

8-4 TBC-2 Power Input versus Aperture Diameter and Mirror Configuration 8-23

9-1 Data Comparison, Different Concentrator Alignments . . . 9-14

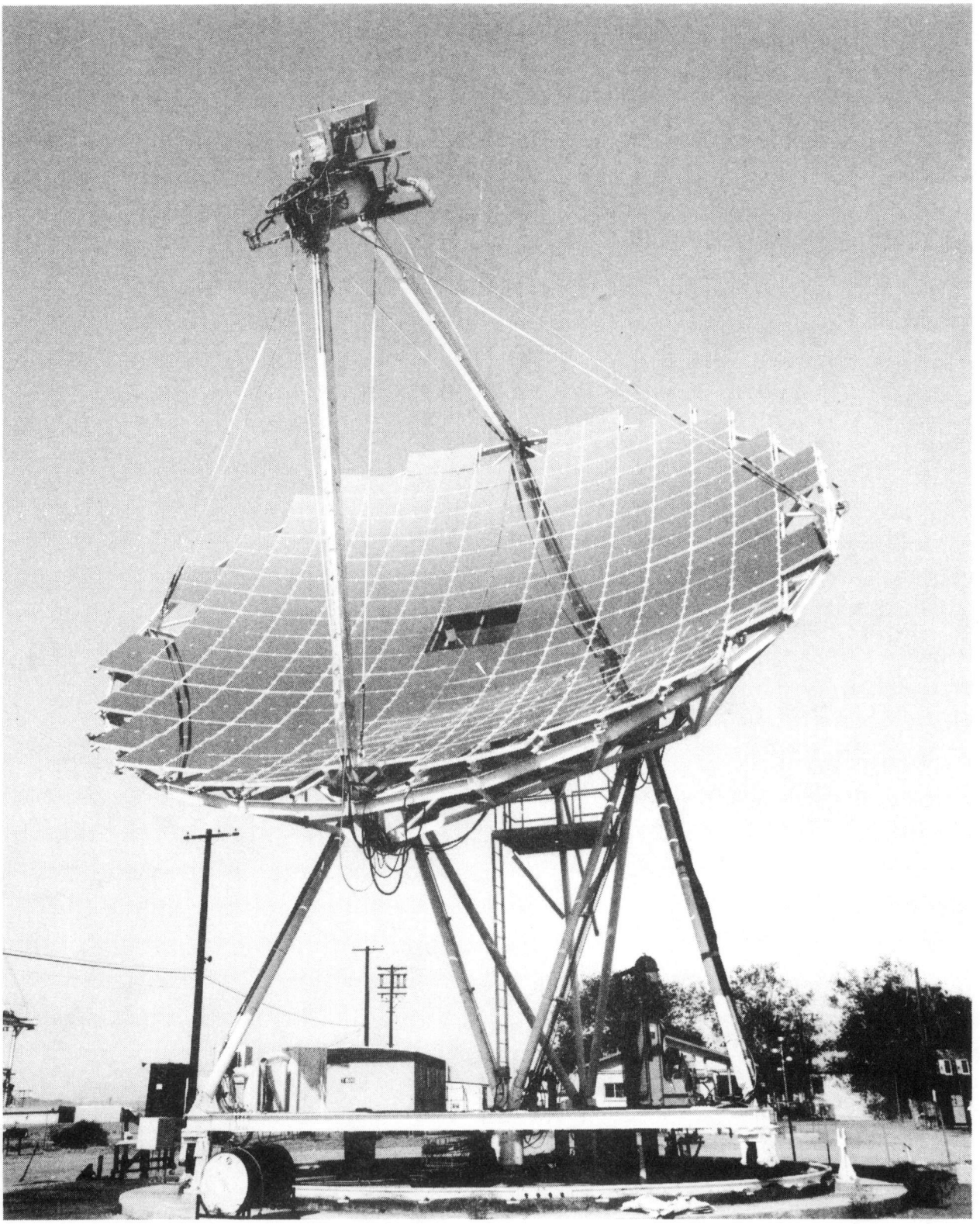

The First 25-kWe Dish/Stirling Power Module

SECTION I

EXECUTIVE SUMMARY[1]

Key accomplishments of the activity included the design of a dish/Stirling electric power system in 1979 followed by successful test and evaluation of such items as (1) concentrator reflective panels made of back-silvered fusion-glass superstrate with thick foamed-glass substrate and (2) components for a metallic sodium heat pipe solar receiver equipped with an integral eutectic salt thermal energy storage medium. From the design and development activity, the appropriate solar thermal technology required for a prototype electric generating module evolved. From 1979 to 1981, test and evaluation of the first 25-kWe dish/Stirling power module demonstrated the use of a practical Stirling engine power conversion unit coupled with the high-performance test bed concentrator. Even though the combined solar with natural gas combustion heating of the Stirling engine/receiver proved to be too difficult to control, experience was gained in how to redesign the hybrid receiver for future application. In 1982, after four years of system definition, design and development, and test and evaluation, outstanding success was achieved with an improved solar-only Stirling engine/receiver. This improved dish/Stirling module could regularly operate 13.5 h each summer day while generating up to 24 kWe with a 28% peak overall conversion efficiency of solar power in to electric power out -- a new record! Moreover, the module could generate over 250 kWe-h each clear summer day. Advances resulting from this development effort are being used in dish/Stirling electric power system ventures pursued by Advanco Corporation (the Vanguard Project) and by McDonnell Douglas Astronautics/United Stirling of Sweden.

Some lessons learned from the activity that may apply to future developments include the following:

(1) The advantages of the excellent thermal transport, stable and uniform operating temperature, and stored energy inherent in the heat pipe solar receiver with eutectic salt thermal energy storage previously demonstrated are worthy of continued evaluation and improvement.

(2) Dish solar concentrator structural loads encountered in severe winter windstorms and severe summer squalls and thunderstorms are needed by the structural designer. More knowledge of the statistical and unsteady wind velocity characteristics within a dish solar concentrator field during windstorms may significantly reduce the extreme stand-alone strength requirements now imposed by structural designers.

(3) The hybrid solar/natural gas combustor receiver could be redesigned with much simpler silicon carbide ceramic components to eliminate the adverse effect of nonuniform heating experienced with the tubed heavy metal heat exchanger. A more suitable natural gas flow control subassembly should be developed.

---

[1]See body of the report for references pertaining to material in the Executive Summary.

(4) Larger temperature differences than expected were seen on the heater cage in the solar-only receiver tests. These temperature differences reduce the effectiveness of the engine by imbalancing the power output of the four pistons. Though not proven, the solar flux pattern on the heater cage appears to be irregular and to contribute to the imbalance.

(5) Other Stirling engines should be developed and/or modified for solar applications. A new generation of Stirling engines is being developed for a wide variety of non-solar applications, and these engines may be able to be modified for solar application.

A. DISH/STIRLING ELECTRIC POWER SYSTEM

Development of a dish/Stirling electric power system has been pursued by the United States Department of Energy (DOE) at the Jet Propulsion Laboratory (JPL) since October 1977. This engineering development activity was transferred to Sandia National Laboratories-Albuquerque (SNLA) during FY 1984. Highlights and accomplishments of the dish/Stirling electric power system development activity over the six-year period are presented herein.

The dish/Stirling electric power system is a modular solar-thermal-powered electricity generating plant. With each dish/Stirling power subsystem module, the direct insolation irradiating the Earth is focused onto a small prime mover heater surface by pointing a large paraboloidal reflector or Fresnel refractor continually at the sun. On each module, the solar-thermal-powered Stirling engine prime mover then drives an electric generator to produce electricity. The dish/Stirling electric power system is composed of a field array of these distributed dish/Stirling power subsystem modules, in addition to an interconnecting electric power subsystem, a distributed control subsystem, and a centralized information display subsystem.

B. ACTIVITY OBJECTIVES

The objectives of the development of a dish/Stirling electric power system were to identify subsystems development requirements through analyses; to implement with industry the design, construction, and factory test of subsystems; and to operationally test and evaluate subsystems in the field.

C. DEVELOPMENT REQUIREMENTS IDENTIFICATION

In order to identify subsystems development requirements, economic projections were made beginning in late CY 1977 and ending in early 1980. Of the solar distributed-collector electric power systems envisioned for years 1990 to 2000, the dish/Stirling electric power system was projected to produce the lowest electricity cost but have the highest developmental risk. Results of the first analysis in 1977 pointed to the necessity of reducing the cost of the solar concentrator unit, while simultaneously improving the efficiency of the power conversion unit through a balanced dish/Stirling power subsystem development activity. Continuing projected economic analyses further

substantiated the key characteristic of superior solar thermal electric power systems as being an efficient low-cost solar concentrator unit combined with an efficient power conversion unit operating at maximum working gas temperatures from 816°C (1500°F) to 1094°C (2000°F). Both projected cost and power improvements foreseen in 1978 for both distributed and centralized solar thermal electric power systems indicated that solar plants could approach the goal of a capital cost of $960 to 1600/kWe and an energy cost of 80 to 96 mills/kWe-h.[2] As part of the analysis, a comprehensive survey of power conversion prime movers in 1978 showed the Stirling engine to have the best potential for high efficiency and low cost even when properly accounting for the high risk associated with the improved Stirling engine technology. Another analysis of plant siting effects on solar thermal electric power system performance and energy cost completed in 1980 concluded that both the dish/Stirling electric power system and the central receiver/Brayton-Rankine electric power system could achieve energy costs competitive with conventional electricity generation peaking plants for all sites studied in the United States after the year 2000. The most promising of sites for solar thermal electric power systems were found to be in the Southwest sunbelt, as expected.

D. SYSTEM CONCEPT DEFINITION

After an organized system analysis, system design and subsystem conceptual design activities were performed in late 1977 at JPL, and a dish/Stirling electric power system design concept for post-1985 applications was defined. The design concept satisfied the systems design objectives of (1) meeting operational requirements, (2) satisfying system performance requirements reducing the cost of electricity, and (3) employing modern, proven technology.

The dish/Stirling electric power system would operate as a peak-load electricity generating power plant in the year 2000 time frame because of its insolation-dependent characteristics. In the utility generation grid network, the system would compete with conventional peak-load, oil-fired and natural gas-fired, open-cycle gas-turbine electric power systems to provide a small fraction of total electricity production. Baseload fossil-fired and nuclear-fueled steam turbine electric power systems would generate the major fraction of total electricity.

The principal function of the dish/Stirling electric power system would be to provide electricity from direct insolation. The system would also perform maintenance, data collection, internal power distribution, and interfacing functions. The system consists of four subsystems: a distributed dish/Stirling power subsystem, a distributed electric power subsystem, a distributed control subsystem, and a centralized control and information display subsystem.

The distributed dish/Stirling power subsystem collects direct solar energy and converts it to electric power. An array of large solar

---

[2]For consistency, all dollar figures in this report have been converted to constant 1984 dollars (see Section IV.A.1, "Accounting for Inflation in Economic Projections").

concentrator units tracks the sun and focuses the direct insolation intercepted by the optical reflector or refractor onto a small heater of the power conversion unit. The Stirling engine converts the absorbed solar thermal power into electrical generator shaft power, which is then converted to electricity. The distributed electric power subsystem collects and distributes electric power to all subsystems and to the interface with the electrical utility grid. The distributed control subsystem generates and controls all signaling and data for external and internal control circuits. The centralized control and information display subsystem provides for the human interface and interprets the operator commands for the control subsystem.

E. SYSTEM REQUIREMENTS

The dish/Stirling electric power system requirements were derived from the system objectives formulated early in the development process. The general requirement is for the system design to be based upon the application and adaptation of proven technology where possible with the objectives of reducing the life-cycle cost and minimizing technical risks. The system is required to function reliably and perform in the operational environment of an electric utility network. Where state-of-the-art components are employed in the system, these components must have proven reliability based upon documented operational history in the expected environment. In contrast, the new solar-related components must demonstrate the potential for reliability through the present development process.

The system would have to be designed and constructed for a service life of 20 years while operating autonomously from sunrise-to-sunset, 7 days per week, 365 days per year. The electricity generating plant size will be determined by the particular application. Because the dish/Stirling electric power system is modular, size variations can be readily accommodated with the economic advantage of a short construction period and readily expandable plant.

The plant must be available for generating electricity upon demand by the operator. Due to the modular nature of the plant, the plant would automatically reconfigure in the event of a failed module in order to continue operation. Clouds, wind, snow, and ice can impair the availability of the plant on a local level; however, where several dish/Stirling electric power system plants are operating in differing locales, the coupled availability of the aggregate plants needs to be considered.

For a 10-MWe plant, a staffing goal for maintenance would be two trained but unskilled maintenance persons available on a one-shift-per-day basis, 5 days per week.[3] During the remainder of the time, a maintenance person would be "on call." Self-diagnostics with the capability of interfacing with maintenance persons or a remote operator would be incorporated. After identification of a failure, the control subsystem would isolate the defective module. The isolated module would be serviced without disruption to the rest of the plant.

Economic analyses point to the requirements of producing electricity in the years 1990 to 2000 at or less than a levelized busbar cost of 80 to

[3]This goal is based on allowable maintenance costs for a 10-MWe plant.

96 mills/kWe-h. In order to do this, the system must achieve an energy conversion efficiency of 35% by 1990 and achieve an up-front capital cost of $960 to 1600/kWe for a 10-MWe plant. Reliability, maintainability, and availability must also be attained to achieve a maintenance life-cycle cost competitive with conventional power systems.

F. DEVELOPMENT OF A YEAR 1985 SYSTEM

A system development task was organized to design, construct, and test solar components for the advanced system. Successful completion of component testing would set the stage for a decision to test a prototype to verify the performance of the solar components when operated as a system. Solar concentrator units, power conversion units, energy storage and transport units, and the electric power subsystem would be developed. At JPL in 1978 a small dish/Stirling electric power system was conceptually designed using projected 1985 technology that could achieve the system requirements. The system concept was defined only to the extent necessary to assure adequate technology direction at the subsystem and unit level. One solar concentrator unit was conceptually designed for industry implementation.

The solar concentrator unit consisted of mirrored glass gores installed in a cantilever configuration on a truss-type support ring of a triangular cross section to form a complete, but physically discontinuous reflective surface having about a 10-m-diameter aperture. Each reflective gore was to be fabricated of thin, back-silvered glass mirror bonded continuously over a contoured substrate of cellular glass. An all-truss structure would serve as an intermediate structure between the reflector assembly and the pedestal assembly, which provides the azimuth and elevation movements necessary for sun tracking. The Acurex Corporation was selected in 1979 to develop the solar concentrator unit through preliminary design, detailed design, and fabrication processes. The key results of the Acurex preliminary design activity were (1) the optimization process to select a diameter of 10.9 m, (2) the extensive design/analysis efforts to produce a minimum weight solar concentrator unit, and (3) the final installed cost estimate of $198/m^2 of aperture, which was 33% higher than the target.

After the solar concentrator unit preliminary design process, Acurex studied the problem of installation costs associated with site preparation, foundation installation, and field erection of the wide-base, perimeter drive configuration. A new concept emerged that retained the advantage of the mirror cellular glass reflector assembly, but eliminated the costly wide-base configuration. A new turret drive/pedestal mount configuration would require a more costly drive unit, but the reduced site assembly and foundation installation costs more than offset this penalty. The total installed cost of the new concept was estimated to be $161/m^2.

Acurex proceeded to detail the design of the reflector surface element: the fusion glass superstrate/foam glass substrate mirrored gore. Several full-scale prototype gores were fabricated by Acurex and subsequently tested by JPL. Optical tests conducted within the 25-ft-diameter Space Simulation Chamber indicated 100% of the reflected light from a point source would be intercepted within a 12.7-cm (5-in.)-diameter solar receiver assembly on an

advanced solar concentrator unit. Calculation further predicted that 100% of the sunlight would be intercepted within a 15-cm (6-in.)-diameter solar receiver. Two gores were tested and both withstood severe environmental tests without adverse effects.

A Stirling solar engine development plan was formulated by the Lewis Research Center (LeRC) in 1978 to support the dish/Stirling power subsystem conceptual design activity. LeRC was chosen to manage the activity because of their involvement with the DOE Automotive Stirling Engine development program in addition to other Stirling engine development activities. The plan was to proceed from an advanced high-efficiency engine concept to a 15-kWe test-bed Stirling engine for full-scale testing. The key goal of the activity was to design a 40%-efficient engine assembly in both the advanced version (1985 and beyond) and the near-term test-bed version. Both kinematic and free-piston engines were considered as candidates for the system. The kinematic engine was more developed and had well defined problems such as limited seal life, difficult heat transfer and fluid flow characteristics, and use of costly materials and production methods. The free-piston engine presented a difficult design problem with two oscillating masses actuated by interdependent springs and with linear alternators in early stages of development. Conceptual designs for both free-piston and kinematic engines were undertaken by Mechanical Technology, Inc. (MTI) in August 1978. United Stirling of Sweden AB (USAB) was engaged by MTI to work on the kinematic engine while Sunpower, Minneapolis-Honeywell, Dynatherm, Masco, and MTI worked on the free-piston engine. It was anticipated that at the end of this conceptual design phase, a reasonably clear choice could be made between pursuing the kinematic-type or the free-piston-type Stirling engine.

Results of the conceptual design of a free-piston engine indicated the ability for a 15-kWe maximum power engine to have an overall engine/alternator efficiency of 30% -- just meeting the goal for combined engine/alternator efficiency. The conceptual design hermetically sealed all components within a pressure vessel for long, maintenance-free operation. Production cost (labor plus material) for the engine was estimated to be $3450 in production quantities of 25,000 per year.

The USAB selected kinematic-type Stirling engine conceptual design was a four-cylinder double crankshaft engine with annular regenerators. The engine heater head design was examined for both focused insolation directly impinging on the heater tubes and condensing sodium heat transfer via heat pipe transport. Calculated results show a near-term efficiency of 42% for the 20-kWe engine -- slightly above the 40% goal.

The choice between the two types of Stirling engine was never made because of redirection of priorities within the overall solar thermal program. However, a substitute solar modification of the USAB Model 4-95 Stirling engine adequately satisfied the requirements for a test-bed solar engine. In addition, the advanced development task continued the conceptual design of the free-piston engine improvements. The University of Washington with Flow Industries, Inc., in 1982 was able to develop a preliminary design for a long-life hydraulic converter capable of interfacing with the free-piston solar Stirling engine design by MTI. The hydraulic converter would produce hydraulic flow at pressures suitable for operating a

ground-based commercial hydraulic motor/electric alternator set. For this free-piston engine application, the hydraulic assembly would replace the linear alternator assembly with some cost advantages and less development of new technology. Energy Research and Generation, Inc. (ERG) also addressed the advanced free-piston Stirling-engine-driven 15-kWe power linear alternator conceptual design. ERG designed and analyzed critical components and subassemblies, assessed and optimized the thermodynamic and dynamic performance through computer simulation, and performed a preliminary design of a resonant free-piston engine-driven 15-kWe power linear alternator. The results of the ERG study indicated attainment of 60% power conversion efficiency, a cost of $76/kWe, absence of strategic materials, and achievement of high reliability and lifetime.

Beginning in FY 1978, the General Electric Company (GE) developed a power conversion unit (PCU) with a heat pipe solar receiver coupled to a thermal energy storage assembly. The PCU featured latent heat thermal energy storage, excellent thermal stability, and self-regulating, effective thermal transport at a low assembly temperature difference. PCU development was supported by component testing of heat pipes and of thermal storage in addition to energy transport models that defined the expected performance of the PCU. All preliminary and detailed design was completed, and most of the components were fabricated before funding was terminated.

The GE heat pipe solar receiver with thermal energy storage (TES) is a high-efficiency assembly for use as part of a self-contained 15- to 25-kWe power conversion unit operating at 827°C (1520°F) maximum engine temperature. High-temperature sodium heat pipes transport heat from a cavity solar receiver subassembly through an $NaF-MgF_2$ eutectic salt latent heat storage subassembly to the USAB Model 4-95 Solar Mk I engine assembly. Another feature of the PCU is a flame impingement combustor subassemly on the TES shell that provides heat to the PCU in the absence of direct insolation. With about 0.8 hours of latent and sensible heat storage, the entire PCU should weigh about 1315 kg (2900 lb).

G. FIRST DISH/STIRLING POWER SUBSYSTEM MODULE DEVELOPMENT

In FY 1979, the DOE Solar Thermal Technology Program elected to demonstrate a subsystem module solar-to-electric conversion efficiency of 24% by pursuing an interim experiment to be demonstrated by FY 1981. It was reasoned that the ultimate system requirements would necessitate many years of advanced development by government and industry to improve performance, operations, reliability, and maintainability and to reduce manufacturing costs. Therefore, an interim experiment achievable within the resources available could provide a means to explore the qualities of the solar subsystem when operated at the Parabolic Dish Test Site (PDTS), Edwards Air Force Base, California.

The interim dish/Stirling power subsystem module would consist of a solar concentrator unit and a power conversion unit. Two solar concentrator units were designed, built, and installed at the Parabolic Dish Test Site by E-Systems, Inc., from September 1978 through October 1979. These were named test bed concentrators and were based upon a 13-m-diameter communications

antenna structure designed for the RCA Domestic Satellite System. The antenna structure was significantly modified and supplemented to serve as a test bed concentrator (TBC). The diameter was reduced to 11 m, the focal length was about doubled, the focal point weight load was increased by a factor of 10, the solar reflector panels were reduced to only a small fraction of the radio reflector panels, and the tipping structure of the antenna required an entirely new pedestal because the radio antenna moved only 60 deg in azimuth to track artificial satellites.

The TBC structure was designed and analyzed using modern finite element techniques while constrained by deflection criteria. The control assembly provided for active sun tracking as well as program tracking.

The TBC reflector surface consists of 224 individual reflector panels fastened to a parallel tube matrix attached to the backup support structure. (Because of shadowing, four center facets were subsequently removed.) Each reflector facet is composed of a thin silver-mirrored fusion glass superstrate bonded continuously to a thick, spherically contoured cellular glass substrate. After manufacture of each reflector panel, the focal length and standard slope error is determined by optical measurement. The alignment of all panels on one concentrator took about two weeks of night work. Subsequent realignment typically took only two nights. The alignment light source was placed on a hill some 5.8 km (3.6 miles) southwest of the test site. In order to align the reflected image of the light source from each facet, the light source was aimed at the TBC. The TBC was then boresighted to the light source, a focal plane target attached to the TBC, and each facet individually uncovered and moved to center the image on the focal plane target.

After alignment of the 220 reflectors, the TBC focal zone radiative energy flux distribution was measured with a "flux mapper." The flux mapper consists of a radiometer attached to a mechanical raster device capable of moving the flux sensor through the concentrated sunlight in a series of planes perpendicular to the optical axis. The recorded energy flux can be presented in various formats as the user requires. The flux mapping results after initial mirror alignment indicated a peak flux of 1500 W/cm^2 with direct insolation of 0.1 W/cm^2, and 98% of the energy within a 20.3-cm (8-in.)-diameter aperture. Before testing the PCU on the TBC, the reflectors were realigned in May 1981 to evenly distribute the energy flux on the Stirling engine conical heater head not to exceed the 55-W/cm^2 limit established by Fairchild Industries (the receiver manufacturer). The flux-mapper data intensity profile at the receiver cavity aperture was compared to a calculated energy flux distribution -- based on the known radius of curvature and standard slope error -- with very close agreement. The excellent agreement confirmed the validity of the numerical radiative flux model. Subsequent reflector realignments could then be based upon numerical computations of radiative flux distribution rather than by a tedious trial-and-error method.

Cavity receiver aperture radiative energy rates were measured with a calorimeter placed behind a simulated focal plane 20.3-cm (8-in.)-diameter aperture. In order to simulate several levels of radiative energy rates even on a clear day, calorimeter measurements were made with 220, 176, 112, and 56 reflectors uncovered. Also, the cavity receiver aperture was reduced to

10.16 cm (4 in.) and 15.24 cm (6 in.) and increased to 25.4 cm (10 in.) for additional radiative energy rate tests. For a 20.3-cm-diameter aperture, the maximum radiative energy rate was determined to be 77.3 kWt for all 220 reflectors uncovered with a direct insolation of 0.1 W/cm^2.

Fairchild Industries, Stratos Division (FSD) in conjunction with United Stirling AB designed, fabricated, assembled, and factory tested the first dish/Stirling power conversion unit beginning in 1979 and ending in 1981. The PCU consisted of an FSD dish/Stirling hybrid receiver assemby, a USAB Model 4-95 Solar Mk I engine, and a GE alternator. The PCU was ultimately mounted on a TBC at the PDTS to form the first dish/Stirling power subsystem module.

A USAB Model 4-95 engine was redesigned for solar application by USAB in 1980. While the solar concentrator unit tracks the sun, the engine assembly is inclined from 90 to 180 deg to the normal upright position on the ground. The engine lubrication subassembly was extensively redesigned and the engine cooling subassembly was moderately redesigned to operate in the near inverted position. The engine casing was redesigned to couple with the alternator assembly, and both were supported in a main frame by six flexible mounts. With the hybrid receiver assembly entirely supported by the engine, the PCU with the main frame was designed to mount to the TBC-2 receiver support structure. The engine electronic control subassembly interfaced with the PCU electronic control assembly. With a combustor subassembly within the receiver assembly, the power output of the engine was held constant by manually setting the maximum working gas pressure at a fixed level and keeping the temperature of the receiver constant by adjusting the firing rate of the natural gas combustor. The engine start-up sequence was the most complex control problem and was initiated in the combustor mode only. Any stop sequence was initiated by turning the solar concentrator away from the sun and closing off the fuel supply. The 22.5-kW shaft power of the engine at 15 MPa mean working gas pressure and 710°C heater tube outer wall temperature was calculated to be 35% of the heat absorbed by the working gas with the hybrid receiver assembly, or about 2 kW (shaft) lower than that obtained with a standard heater.

By September 1, 1980, USAB began procuring components for the baseline 4-95 Stirling engine, and the engine was assembled before the end of the month as the conventional fossil-fuel-fired configuration. Acceptance testing of the engine began on November 13 with dynamometer run-in and was completed on December 8 after 48 hours total running time. Performance of the engine during the acceptance test indicated that the engine power at 1800 rev/min ranges from 20 kWe at 11 MPa mean helium working gas pressure to 27 kWe at 15 MPa mean pressure with only the solar auxiliaries (oil pump and helium pump). After completion of the dynamometer tests, the lubrication subassembly was modified to allow inverted operation, and the engine/alternator assemblies on the main frame were mounted to the mock TBC-2 mounting ring. For testing in the USAB laboratory, the complete unit could be rotated on an axis to the inverted position. With the alternator interfacing with the Swedish electrical utility (3-phase, 50-Hz), the engine speed was 1500 rev/min under all load conditions. The engine/generator assemblies were operated successfully for a total of 350 hours under simulated solar dish attitude. Performance at 1500 rev/min and 720°C outer heater tube temperature was measured as 22-kWe output with an overall efficiency from fuel to electricity of 31.5%. Based upon an alternator efficiency of 93% and a combustor

efficiency of 89%, the predicted solar efficiency was calculated to be 38% using helium working gas. After completion of the testing in Sweden, the engine/alternator was shipped to the Parabolic Dish Test Site for integration with the solar receiver assembly and the test bed concentrator.

The solar/gas-fired receiver assembly designed, built, and factory tested by FSD was known as the dish/Stirling solar receiver (DSSR). The principal function of the DSSR was to convert concentrated sunlight and/or to burn natural gas with air in order to supply the heat directly, efficiently, and uniformly to the Stirling engine hot end. The gas-fired combustion augmentation provides capability to supplement heat available from the sun on cloudy days or at night so the dish/Stirling power subsystem can provide a predictable electrical output. The DSSR is composed of two sections, a section containing the optical receiver cavity covered by a conical ceramic aperture plate and a section containing the combustion subassembly. The two sections are separated by a conical heater head made of copper encapsulated in Inconel 617 for oxidation protection and structural rigidity. Forty-eight equally spaced Inconel 617 engine heater tubes are embedded with the copper to channel the engine working gas. The engine heater tubes extend from the lower surface of the heater cone to the regenerators and have Inconel-617-clad copper sleeves providing the heat transfer surface for the combustion gas to working gas heat exchanger. Thermocouples on these lower tubes sense the temperature used to control the natural gas/air flow rates to the eight combustor nozzles within the combustion chamber. The combustion air is preheated to 760°C (1400°F) by combustion exhaust gases within an annular fin-type counter-flow heat exchanger. The combustion air blower powered by a 1-kWe power motor was selected for its high head pressure and low flow rate characteristics. Air and fuel control valves supplied by Honeywell were modified by FSD. The combustor subassembly was thoroughly tested before integration with the solar receiver assembly and the PCU.

Advanco Corporation performed initial testing of the DSSR with the USAB Model 4-95 solar engine on a ground pad at the PDTS beginning on September 22, 1981. The combustion was reported to be excellent with control maintained in a semi-automatic mode; however, the natural gas flow was difficult to control with an adjustable potentiometer. The complete power conversion unit was then installed on TBC-2 on October 2, 1981, with initial low power solar testing beginning on November 9 and ending on December 8, 1981, with a braze joint failure. Problems encountered in the tests included poor control of the combustor subassembly, multiple failures in the heater tube due to heater head braze joints, lack of good combustor gas oxygen sensing capability, few thermocouples on the heater tubes, and continued inability to properly adjust the natural gas flow rate. Even so, the feasibility of a natural gas-fired hybrid solar Stirling engine receiver was demonstrated. Considerable future development is required to attain proven technology. During all of these tests, the Model 4-95 Solar Mk I engine performed flawlessly.

H. DEVELOPMENT OF AN IMPROVED DISH/STIRLING POWER CONVERSION UNIT

During the solar Stirling engine conceptual design activity in 1978, United Stirling with MTI designed five direct solar-only engine heater heads.

At least two of these designs were subsequently modified by USAB for use on the Model 4-95 Solar Mk I engine. USAB recognized the solar-only heater to be the most critical component of a solar Stirling engine because the solar-only heating concept could not meet the optimum cycle requirements, such as small dead volume and uniform temperature distribution. The design of a heater for direct solar heating required a detailed analysis of engine performance, including the radiative flux distribution on the heater tubes, because the design of all of the other Stirling engine components are affected by specific qualities of the heater. Two different and conflicting design philosophies for the heater heads were (1) to arrange the gas passages to match the physical needs of the Stirling engine with the receiver radiative flux in order to achieve a uniform temperature distribution on the heater head, or (2) to arrange the gas passages close to each other in a uniform way to completely cover the heater cage area so as to exclude the need for surface extension or buffer material. An intense study of several heaters considered the parameters of tube length, unheated tube length, dead volume between regenerator and heater, and dead volume between cylinder and heater. After completion of the DOE-funded conceptual design study, USAB continued the development program through computer modeling and optical analysis of several solar receiver designs for the Model 4-95 engine. Two different heat exchangers were constructed as well as several solar receiver cavities that incorporated different types of insulation and reflecting surfaces. The heater cage diameter was about 40 cm (15.75 in.) on the two new involute heaters; the standard heater diameter is 28.6 cm (11.25 in.). USAB also developed a digital electronic control for autonomous operation. The all new engine control consisted of both electronic and electric equipment such as solenoid-operated valves, high voltage relays, and meters for grid connection.

Integration and test of the improved USAB dish/Stirling power conversion unit took place in three distinct solar phases. The first two phases occurred from August 1981 through March 1982. The final phase extended 20 months from May 1982 through December 1983. The first phase of the testing took place at the DOE Advanced Components Test Facility (ACTF) located at Georgia Tech Research Institute (GTRI) during the period of August through November 1981. The ACTF consists of a field array of 550 1-m-diameter mirrors that focus the sun's image at the lower level of a tower platform 21 m (70 feet) above the ground. USAB contracted with GTRI to test a power conversion unit nearly identical to the first dish/Stirling power conversion unit being tested at the PDTS. Testing at the ACTF was intended to parallel the PDTS testing and provide additional experience with solar-only receivers. The best run was made on November 18, 1981, with the PCU producing a maximum of 18.5 kWe to the grid near noon with a large 40.6-cm (16-in.)-diameter aperture. The engine operated successfully under automatic control that held the maximum heater head temperature at 720°C. Tests on November 21, 1981, with the second solar-only heater head installed on the engine yielded a power output of 16.5 kWe at the same insolation.

From January through March 1982, the two solar-only receivers plus the standard heater head were tested at the PDTS with the first dish/Stirling power conversion unit then installed upon TBC-2. Even though TBC-2 had been aligned for the FSD dish/Stirling solar receiver, the radiative flux on the new heater heads was uniform at about 50 W/cm^2 with no high peaks -- however, the radiative flux level on the cavity walls was fairly high. Results of

these tests confirmed part of the earlier heater head parametric analysis and showed that the largest diameter heater head with the calculated lowest Stirling-cycle performance gave the highest power output and conversion efficiency while the standard heater head with the best calculated Stirling-cycle performance produced the lowest power output and efficiency. Clearly, much needed to be learned from continued activity.

In May 1982, USAB and JPL installed (upon TBC-2) the improved dish/Stirling power conversion unit formerly tested at Malmo, Sweden, and at the ACTF. Thus began a long sequence of tests concerned with improving the performance of the power conversion unit. Over the next 20 months, USAB with JPL would characterize solar receivers, conduct full-day performance tests of the subsystem, test new cavity and aperture glass windows, image the temperature distribution on the heater head with an infrared video camera, conduct radiator subassembly tests, and conduct control subassembly tests.

More was also being learned about the effect of solar concentrator alignment upon PCU performance. TBC-2 was realigned in order to concentrate all radiative flux on the receiver heater tubes. After realignment, the radiative flux distribution proved to be the shape of a doughnut completely covering the heater tubes but not spilling over on the cavity walls or the central ceramic plug. The peak performance of the improved dish/Stirling power subsystem was now 24.2 kWe power at a conversion efficiency[4] of 33.6% compared to the 19.5 kWe power, 28.4% efficiency of the first dish/Stirling power subsystem equipped with a solar-only receiver measured in March 1982.

Testing was performed to find the optimum operating conditions for the receiver and the complete power conversion unit. Parameters investigated were working gas temperature, front tube temperatures, cavity temperatures, engine pressure, temperature distribution, power output, and engine location in relation to the concentrator focal point. The optimum engine location is where the heater cage intercepts almost all radiative flux in a near uniform distribution and the tube temperatures are balanced between inner and outer tubes. The relationship between power output, pressure, tube length, and cage diameter was optimized in a later solar-only receiver heater (ESOR-III) to improve performance. Additionally, the relatively lower operating pressure for ESOR III for same power output can be attained with no more than a 20-MPa maximum working gas pressure -- the engine operating limit.

The DOE-owned Model 4-95 Solar Mk I engine was updated temporarily by USAB with a new electronic digital control, a new solar-only receiver assembly, and a complete engine-mounted cooling system. After TBC-1 was realigned by a newly devised rapid method evolving from the Stirling PCU test sequence, the improved DOE-owned PCU was mounted and tested. The results were 22.4 kWe maximum power with helium working gas at an ambient temperature of 28°C. Maximum cooling water temperature never exceeded 51°C with a total cooling fan power of 0.790 kWe -- a design criterion. Maximum parasitic power of 1.5 kWe for the engine cooling subassembly was 4 to 5 kWe less than that demonstrated by the first FSD dish/Stirling power subsystem.

---

[4]Efficiency numbers do not include parasitic losses.

The improved PCU on TBC-2 was operated for a full day on several occasions. The improved dish/Stirling power subsystem performance for these all-day tests can be highlighted by the following record performance figures:

(1) Net electric power output = 24 kWe

(2) Net solar to electric efficiency = 28%

(3) Daily net energy generation = over 250 kWe-h

(4) Time of continuous operation = 13.5 h

I. TECHNOLOGY TRANSFER

While the previously described development of the USAB Model 4-95 was in progress, the engine was selected by the Advanco Corporation and DOE for a cooperative agreement to build a prototype solar parabolic dish/Stirling engine system module. The Stirling engine used in the Vanguard project is the first of a new generation of engines manufactured by United Stirling called the 4-95 Mk II Solar SE. The engine was delivered and installed upon the Vanguard unit at Rancho Mirage by December 1983. The performance of the Vanguard dish/Stirling electric power system module has exceeded the previous performance of the 4-95 Mk I Solar SE on TBC-2 at the PDTS.

United Stirling AB joined with McDonnell Douglas Corporation in November 1983 to jointly develop, manufacture, and market worldwide the dish/Stirling solar electric generating system. The solar PCU proposed for the system is a USAB Model 4-95 Mk II Solar SE. The PCU is mounted upon a McDonnell Douglas concentrator, which allows access to the engine by lowering it to ground level. The extensive solar engine development initiated and supported by the DOE Solar Thermal Technology Program and the solar testing conducted by USAB at the PDTS led directly to this major DOE accomplishment of stimulating industry to commercialize the dish/Stirling electric power system.

J. FUTURE DISH/STIRLING ELECTRIC POWER SUBSYSTEM DEVELOPMENT

Future solar concentrator unit development applicable to the dish/Stirling electric power subsystem includes non-destructive quality assurance tests, system reliability tests, and a preventive maintenance demonstration of the joint DOE/Advanco Vanguard project. Another ongoing activity of considerable interest to the development of solar concentrator units is the Innovative Point Focus Solar Concentrator project being pursued by the DOE Albuquerque Operations Office (DOE/ALO) in conjunction with SNLA and three private-sector organizations. The privately funded efforts by McDonnell Douglas, LaJet Energy Company, and others also are improving the state of solar thermal electric dish technology. Beyond these ongoing development efforts, environmental loadings on concentrators due to wind, ice, snow, hail, and earthquakes need to be better understood by designers in order to apply a modern statistical stress/strength approach to designing toward a desired reliability. Meteorological instrumentation on distributed wind

towers, several instrumented heliostats, and complete data acquisition equipment at the Solar One solar thermal central receiver pilot plant are acquiring the needed wind data within and adjacent to a heliostat field array.

Future dish/Stirling power conversion unit development is now addressing the need for additional, newer Stirling engines beyond the USAB Model 4-95. These new Stirling engines will be explored in relation to the needs of the Solar Thermal Technology Program. Where an engine is found to have considerable value in projected solar applications, the engine should be redesigned, modified, tested, and evaluated for this application. Under contract to the Gas Research Institute and in conjunction with DOE/ALO, the Advanco Corporation through a subcontractor will design, build, and test a hybrid solar receiver with natural gas combustion for the present Vanguard module. In order to synchronize the dish/Stirling electric power system generating schedule with the peak power demands of the electric utility, both thermal energy storage along with natural gas combustion in the PCU will have to be examined. In addition to the development of dish/Stirling PCU's, the Solar Thermal Technology Program should include an adequate technology base activity for engine research and development to increase the efficiency and lifetime of Stirling engines and components while lowering the cost of operations and maintenance.

SECTION II

INTRODUCTION

A solar dish concentrator with a Stirling engine generator system has been under development by the United States Department of Energy (DOE) through the Jet Propulsion Laboratory (JPL) over the past several years. The Solar Thermal Power Systems Project at JPL was terminated in September 1984. Engineering development of the Dish/Stirling electric power system will continue to be pursued by DOE at Sandia National Laboratories in Albuquerque, New Mexico (SNLA).

The solar dish concentrator with Stirling engine/generator electric power system is one of the solar thermal renewable energy technologies showing substantial promise as an alternative to conventional sources of energy supply (Reference 1). Unlike conventional power plants, the modularity of the dish/Stirling electric power system also makes possible a gradual growth of generating capability to match the prevailing electricity demand.

A solar dish concentrator with Stirling engine/generator electric power system consists of a distributed dish/Stirling power subsystem, a distributed electric power subsystem, a distributed control subsystem, and a central information display subsystem. The ideal system would be designed to minimize the life-cycle cost to the user. A 1977-78 comparative system analysis study (Reference 2) concluded the following:

(1) "Two-axis tracking concentrators...have the highest optical collection efficiencies and are therefore the most promising advanced technologies for achieving the high temperatures necessary for efficient electric power production."

(2) "Highest power plant system efficiencies (two-axis tracking systems) occur between [816 to 1093°C] 1500 to 2000°F as a result of a trade-off between increasing engine performance with temperature and higher heat losses from the receiver."

(3) "Advanced high temperature systems using technologies such as advanced Stirling and Brayton engines...improve the probability of success for achieving the target energy cost[1] (80 to 96 mills/kWe-h) by factors as high as 4 to 5 compared to present generation (Barstow pilot plant) central receiver systems..."

(4) "Stirling engines achieve the highest projected efficiencies over a wide size range and are therefore identified as being the most attractive advanced energy conversion technology."

---

[1]For consistency, all dollar figures in this report have been converted to constant 1984 dollars (see Section IV.A.1, "Accounting for Inflation in Economic Projections"). The energy cost quoted in Reference 2 is 50 to 60 mills/kWe-h in 1977 dollars.

The JPL subsystem development task resulted in the operational test and evaluation of two unique solar power conversion units, one by Fairchild Industries, Stratos Division (FSD) and the other by United Stirling AB (USAB) at the JPL Parabolic Dish Test Site, Edwards Air Force Base, California, from 1981 to 1983. The Advanco Corporation chose to use the results of this previous development in their successful bid for the Solar Parabolic Dish Stirling Engine System Module Project, undergoing operational test and evaluation at the Southern California Edison Company Santa Rosa Substation, Rancho Mirage, California, in 1984. Also the development of an advanced solar parabolic dish concentrator unit in 1977-80 for the dish/Stirling power subsystem resulted in the design of such a unit and the test and evaluation of a fusion-glass superstrate/foamed-glass substrate gore-shaped reflector surface subsequently incorporated into Acurex Corporation's solar parabolic dish concentrator unit.

SECTION III

OBJECTIVES OF THE DISH/STIRLING ELECTRIC POWER SYSTEM DEVELOPMENT ACTIVITY

A. OBJECTIVE 1: IDENTIFICATION OF SUBSYSTEMS DEVELOPMENT REQUIREMENTS THROUGH ANALYSES OF ADVANCED DISH/STIRLING ELECTRIC POWER SYSTEMS

Clear-cut objectives of the DOE Solar Thermal Technology (STT) Program's development of dish/Stirling electric power systems were based upon application of the proven systems approach practiced at JPL. Using the systems analysis process, engineering requirements for the several subsystems were formulated for initiating contractor subsystem development.

B. OBJECTIVE 2: IMPLEMENT WITH INDUSTRY THE DESIGN, CONSTRUCTION, AND FACTORY TEST OF ADVANCED SUBSYSTEMS

Those subsystems, units, and assemblies requiring development before incorporation into an advanced dish/Stirling electric power system were pursued with industry through competitive procurement activities. Industrial firms designed subsystems to meet advanced functional, performance, endurance, operational, maintenance, cost, and other requirements. Subsequently, they constructed and factory tested these subsystems. The policy of the DOE/STT Program has been to engage industry as much as possible in implementing developmental subsystems in order to stimulate industrial interest in private commercial ventures utilizing the developed, proven subsystem.

C. OBJECTIVE 3: OPERATIONALLY TEST AND EVALUATE ADVANCED SUBSYSTEMS

In order to prove the advanced design and/or further develop the subsystem, unit, or assembly, operational testing and evaluation were conducted at characteristic operational test sites. The natural environment of the test site in addition to the presence of an operational test crew over several months stressed the subsystem to the level expected to be encountered in commercial installations. A Parabolic Dish Test Site was prepared at the JPL Edwards Test Station, Edwards AFB, California, for operational test and evaluation.

SECTION IV

IDENTIFICATION OF SUBSYSTEMS DEVELOPMENT REQUIREMENTS

A. PROJECTING ECONOMICS FOR DISTRIBUTED COLLECTOR ELECTRIC POWER SYSTEMS

1. Accounting for Inflation in Economic Projections

In this report, economic projections were determined by studies conducted in earlier years of the project. This subsection provides an explanation of how these projections, which were originally in prior year dollars, all have been converted to constant 1984 dollars. The text of the following explanation and table showing gross national product implicit price inflators is taken primarily from Economic Analysis of Investment and Regulatory Decision - A Guide, Federal Aviation Administration, U.S. Department of Transportation, APO-82-1, January 1982:

Changes in the value of the dollar over time with respect to any particular commodity or group of commodities are measured using an index number. Such a number is a measure of relative value. It indicates the price of any particular commodity or group of commodities in one year relative to its value in some other year. By convention, index numbers are usually computed as the ratio of this price in one year divided by the price in the base year. The resulting ratio is then multiplied by 100 to produce the index number. Repeating the process for a number of years results in a series of index numbers.

To grasp the methodology of working with index numbers, consider the gross national product implicit price deflator, which is reported in the following table for 1972 through 1984 third quarter.

	Index (Base Year)	
Year	1972	1984
1972	100.00	44.6
1973	105.69	47.1
1974	114.92	51.2
1975	125.56	55.9
1976	132.11	58.9
1977	139.83	62.3
1978	150.05	66.9
1979	162.77	72.5
1980	177.36	79.0
1981	195.14	86.9
1982	207.38	92.4
1983	215.34	96.0
1984 (third quarter)	224.44	100.0

Note first that 1972 has a value of 100. Known as the base year, it is an arbitrary selection which is changed from time to time. It indicates that all other values are measured relative to 1972 being equal to 100. Moreover, the entire index may be restated in terms of any other base year by dividing each value by that of the new base year. In column three of the table, the index for 1984 as the base year has been computed.

2. Projections of Solar Thermal Power Plant Economics

A preliminary comparative evaluation of distributed collector solar thermal power plants was undertaken in FY 1977 by projecting power plant economics of selected systems to the 1990-2000 time frame (Reference 3). The selected systems include (1) fixed orientation (non-tracking) collectors with concentrating reflectors and vacuum tube absorbers, (2) one-axis tracking linear concentrators including parabolic trough and variable slat designs, and (3) two-axis tracking parabolic dish systems including concepts with small heat engine/electric generator assemblies at each focal point as well as approaches having steam generators at the focal point with pipeline collection to a central power conversion unit.

Comparisons (Figure 4-1) were presented primarily in terms of energy cost (mills/kWe-h) and capital cost over a wide range of operating load

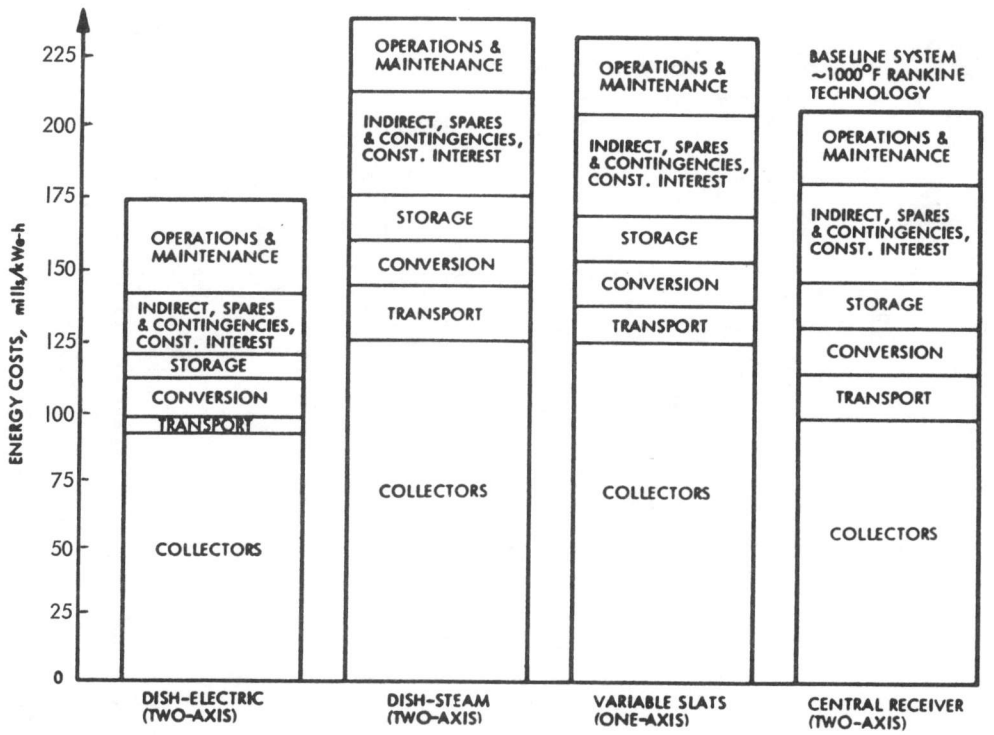

Figure 4-1. Comparative Energy Costs for 100-MWe Plants. (Annual Load Factor = 0.55, Year 2000 Start-Up)

factors. Sensitivity of energy costs for a range of efficiencies and costs of major subsystems/components was presented to delineate critical technological development needs.

It was concluded from the economic analysis that the most promising distributed collector system, particularly for small power applications, is the dish-electric system. However, this system had the greatest uncertainties and required more technology development than the other systems.

An examination of subsystem sensitivities indicated that collector costs are a dominant parameter. The overall system efficiency involving all the subsystems from concentrator to energy conversion is also a powerful cost driver because higher efficiencies allow use of a smaller and, hence, less costly collector field for a given power plant rating. These sensitivity results indicated that cost reduction activities should emphasize the collector (concentrator plus receiver) system while advanced technology efforts should concentrate on improving efficiencies of components such as receivers coupled to engines.

B. TECHNO-ECONOMIC PROJECTIONS OF POWER SYSTEM CHARACTERISTICS

Advanced technologies applicable to solar thermal electric power systems in the 1990-2000 time frame were delineated for power applications that fulfill a wide spectrum of small power needs with primary emphasis on power ratings of <10 MWe (Reference 2). Techno-economic projections of power system characteristics (energy and capital costs as a function of capacity factor) were made in FY 1978 based on development of identified, promising technologies. These projections were used as the basis for comparing technology development options and combinations of these options to determine developmental directions offering potential for significant improvements (Figure 4-2).

The key characteristics required are efficient low-cost solar energy collection to achieve high temperatures for efficient energy conversion at appropriate costs. Two-axis tracking systems such as the central receiver (or power tower concept) and distributed parabolic dish systems possess the potential for achieving these characteristics. For these two basic concepts, advanced technologies, including conversion systems such as Stirling engines and Brayton/Rankine combined cycles and storage/transport concepts encompassing liquid metals and reversible-reaction chemical systems were considered. In addition to techno-economic aspects, technologies were also judged in terms of factors such as developmental risk, relative reliability, and probability of success.

Improvements potentially available to projected advanced technology systems, both central receiver and parabolic dish systems, indicate that pursuit of advanced technology across a broad front can result in post-1985 solar thermal systems having the potential for approaching the goal of competitiveness with conventional power systems, i.e., capital costs[2] of $960 to 1600/kWe and energy costs of 80 to 96 mills/kWe-h (Reference 2).

---

[2]The capital costs quoted in Reference 2 are $600 to 1000/kWe in 1977 dollars.

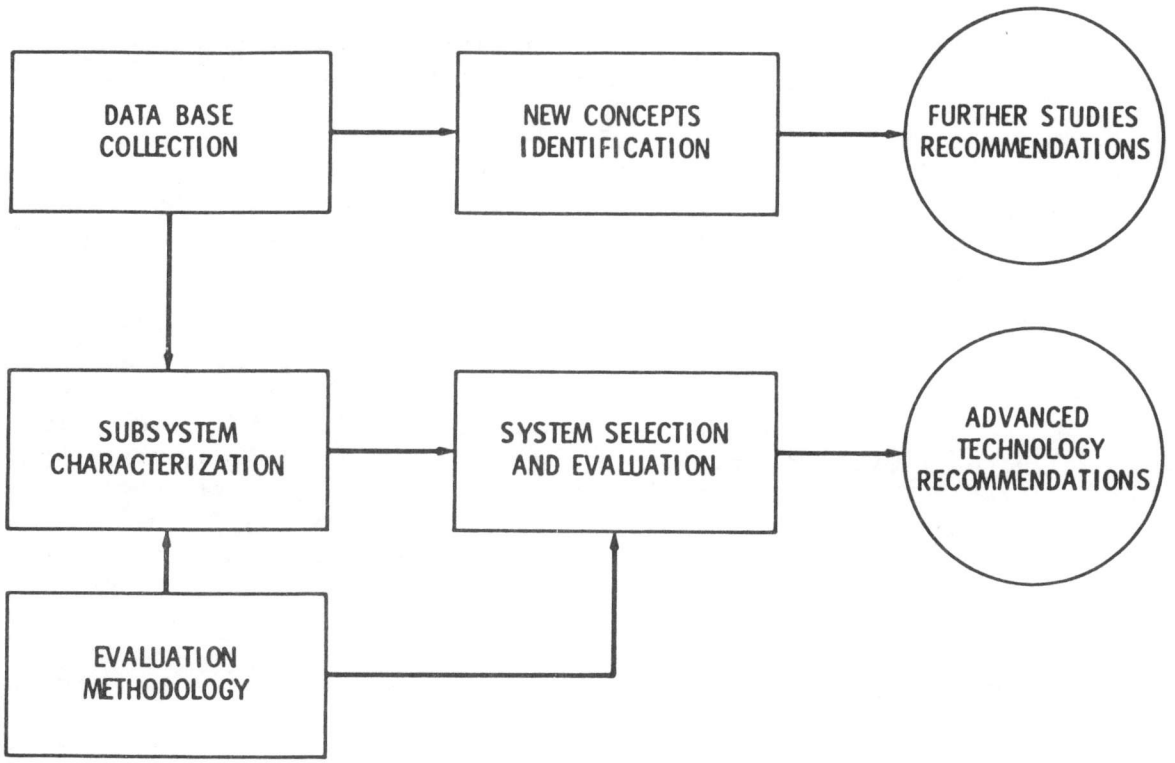

Figure 4-2. Study Plan Flow Diagram

A probabilistic evaluation methodology was used in the FY 1978 projection to compare the most promising systems. Benefits of advanced systems were determined by cost savings resulting from operation of the advanced system as compared to the baseline. Technical risks associated with factors such as materials availability, technology development status, safety, etc., were assessed as the basis for determining the probability of success. The projected benefits/cost savings multiplied by the probability of success determined the allowable expenditure for research and development.

A comprehensive survey in FY 1978 of advanced energy conversion systems indicated that Stirling engines have the highest potential in terms of both efficiency and cost. Therefore, both the central receiver and distributed dish systems employing the Stirling engine showed the highest gains even when the higher risk of the Stirling was compared to the relatively well established Brayton and combined cycles. Brayton and Brayton/Rankine combined cycles were shown to be highly promising options that could be implemented with relatively small additional advanced technology expenditures because they would use the same collectors, storage, and transport as the systems employing Stirling engines. Generally, the study indicated that the largest benefits would result from focusing advanced technology efforts on the achievement of the highest possible conversion efficiencies in the 816 to 1093°C (1500 to 2000°F) temperature range.

C. EFFECT OF SITING ON ADVANCED SOLAR THERMAL ELECTRIC POWER SYSTEM PERFORMANCE AND ENERGY COSTS

A study completed in FY 1980 determined the performance and cost of four 10-MWe advanced solar thermal electric power plants sited in various regions of the continental United States. Each region has different insolation characteristics and costs of conventional energy, which result in varying collector field areas, plant performances, capital costs, and energy costs (Reference 4).

In the context of advanced technology, solar plants were conceptualized to begin commercial operation in the year 2000. It was assumed that major subsystem performance would have improved substantially as compared to that of pilot plants currently operating or under construction. The net average annual system efficiency was therefore roughly twice that of current solar thermal electric power plant designs. Similarly, capital costs reflecting goals based on high-volume mass production that are considered to be appropriate for the year 2000 have been used. These costs, which are approximately an order of magnitude below the costs of current (FY 1980) experimental projects, are believed to be achievable as a result of the anticipated sizable solar penetration into the energy market in the 1990 to 2000 time frame.

From Figure 4-3, it can be inferred that paraboloidal dish/Stirling and central receiver Brayton/Rankine solar thermal peaking (solar-only) plants could achieve energy costs that are competitive with residual-oil, gas-turbine peaking plants for virtually all sites studied within the continental United States. (The parabolic trough could be competitive only in the sunbelt.) To reach this competitive status would require advanced technology development, low-cost designs suited to mass production, and sufficient market penetration to achieve the high-volume production associated with low costs.

The primary conclusion from the study was that the two-axis tracking solar thermal systems (namely, the central receiver and paraboloidal dish/Stirling systems) are potentially attractive for electric power generation in virtually all regions of the continental United States, and the relative advantages of these systems over other configurations are true for all regions. The most promising region is the Southwest sunbelt. However, in the context of large uncertainties regarding future energy costs from fossil and nuclear power plants, solar thermal power generation is potentially viable, even in the Northeast.

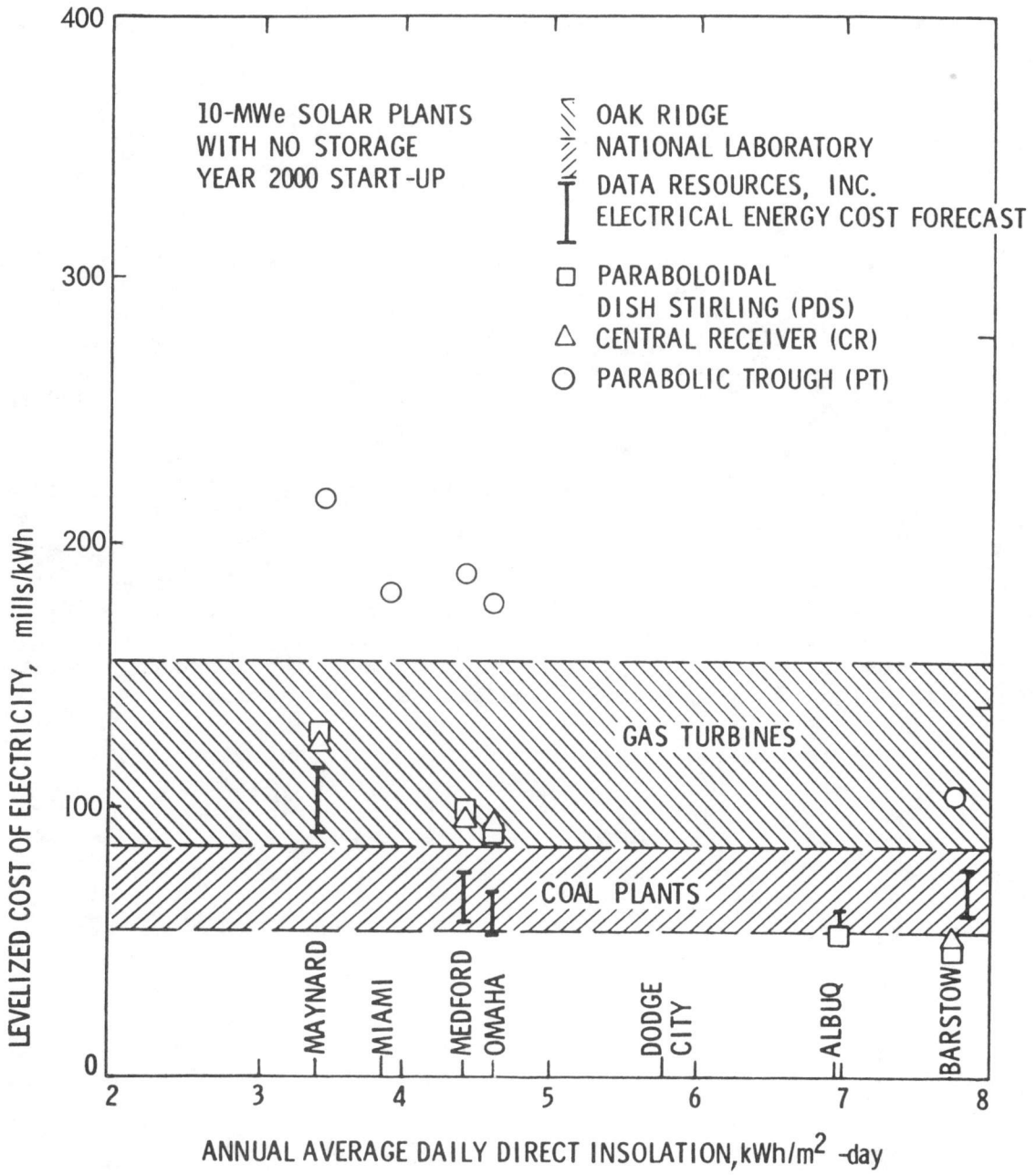

Figure 4-3. Projected Solar Thermal and Conventional Power Plant Energy Costs at Selected Sites

SECTION V

DISH/STIRLING ELECTRIC POWER SYSTEM CONCEPT DEFINITION

A. APPROACH TO SYSTEM CONCEPT DEFINITION

Starting with the dish/Stirling electric power system design objectives of (1) meeting operational requirements, (2) satisfying system performance criteria, (3) reducing the cost of electricity, and (4) employing modern, proven technology, a system design team was formed by the DOE Solar Thermal Technology Program in October 1977 at JPL to (1) pursue the conceptual design, (2) identify costly and/or unproven technology, (3) implement technology improvements with industry, and (4) test and evaluate these technology improvements.

The system design, system analysis, and subsystem conceptual design activity resulted in a dish/Stirling electric power system concept definition that satisfied all system objectives.

B. DISH/STIRLING ELECTRIC POWER SYSTEM CONCEPT DESCRIPTION

1. Operational Environment

The dish/Stirling electric power system will probably operate as a peak-load electricity generating power plant in the year 2000 time frame because of its insolation-dependent characteristics. Other conventional peak-load electricity generating power plants operating in the year 2000 environment will likely be oil-fired and natural gas-fired, open-cycle, gas-turbine electric power systems. The dish/Stirling electric power system will likely generate a small fraction of the total electricity production while operating in an environment composed mainly of baseload fossil-fired and nuclear-fueled steam turbine electric power systems within an electrical utility generation grid network.

2. System Functions

The principal function of the dish/Stirling electric power system is to provide electricity from direct insolation. The system also performs a maintenance function, data collection, internal power distribution, and interfacing functions. Potential users include public and private utility companies and other users not connected to an electrical utility grid network.

Given the direct insolation, mean wind speed and direction, and ambient air temperature, the system power available should be predictable and repeatable. The characteristics of the generated electrical power should conform to national and local standards and codes.

The dish/Stirling electric power system should operate autonomously and perform self-diagnosis, fault identification, fault isolation, fault correction, and real-time quality control.

The system should have data collection, reduction, and analysis features permitting operation and maintenance personnel to understand and improve the system performance and scheduling. Data obtained from several interconnected dish/Stirling electric power systems at several locations may prove the coupled plant availability and plant capacity factor to be greater than the isolated plant.

The internal power distribution function of the system consists of distributing the electrical utility grid power, the self-generated power, and the uninterruptible power to all subsystems.

System interfacing functions include the generation, reception, and interpretation of proper signals to and from operations and maintenance personnel. Where the system interfaces with the electrical utility grid, it must sense and properly interpret normal and abnormal conditions and take appropriate action as required.

3. System Functional Block Diagram

The dish/Stirling electric power system can be represented by the following functional blocks as seen in Figure 5-1:

a. Distributed Dish/Stirling Power Subsystem. The dish/Stirling power subsystem collects solar energy and performs the solar-thermal-to-electric power conversion. An array of solar concentrator units tracks the sun and focuses the direct insolation intercepted by the concentrator apertures into the receiver apertures on the power conversion units (PCUs). Each dish/Stirling power subsystem module is composed of a solar concentrator unit and a power conversion unit (as seen in Figure 5-2).

Solar Concentrator Unit. The mirror reflector assembly of the solar concentrator unit intercepts and reflects solar radiative power to the PCU while it maintains the proper optical rigidity through support by a backup structural assembly. The backup structural assembly is supported and pointed in space by a gimbal assembly attached to the foundation.

Power Conversion Unit. On each dish/Stirling power subsystem module, the power conversion unit consists of a solar receiver whose aperture accepts solar radiative power from the solar concentrator unit. Its heat exchanger surfaces absorb most of the solar radiative power and conduct this thermal energy to the Stirling engine. The Stirling engine converts the thermal power into shaft power for driving an electrical generator.

b. Electric Power Subsystem. The electric power subsystem collects and distributes electric power to and from the dish/Stirling power subsystem and to and from the electric interface of the electrical utility grid. The electric power subsystem also distributes electric power to the control and information display subsystems. An emergency electric power unit provides electrical power for system-wide distribution in the event of loss of connection to the electrical utility grid.

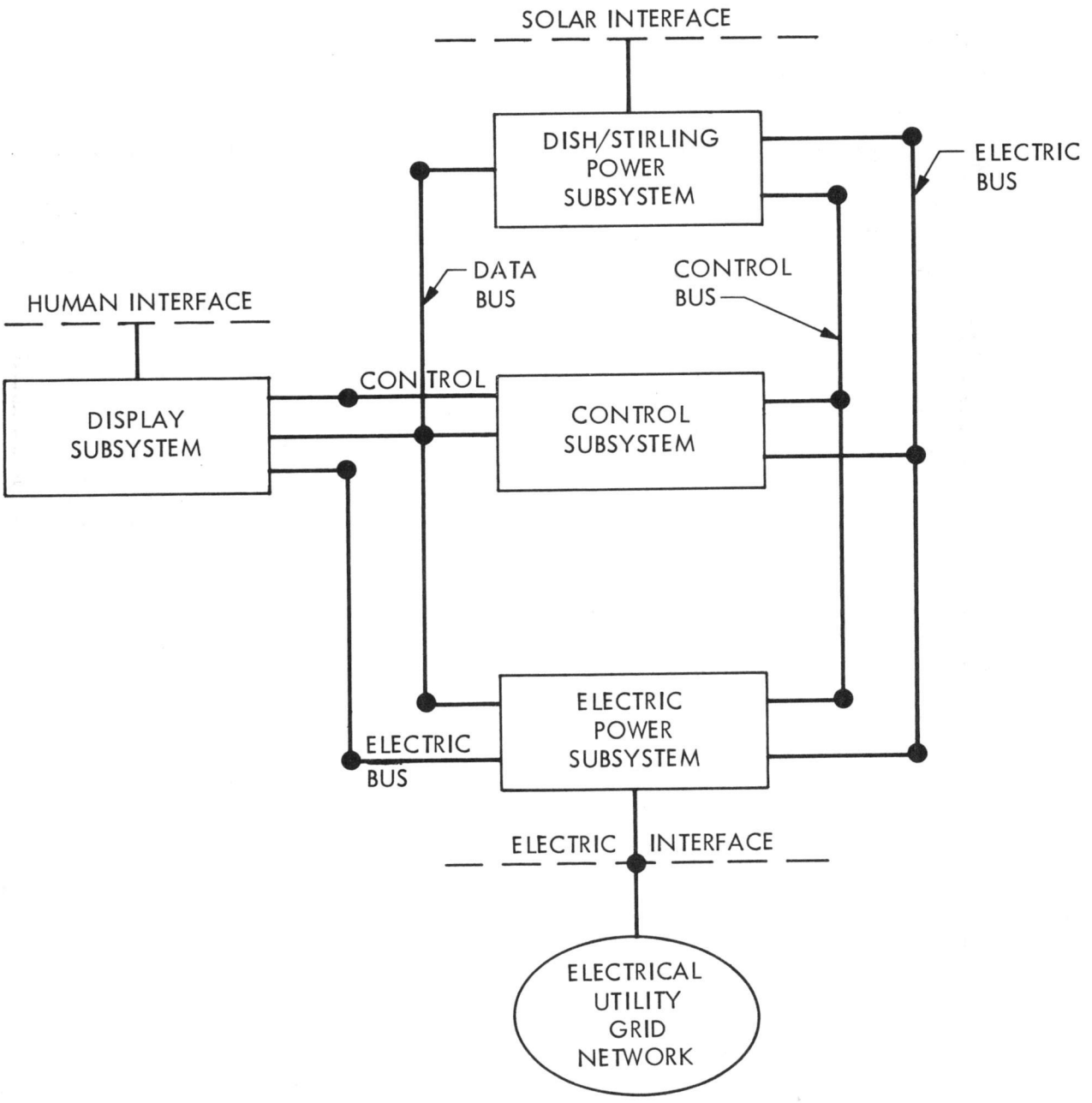

Figure 5-1. Dish/Stirling Electric Power System Functional Block Diagram

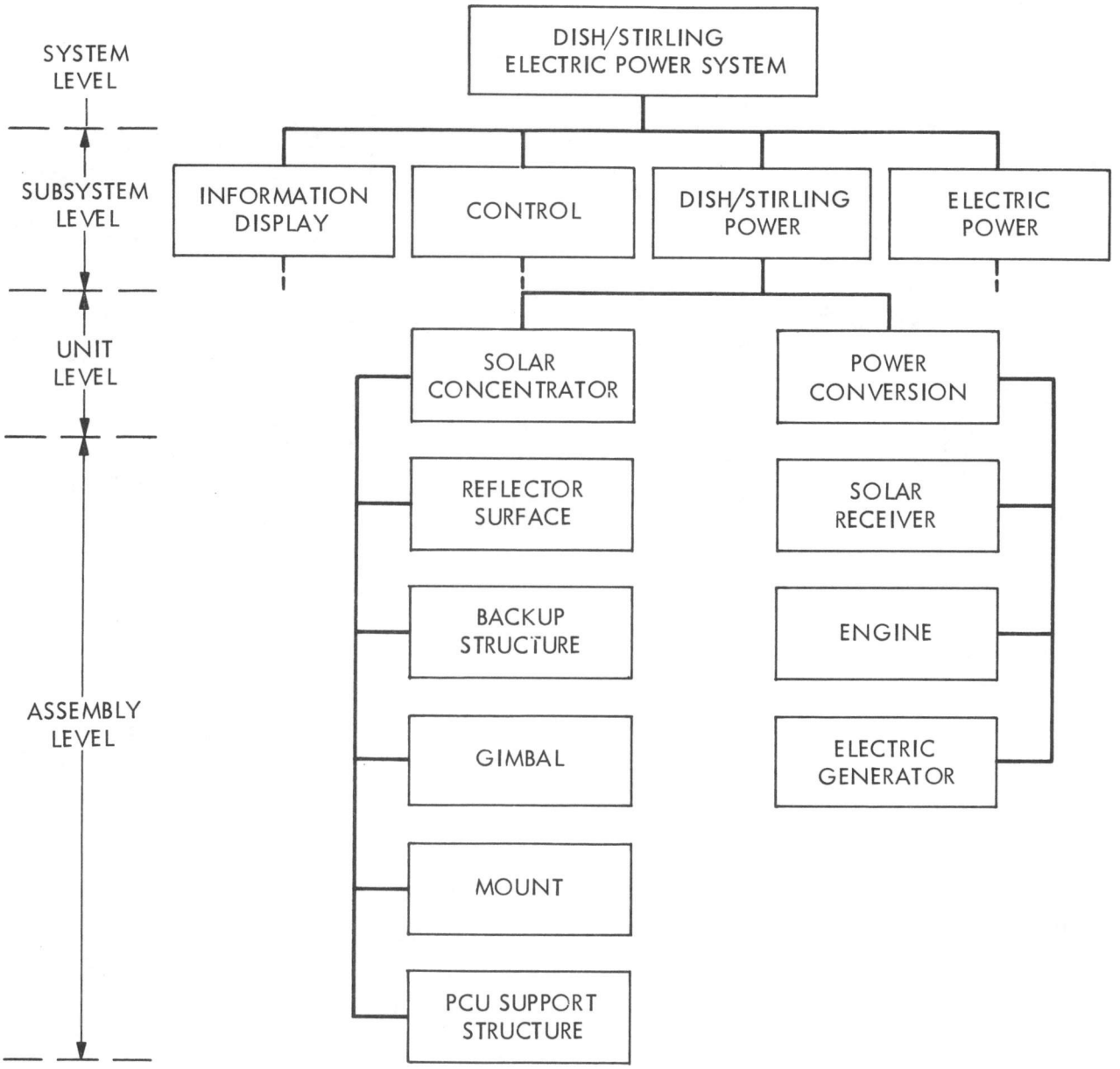

Figure 5-2. Dish/Stirling Electric Power System: Hardware Hierarchy

c. Control Subsystem. The control subsystem generates and controls all signaling and data for external and internal control circuits. It also controls the system generating configuration, receives other reconfiguration commands from the plant supervisor or maintenance positions, and disseminates information to the dish/Stirling power subsystem, the electric-power subsystem, and the information display subsystem to execute all changes. The subsystem controls the interfaces with the electrical utility grid and the data acquisition unit and performs real-time quality control.

d. Display Subsystem. The display subsystem provides the information necessary for the operator, interprets operator commands, and passes the information to the control subsystem.

SECTION VI

DISH/STIRLING ELECTRIC POWER SYSTEM REQUIREMENTS

A. GENERAL REQUIREMENTS

The dish/Stirling electric power system requirements are derived from the system objectives formulated early in the development process. As far as possible, the system design is based upon the application and adaptation of proven technology with the objective of reducing the life-cycle cost and minimizing technical risk. The factors of reduced maintenance and operator productivity have been emphasized in the system design.

The system design assures that all functional and performance requirements can be achieved. For those subsystems using state-of-the-art components, proven reliability based upon documented operational history must be obtained. All new solar component designs were to achieve proven reliability through the developmental process.

B. SYSTEM DESIGN CRITERIA

1. Lifetime

The system must be designed and constructed to have a service life of at least 20 years with cost-effective preventative and corrective maintenance practice. During the service life, the dish/Stirling electric power system must be capable of continuous, autonomous, normal operation from sunrise to sunset each day, 7 days per week, and 365 days per year.

2. Size

The dish/Stirling electric power system size will be determined by the electrical utility application or the off-grid electrical load characteristics. Because of the modular nature of the dish/Stirling electric power system, plant size variations and differences in operational environment from one installation to another can be readily accommodated.

3. Availability

The availability for generating electricity of the dish/Stirling electric power system is subject to local weather conditions in addition to system failures. Clouds, wind, snow, and ice can all impair system availability on the local level.

Due to the system's modular characteristics, failures and subsequent corrective maintenance should not have a large impact on system availability.

C. SYSTEM FUNCTIONS AND FEATURES

1. Electrical Generation Functions

The dish/Stirling electric power system provides the capability to supply all generated power to an electrical utility grid or other non-grid electrical loads. The system automatically configures to supply the generated power and automatically reconfigures to adjust to changes in power from predetermined circuit diagrams. The system confirms supply of generated power by signalling the plant operator.

2. Maintenance Functions

Operation and maintenance cost goals for the first year of operation were set at about 1% of the total capital investment cost. These costs were escalated at the rate of about 7% per year for labor and 4.3% per year for manufactured goods (see Reference 2, Appendix C). The operation and maintenance cost was considered to be composed of 75% labor and 25% goods with a combined annual growth rate of 6.3%. A 10-MWe dish/Stirling electric power system would be operated autonomously; therefore, most of the cost goal would be allotted to maintenance. With preventive maintenance principally concerned with mirror cleaning and PCU check-up, and with corrective maintenance consisting of replacing the failed lowest replaceable units within the subsystems, a staffing goal for a 10-MWe dish/Stirling electric power system would be two trained but unskilled maintenance persons available on a one-shift-per-day basis, 5 days per week. During the remainder of the time, a maintenance person would be "on call."

Self-diagnostics with the capability of interfacing with maintenance persons or a remote operator would be an integral part of the design. The system would include capability for detection of failures and faults. After identification of a failure, the system would isolate the defective module and automatically configure its function around the problem. The isolated faulty module could then be serviced without disrupting the ongoing operation. Intermittent faults would be reported for maintenance testing and correction.

D. SYSTEM PERFORMANCE REQUIREMENTS

In order for alternative electricity generating plants to compete with conventional electricity generating plants in the years 1990 to 2000, the cost (on a levelized basis) of electricity generated by the alternative plants would have to be less than conventional generation. Economic analyses pointed to a requirement of producing electricity in 1990-2000 at or less than a levelized busbar cost of 80 to 96 mills/kWe-h. The levelized busbar electricity cost requirement was clearly beyond the current capability of solar thermal electric power systems. The life-cycle cost requirement of the dish/Stirling electric power system could be achieved by attaining a dish aperture solar power to generator electric power conversion efficiency of 35% by 1990 while at the same time achieving the up-front capital cost of $960 to 1600/kWe for a 10-MWe plant. Reliability of the system components would have to be attained to achieve a preventative plus corrective maintenance life-cycle cost competitive with conventional power systems.

SECTION VII

DEVELOPMENT OF A PROJECTED YEAR 1985 DISH/STIRLING ELECTRIC POWER SYSTEM

A. APPROACH

During FY 1978, DOE identified the dish/Stirling electric power system as the most promising candidate for distributed systems applications. An advanced system development task would conduct design, construction, and testing of the components for the advanced system. Successful completion of the testing of components would set the stage for a decision to test the components as a prototype subsystem integration experiment. The purpose of the proposed subsystem integration experiment was to verify the performance of the components when operated in the context of a system. Completion of the subsystem integration experiment would establish the technical and cost feasibility of the system and establish its readiness for subsequent application. Solar concentrator units, power conversion units, energy storage and transport units, and electric power subsystems would be developed. Throughout the course of the development, progress was reported at various forums including semiannual and annual nationwide DOE solar thermal technology reviews. The reviews were not only programmatic, but were intended to disseminate information about key technical innovations of value or interest to technological corporations engaged in research and development of solar thermal electricity generating plants.

Task members at the Jet Propulsion Laboratory and the Lewis Research Center (LeRC) defined the advanced dish/Stirling electric power system, specified the major system requirements, and directed system test and operations. Industry was utilized in the performance of technical work to the maximum extent feasible consistent with JPL and LeRC roles. Some implementation tasks were performed by JPL and LeRC task members in order to maintain technical proficiency.

First, JPL conceptually designed a small (less than 10 MWe) dish/Stirling electric power system using projected 1985 technology that, in mass production, could achieve the capital cost target of about $960 to 1600/kWe. Operation and maintenance costs would be sufficiently low so that the cost of electricity from the system would be about 80 to 96 mills/kWe-h. An engineering prototype model of a 15-kWe module of the dish/Stirling power subsystem was conceptually designed and presented at the November 15-17, 1978, semiannual review held at Golden, Colorado (Reference 5).

B. SYSTEM CONCEPT

The system concept was defined only to the extent necessary to assure adequate technology direction at the subsystem and assembly level. Versatility and scalability of the technology were emphasized. One module of the advanced dish/Stirling power subsystem is shown in Figure 7-1. The advanced dish/Stirling subsystem module consists of a solar concentrator unit and a power conversion unit. Projected efficiencies and power outputs of the various dish/Stirling subsystem assemblies are shown in Table 7-1.

Table 7-1. Dish/Stirling Electric Power System Component Efficiency and Power Level Projections

Component	Efficiency, %	Power Output	
		Peak	Average[a]
10-m Concentrator (clean) (Geometric concentration ratio = 2000)	83	64.0 kWt	55 kWt
Receiver (including TES)	85	55.0 kWt	47 kWt
Stirling Engine (kinematic)	35[b]	19.0 kWs	16 kWs
Alternator	90	17.5 kWe	15 kWe

[a]Specified cloud-free insolation is 0.845 kW/m^2.

[b]An engine efficiency of 42% was to be demonstrated by 1985.

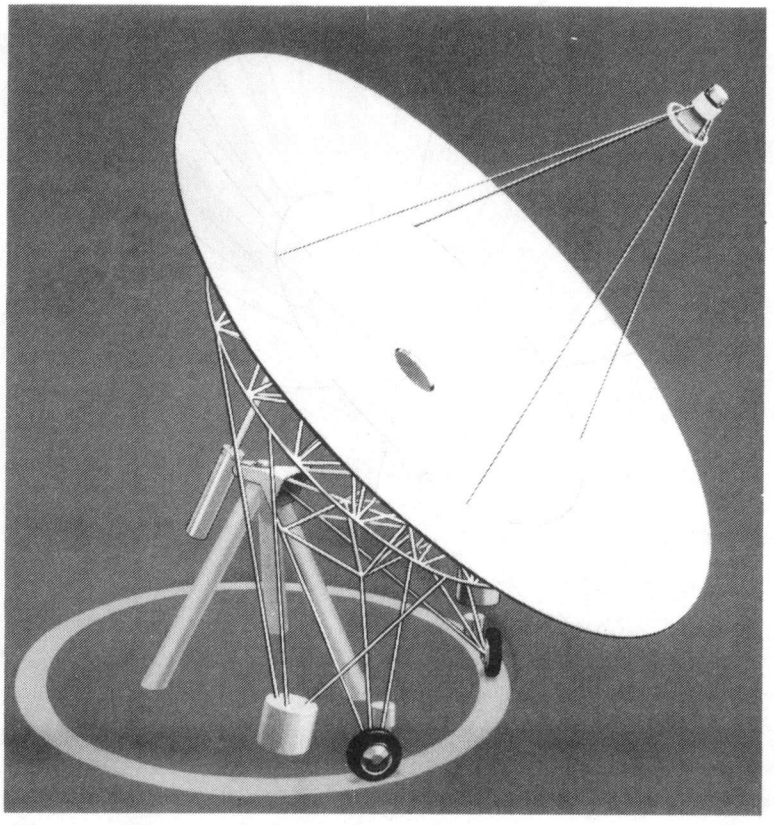

Figure 7-1. Dish/Stirling System Concept

1. Advanced Solar Concentrator Unit (Parabolic Dish Concentrator No. 2)

The advanced solar concentrator unit concept selected was the deep-dish configuration, as shown in Figure 7-2. This advanced concentrator conceptual design consists of mirrored glass gores installed in a cantilever configuration on a truss-type support ring of triangular cross section to form a complete but physically discontinuous reflective surface. Two groups of independent, optical-quality reflective gores form a paraboloidal concentrator surface with an aperture diameter of about 10 m. The focal length to aperture diameter ratio (f/D) is 0.6. Each reflective gore was to be fabricated of thin, back-silvered glass mirror bonded continuously over a contoured substrate of cellular glass. An all-truss structure would serve as an intermediate structure between the concentrator surface assembly and the pedestal, which would provide the azimuth and elevation movements of the concentrator. Analysis of tracking sensors, drive elements, control, and structural deformation was performed during the design phase.

A prototype advanced concentrator of the deep-dish paraboloidal configuration would be procured and installed in a system technology demonstration. The technology demonstration would provide empirical concentrator performance data and integration of the concentrator unit with

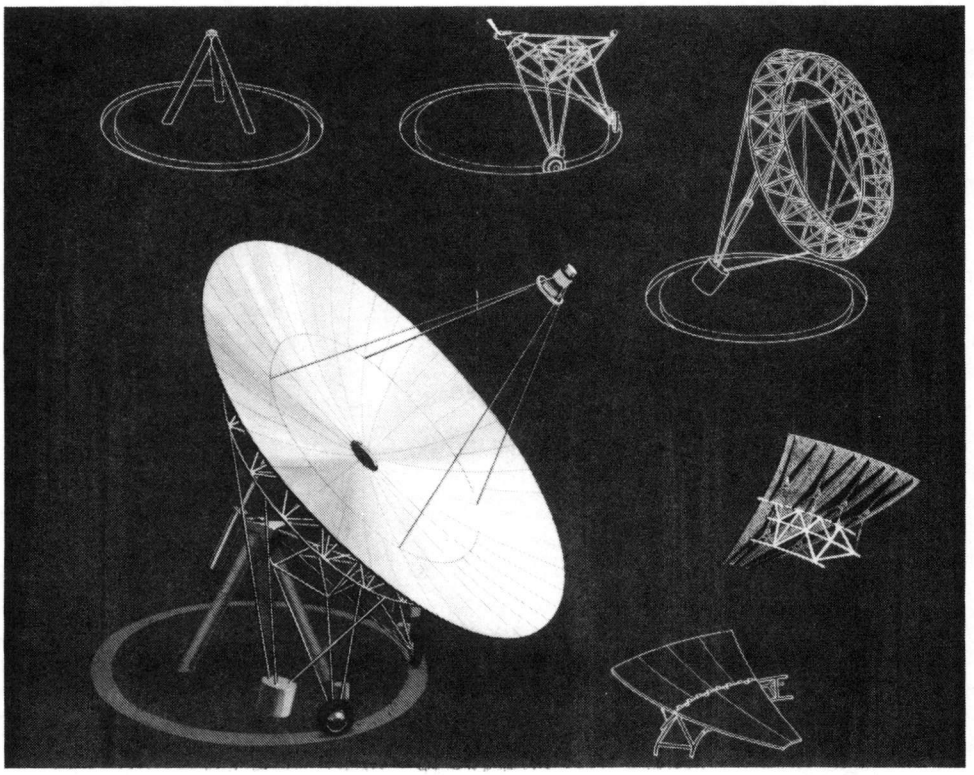

Figure 7-2. Deep-Dish Point-Focusing Concentrator

the receiver assembly and power conversion unit that would be developed in parallel. Selection criteria for making this choice were as follows:

(1) Representative of mid-range technology for dispersed solar thermal systems.

(2) Compatible with a selected Stirling engine-generator.

(3) Within the limits of existing fabrication capability.

(4) Consistent with project funding constraints.

a. Preliminary Design of an Advanced Solar Concentrator Unit. The overall objective of this task, contracted to Acurex Corporation, was to develop a minimum cost per kilowatt solar concentrator design within the constraints of 1985 mass-production technology. As the thermal output of the concentrator had been specified, this goal could be expressed in terms of $\$/m^2$ of aperture area. An installed cost[3] of \$112 to $161/m^2$ was the target (Reference 6).

The key element of the second-generation (advanced) concentrator design is the lightweight, self-supporting reflective panel made possible by the use of cellular glass as a reflective mirror substrate material (References 6, 7, and 8). The effect of the low weight of the panels cascades down through the other concentrator subsystems: A lightweight, self-supporting panel allows the design of a lightweight supporting structure, which in turn yields low drive and foundation loads and low installation labor, all leading to a low-cost concentrator design. Cellular glass is a desirable reflector substrate material because of its high stiffness-to-weight ratio, thermal expansion match to mirror glass, and environmental durability. It is a low-cost material, selling for approximately \$0.30 per board-foot in large volume production in the self-supported insulation market.

Design Description. The design of the cellular glass substrate concentrator is shown in Figure 7-3. The concentrator is a 10.9-m-diameter, two-axis tracking parabolic dish solar concentrator. The reflective surface of this design consists of inner and outer groups of mirror glass/cellular glass gores. The gores are attached as simply supported cantilevered beams to a ring truss support structure to form a complete but physically discontinuous reflective surface. There are five structural support assemblies: the gore support, a quadripod receiver support, a counterweight support, a tripod center pedestal, and a tilted pyramid drive structure. Elevation motion is produced by a ball screw, and azimuth motion by a chain and sprocket perimeter drive. The foundation consists of concrete piers for the center pedestal and a raised steel track also on concrete piers.

The reflective panel or gore design is a sandwiched mirror glass/cellular glass/unsilvered glass configuration. The mirror glass is back-silvered 0.1-cm (0.040-in.)-thick Corning 7809 aluminoborosilicate fusion glass. The cellular glass is 192 kg/m^3 (12 lb/ft^3) Pitt-Corning Foamsil 75 and is specifically tailored to match the coefficient of thermal expansion of

[3]The installed cost quoted in Reference 6 is \$70 to $100/m^2$ in 1978 dollars.

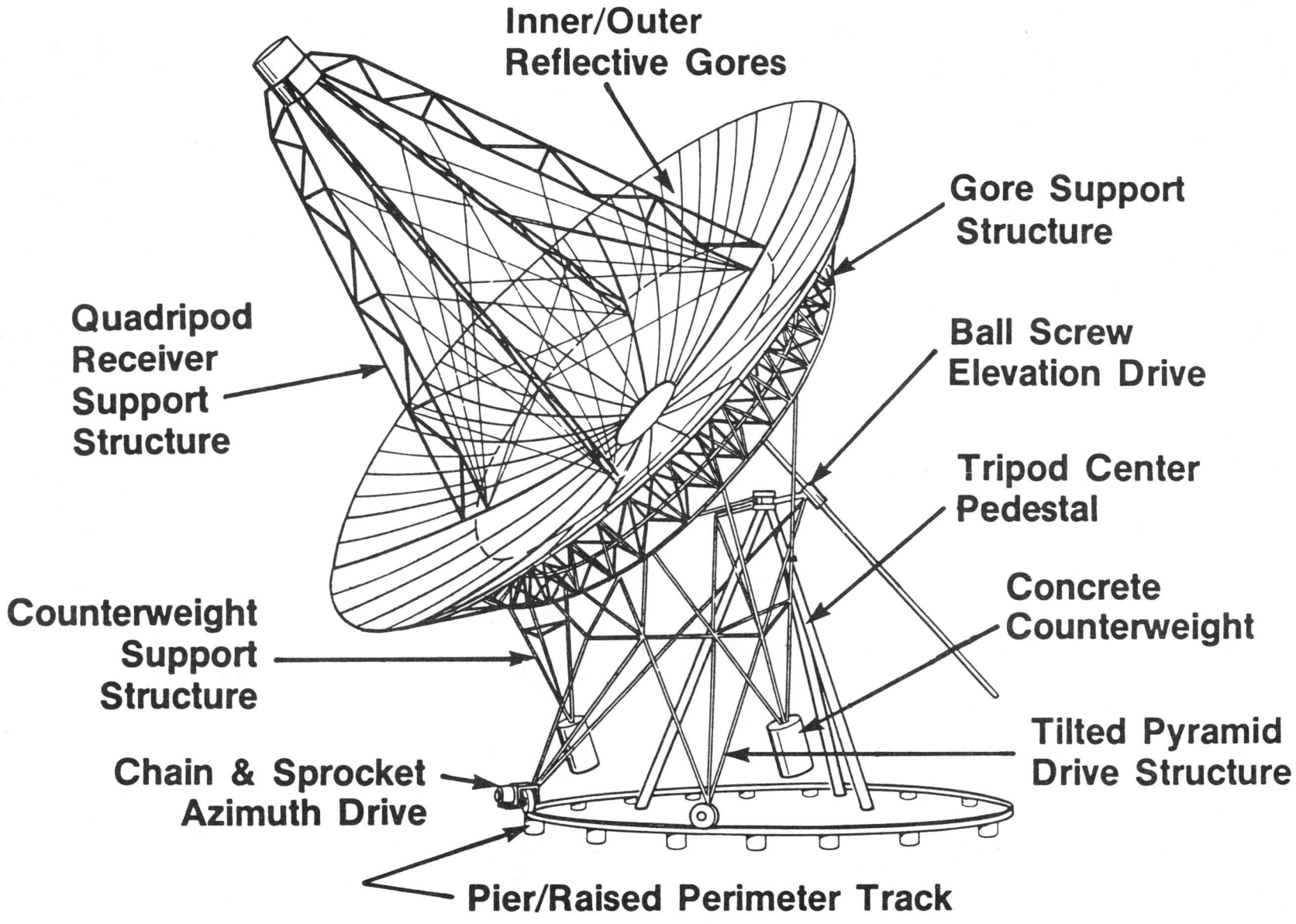

Figure 7-3. Concentrator Design Description

the 7809 mirror glass. The backsheet is an unsilvered piece of 0.1-cm (0.040-in.)-thick Corning 7809 glass. The sandwich configuration was selected because it produces the minimum weight gore. The concentrator design consists of 40 outer gores and 24 inner gores. The maximum gore width is limited by the allowable membrane stress for a single panel per gore. Gore weights, less the attachments, are 22.2 and 14.5 kg (49 and 32 lb) for the outer and inner rings, respectively.

The support structure design features welded steel shop subassembly construction using standard size, commercially available, structural steel members. Finite element analysis techniques were used to optimize the support structure for minimum weight. The concentrator design has a total structural steel weight of 1966 kg (4335 lb) and a concrete counterweight of 4536 kg (10,000 lb).

The drive design features positive traction, rugged, state-of-the-art components. Approximately 100 different combinations of drive power, actuation mechanism, and drive and foundation structure alternatives were evaluated. Life-cycle costs were developed for each of the alternative concepts. Chain/sprocket and cable/drum azimuth drives were found to provide essentially equivalent minimum life-cycle costs. The chain sprocket design was selected over a cable/drum design because of its greater stiffness. A ball screw was selected as the minimum life-cycle cost elevation drive design. Due to the requirement for fail-safe stowing capability, electric motors and a fossil-fueled generator were selected for drive motors and emergency power, respectively, under the assumption that a single generator set would provide power to at least four concentrators in a multi-unit field.

The foundation design features simple installation and adaptability to sloping or rough terrain. The foundation consists of a tubular steel tripod pedestal, which supports the azimuth bearing, and a raised steel track upon which the drive structure rides. Both the pedestal and track are anchored to simple drilled and poured concrete piers. The pedestal angle and number of piers were optimized for minimum cost.

The electrical subsystem consists of off-the-shelf components providing for power distribution and lightning and grounding protection. The instrumentation and control subsystem consists of the tracker control and shaft encoders. A hybrid, two-axis image tracking system is recommended. Coarse synthetic tracking will be achieved through a microcomputer-based control system. Accurate active tracking will be achieved by a two-axis photodetector located at the focal plane that senses the position of the reflected image. Image sensing not only provides inherent gravity compensation but also compensates for steady-state wind deflections.

Key Results. The key results of the project, through the preliminary design phase, were as follows:

(1) The optimized concentrator diameter was determined to be 10.9 m. The concentrator aperture diameter and structural stiffness were optimized given the performance requirement of delivering 56 kWt to a 22-cm (8.7-in.)-diameter receiver aperture with a direct normal insolation of 845 W/m^2 and an operating wind of 50 km/h (31 mi/h).

(2) A minimum weight preliminary design was developed. Extensive design/analysis efforts produced a minimum weight concentrator design. The use of cellular glass as a reflective panel substrate material potentially offers significant weight advantages compared to alternate substrate materials.

(3) The final cost estimate was $\$198/m^2$. Installed cost estimates made from vendor contacts and rule-of-thumb cost per pound guidelines indicated that a cellular glass substrate concentrator would not meet the JPL cost target on a dollar per unit aperture area basis.

b. Modified Design of an Advanced Solar Concentrator Unit (Parabolic Dish Concentrator No. 2). Acurex, under contract to JPL, performed the preliminary design of the advanced solar concentrator, and carried the design of the outer reflective gore through the detailed level. A preliminary cost assessment confirmed the cost-effectiveness of reducing the structural framework required for the reflective dish, but also identified a problem with regard to the balance of the concentrator design. The installation costs associated with site preparation, foundation installation, and field erection of the wide-base/perimeter drive configuration accounted for a major portion of the total installed concentrator cost.

A concept-level trade-off study resulted in a more cost-effective design that retained the advantages of the cellular glass panels, but eliminated the costly wide base configuration. This concentrator was named Parabolic Dish Concentrator No. 2. Its installed cost was estimated to be $\$161/m^2$, slightly more than the cost target.

The resulting Acurex/JPL advanced concentrator is shown in Figure 7-4. It consists of 64 lightweight cellular glass substrate gores (40 outer and 24 inner gores), simply supported from a tubular steel ring truss that is hinged in elevation from an intermediate space-frame structure. The intermediate structure is mounted to a motor-driven turret azimuth drive that sits atop a single pedestal. The reflective dish is driven in elevation by an electric ball screw actuator that couples the gore support ring structure to the intermediate structure. A guyed truss-legged quadripod receiver support structure provides a rigid support for the power conversion package while providing a minimal amount of shading or blocking of the incident and reflected insolation.

The turret drive/pedestal mount configuration requires a more massive and more costly drive unit than the original wide-base/perimeter drive configuration. The significant reduction in site assembly and foundation installation costs more than offset this penalty, however. It is estimated that the installed cost of the single pedestal configuration would be 10 to 20% less than the wide-base design.

c. Reflective Panel Design. The key element of the advanced solar concentrator is clearly the cellular glass substrate reflective gore. As shown in Figure 7-5, each gore is fabricated from a composite of 1.0-mm Corning Glass Works 7809 borosilicate glass and a Pittsburgh Corning Foamsil 75 cellular glass core. The Foamsil 75 has been specially formulated to match the thermal expansion characteristics of the 7809 sheet glass. A

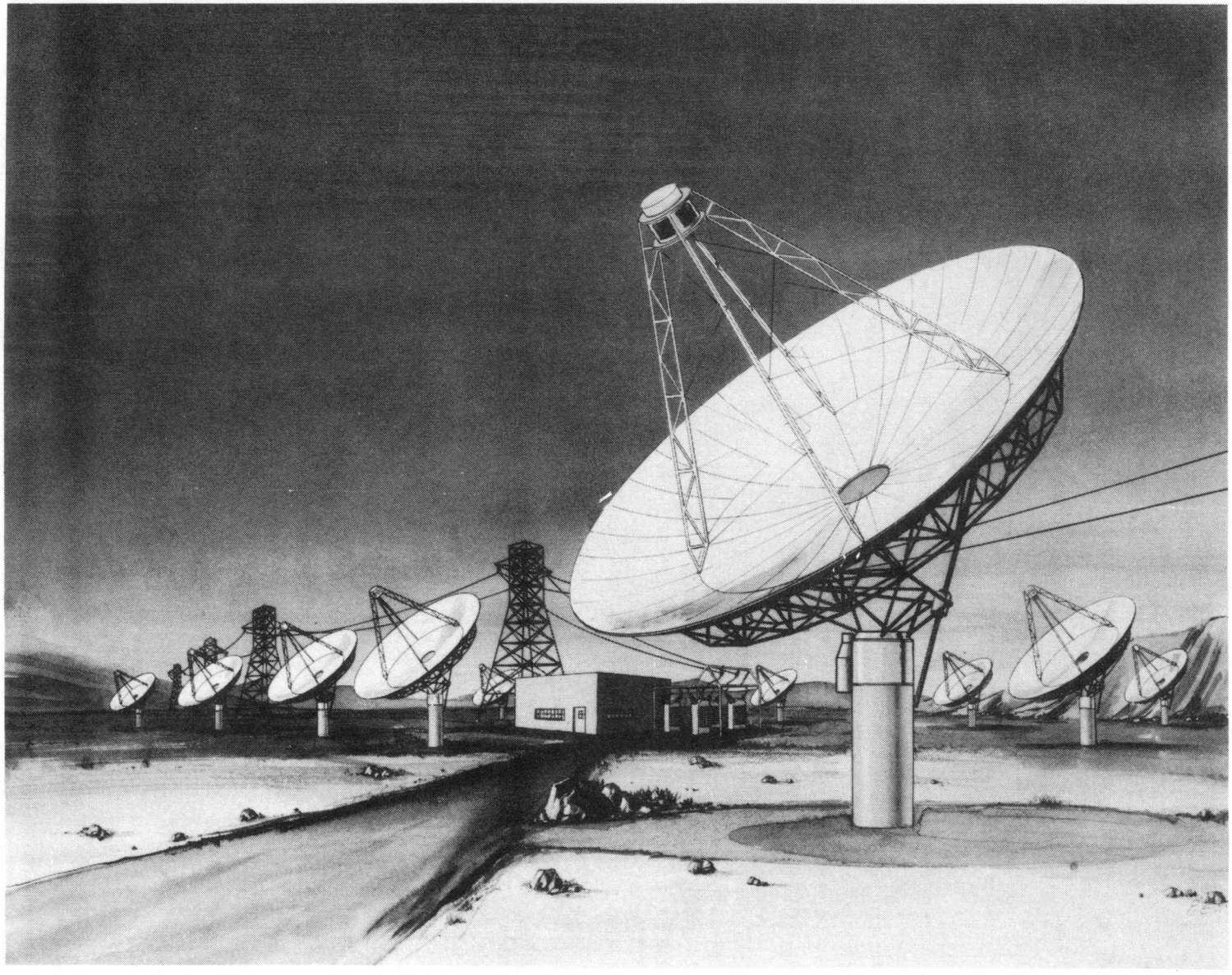

Figure 7-4. Advanced Concentrator (Parabolic Dish Concentrator No. 2)

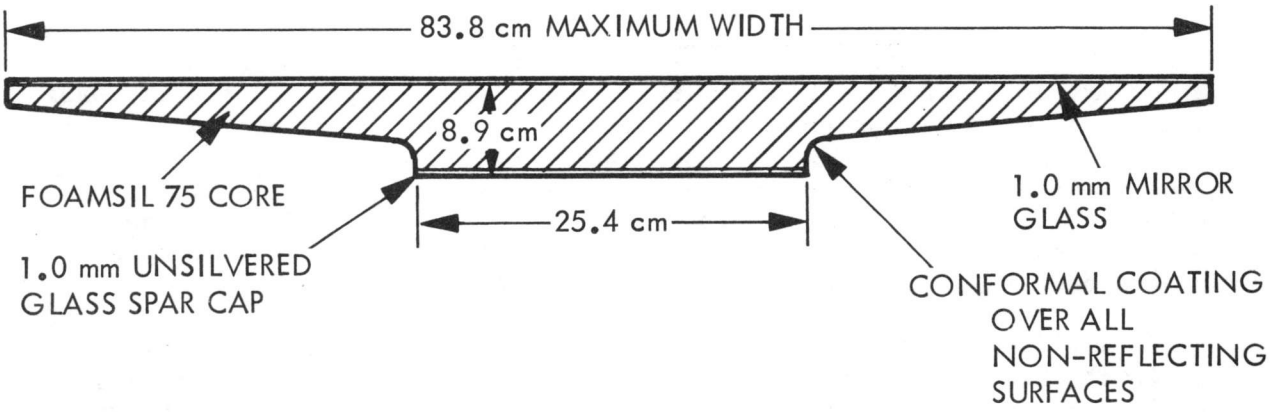

Figure 7-5. Outer Gore Cross Section

single sheet of back-silvered thin glass is continuously bonded to a contoured substrate of the cellular glass material. A narrow strip of unsilvered thin glass is bonded to the outer face of the cellular glass spar running longitudinally along the backside of the gore. The face sheets and the cellular glass core form a composite structure in which the mirror glass and the spar cap carry a significant portion of the aerodynamic and gravitationally induced bending loads. Three compression-molded glass reinforced polyester (GRP) pads are bonded to the gore to serve as attachment points for the interface with the support structure.

Two panel types form the paraboloidal surface. Forty outer gores and 24 inner gores are required. The masses of the outer and inner gores (less attachments) are 23.2 and 15.8 kg, respectively. The width of each gore type is limited by the maximum steady-state curvature stress that the sheet glass can withstand. A maximum panel width of 84 cm for the outer and inner gores limits the steady-state stresses to 14.9 MPa.

A detailed design was developed for the outer gore type only. The resulting gore is stress limited with a 5% probability of failure in the cellular glass core under a governing load condition of a 1-min cumulative exposure to a 110 km/h wind at the worst-case orientation. The peak tensile core stress is 275 kPa under this condition with a corresponding mirror glass stress of 20.1 MPa. Under worst-case operating conditions, the outer gore panel yields a peak deflection slope error of less than 0.3 mrad and an area weighted rms (root mean square) deflection slope error of less than 0.2 mrad. Due to current manufacturing limitations, the maximum block size for the Foamsil material is 46 by 61 by 10 cm. Near-term production, therefore, requires the bonding of several blocks of cellular glass into a large core blank prior to machining. Future developments in cellular glass production may lead to full-size monolithic core blanks or even foamed-to-shape cores.

d. Prototype Panel Fabrication. To verify the fabricability and integrity of the gore design, Acurex fabricated several full-scale prototype gores. These gores were tested by JPL to determine the structural and optical characteristics of the design.

Prototype Design Modifications. Several prototype-specific design modifications were incorporated to reduce cost. Due to limited availability of the 1.0-mm Corning 7809 sheet glass and the Pittsburgh Corning Foamsil 75, the prototype gores were fabricated from 1.5-mm Corning 0317 glass and Pittsburgh Corning's standard Foamglas material. While these materials are not ideally thermally matched and the thicker sheet glass provides a shorter panel life, much insight into the gore design has still been gained. Steel weldments were substituted for the compression-molded GRP attachment pads at a penalty of approximately 2.3 kg per gore.

In addition to these prototype material changes, two significant dimensional changes were also incorporated. To simplify the core machining operation, the rear-side contour was modified from a constant edge thickness configuration to a constant contour angle design, and the spar depth was increased to avoid a local bond joint problem. This change added approximately 10% to the core mass, but allowed the use of a simplified contouring scheme. The front-side contour was also modified to simplify the prototype machining operation. In lieu of the more perfect paraboloidal contour, a compromise of a parabolic contour in the radial direction and constant radius of curvature in the circumferential direction was selected. The effective area-weighted slope error impact of this modification is approximately 0.3 mrad rms.

Fabrication Approach. To minimize prototype fabrication cost, Acurex developed a simple contouring scheme that allows accurate, repeatable substrate fabrication with a minimal investment in tooling. The prototype gore fabrication procedure is essentially a ten-step operation:

(1) Cut cellular glass blocks.

(2) Bond blocks to form core blank.

(3) Cut core blank to planform.

(4) Machine core rear side.

(5) Bond sheet glass spar cap.

(6) Machine core front side.

(7) Bond mirror glass.

(8) Bond attachment pads.

(9) Apply conformal coating.

(10) Package and ship.

Because the optical accuracy of the gore is directly dependent upon the accuracy of the substrate contour, the core contouring apparatus was a key element of the prototype fabrication effort. As shown in Figure 7-6, the cellular glass contouring apparatus consists of a pair of reversible precision parabolic rails that support a hand-drawn cutter carriage. The carriage is designed to accept several interchangeable contoured scraper blades. Two blade configurations are required to generate the rear-side countour, while only one constant-radius blade configuration is required for the front-side contour.

Results. The optical quality of the six prototype gores appeared to be excellent. Visual inspection indicated a slight "print-through" of the bond lines where the cellular glass blocks were joined, but the total distorted area is very small. Simple hand-held imaging tests with the sun as the light source provide a clearly defined image on the order of 10 cm at a focal distance of approximately 6.6 m. This corresponds to roughly a 60% increase over the sun's theoretical image as would be expected for a 1 mrad rms slope error mirror.

The Acurex advanced solar concentrator gores were optically characterized within the JPL 25-ft Space Simulator (Reference 9). The availability of the JPL 25-ft Space Simulator, with its 5.8-m (19-ft) simulated solar light beam, provides an excellent facility for measuring the optical characteristics of parabolic solar concentrator panels and gores. To ensure the accuracy of the measurements and data interpretation, it is important to characterize the simulated solar beam. All measurements were made using one of the illuminating lamps and the center lens uncovered. The three important parameters of the illumination source are the distance from

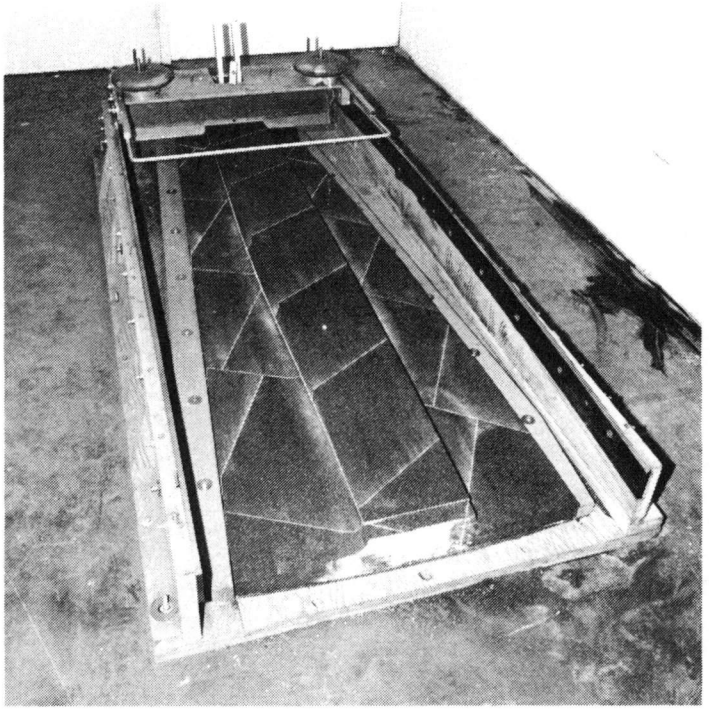

Figure 7-6. Cellular Glass Contouring Apparatus

the chamber floor, the location of the source over the chamber floor, and the angular size of the source. The source is, in fact, a virtual source because of the compound optical system. The calibration measurements made indicate that the virtual illumination source for the 25-ft Space Simulator is located at a distance of 404 m (1320 ft) above the chamber floor at a point approximately 75 cm (30 in.) east and 30 cm (12 in.) north of the chamber's center. To compensate for this, the measurement plane must be located 14.15 cm (5.6 in.) higher than the nominal focal plane, and the gore under test must be positioned as described in this report.

A virtual source angular size is 0.8 $\pm$ 0.2 mrad as seen from the chamber floor. For a perfect parabolic reflecting surface of the assumed dimensions, the source image will have a diameter less than 2.6 cm (1.03 in.) and the corresponding solar image diameter would be 10.2 cm (4 in.). It appears that the source image is sufficiently smaller than the solar image so that the predicted concentrator image size can be derived from the size of the image as measured in the simulator, and the solar image (i.e., the simulator image) can, in practice, be assumed to be a point.

Results of subsequent optical testing of the Acurex gore in the 25-ft Space Simulator are shown in Figure 7-7 for the point source. Results indicate 100% of the reflected light from a point source would be intercepted within a 12.7-cm (5-in.)-diameter solar receiver on an advanced solar concentrator. The optical performance has been projected for sunlight intercepted in Figure 7-8 where calculations (with the indicated assumptions) would predict 100% of sunlight intercepted within a 15-cm (6-in.)-diameter solar receiver.

Structural test of the Acurex reflective panel #A6 under simulated wind loadings, corresponding to the most severe aerodynamic pressure distribution with an equivalent wind velocity of 102 km/h (61 mi/h), was successfully applied to the gore for 744 hours before termination of the test. The test requirement for a 30-year operational life of the gore, as delineated in the Acurex final report (Reference 8) was specified for 8.2 hours under a pressure loading of 80 km/h.

Reflective panel #A1 survived in the environmental test chamber for 190 cycles of freeze-thaw in a high humidity test environment.

With adequate effort expended on its development, the cellular glass substrate reflective panel appears certain to have a significant impact on the future of point-focusing solar technology.

2. Advanced Power Conversion Unit

a. Stirling Solar Engine Development Plan. A Stirling solar engine development plan was formulated by LeRC in FY 1978 to support the dish/Stirling power subsystem conceptual design activity (Reference 10). LeRC was chosen for the activity because of their involvement with the automotive Stirling engine development program and other Stirling engine development programs.

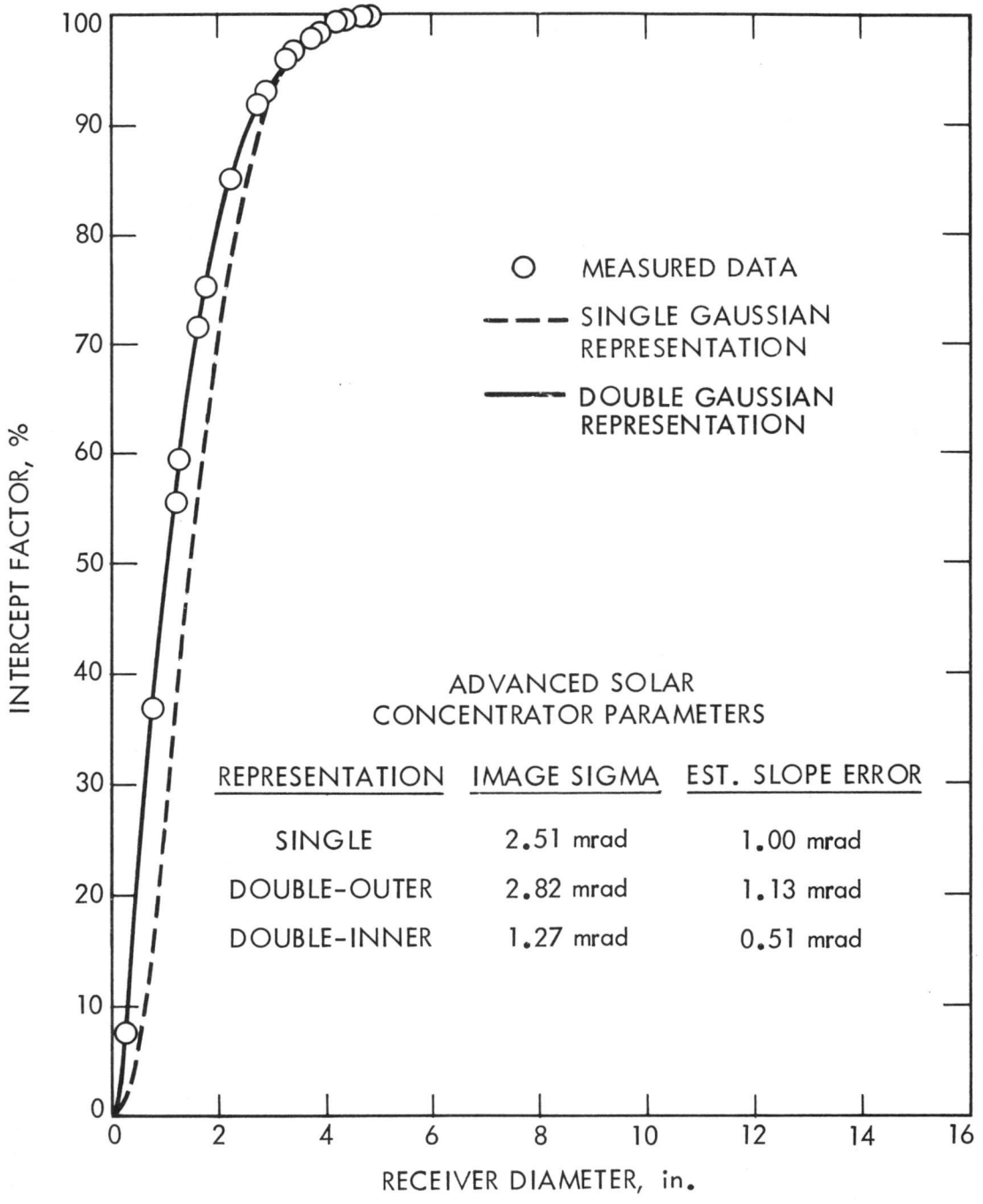

Figure 7-7. 25-ft Space Simulator Data

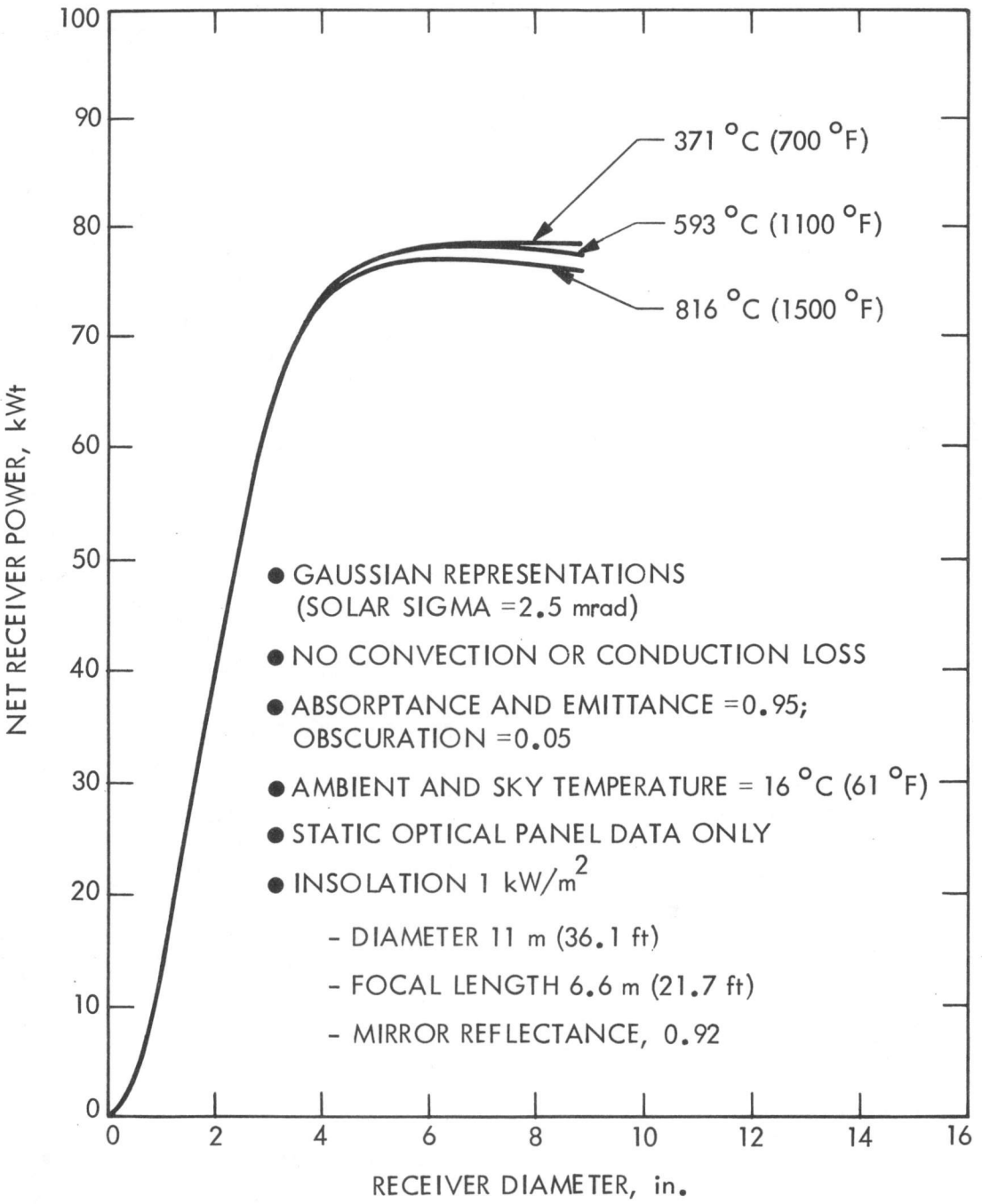

Figure 7-8. Projected Concentrator Performance

The approach taken by LeRC was based on significant utilization of ongoing technology efforts in combination with parallel activities and focused on identifying appropriate solar applications and available engine combinations. The program plan was to proceed from an advanced high efficiency engine concept to be generated through parametric and configuration studies to a 15-kWe test-bed engine for full-scale system testing. The options among existing Stirling engines in the appropriate power range were to be reviewed and compared with the requirements for the test-bed engine to achieve the most technologically advanced and cost-effective test-bed engine. A list of candidates included an 18-kW general purpose test engine then in preliminary design, the United Stirling AB (USAB) Model P-40 engine, the Stirling Power Systems 8-15 kW engine, and a free-piston engine from a GE-AGA-DOE heat pump rated at 3 kW. A flow chart indicating the elements of the LeRC approach and their sequence is shown in Figure 7-9.

As part of the evaluation of on-going programs, the development plan also included a detailed technical status assessment of all Stirling engine research in both government and private industry.

A key goal of the Stirling engine development activity was identified as the design of solar-specific engines with approximately 40% efficiency in both an advanced technology version (1985 and beyond) and a near-term test-bed version. The development of the solar Stirling engine would benefit from Stirling engine development in other areas -- most notably, the automotive area.

Both kinematic and free-piston Stirling engines were candidates for solar energy conversion systems. The kinematic Stirling engine transmits power through connecting rods or other linkages to a rotating alternator. In the free-piston engine, the power piston connects directly to a linear alternator. But the heat input components would be almost identical for both types of engines. The kinematic Stirling engine has a much longer and more extensive development history than the free-piston engine, whose conception is of recent origin. After thousands of hours of engine operation in laboratories in the U.S., Holland, and Sweden, the kinematic Stirling has well defined problem areas: shaft seal life is limited; improvements in heat transfer and fluid flow are required for the achievement of the engine's efficiency potential; and more cost-effective materials and production methods must be identified.

The free-piston Stirling presents a difficult design problem because of the oscillation of two separate masses actuated by interdependent spring systems. However, because there are no mechanical losses between the piston and the alternator, a 20% gain in efficiency over the kinematic Stirling might be achievable. No shaft seals are required because the alternator is housed within the engine. The free-piston Stirling represents a high development risk. Also, linear alternators were only in the early stages of development, and potential problems were not fully known.

b. Stirling Engine Conceptual Designs. The solar Stirling engine development plan allowed for advanced systems and a new concept demonstration. The advanced engine systems would lead to a totally new

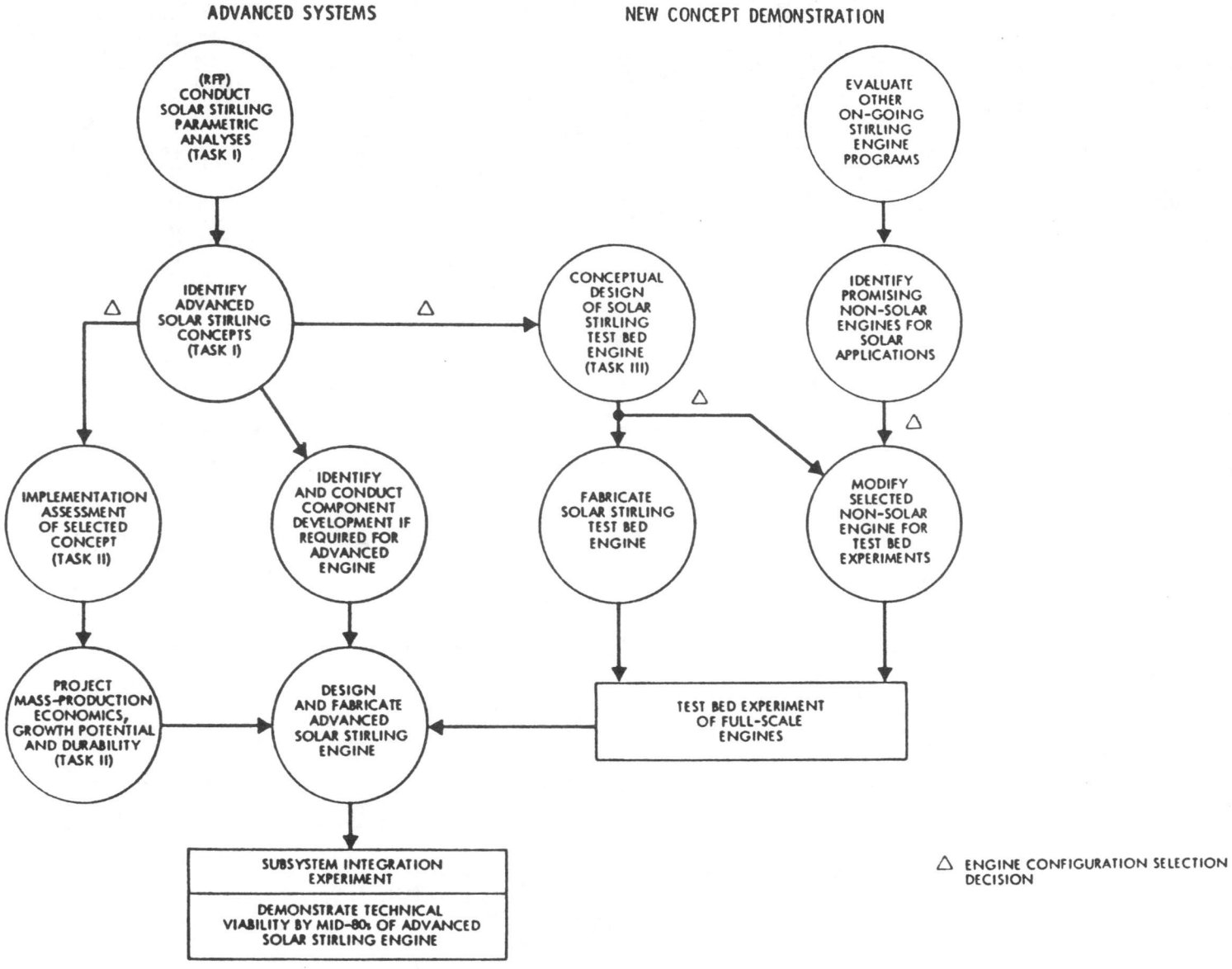

Figure 7-9. Flow Chart for Solar Stirling Engine Development

Stirling engine for solar application whereas the new concept demonstration would rely on modifying a selected non-solar engine for test-bed experiments. In any case, the goal would be the same, i.e., to demonstrate technical viability by the mid-80s of an advanced solar Stirling engine. The plan conceived in FY 1978 was followed and resulted in the demonstration of the highest conversion efficiency of sunlight to electricity by the USAB Model 4-95 Solar Mk II engine at Rancho Mirage, California, in FY 1984.

Design Studies of Free-Piston and Kinematic Stirling Engines for Distributed Receivers. The development plan called for identical six-to-seven-month conceptual programs for both the free-piston and the kinematic Stirling engines. Each program was divided into three main tasks: (1) the generation of several advanced technology engine concepts, (2) a fabrication and economic assessment of one of those concepts, and (3) the conceptual design of a test-bed engine. Under a fourth task, to be active throughout the program, the engine system interface was to be addressed. More detailed task descriptions are given below (References 11 and 12).

Advanced Configuration Definition and Parametric Analysis: Under the first task, advanced engine concepts were to be generated. The meaning of "advanced" is that the concepts would include technology not ready for incorporation into an engine prototype at that time, but which could reasonably be expected to become mature by mid-1980. Heat input concepts for remote as well as closely coupled engine-receiver systems were considered. After an initial screening exercise, a parametric performance analysis would be carried out for three of the most attractive configurations, looking at a heat and coolant temperature range and part-load operation. The basis for the analysis was the energy input derived from daily profiles of the insolation study (by West Associates) of Lancaster, California. A single most promising engine configuration and heat input concept would emerge from this task effort.

Implementation Assessment: Under this task, an assessment of the selected advanced engine concepts was to be made with respect to the technology status of critical components, producibility and cost in various quantities up to 500,000 units per year, durability and failure modes, service requirements, and power growth potential.

Conceptual Design of a Test-Bed Engine: Under this task, the advanced engine configuration concept selected was to be translated into a conceptual design of a near-term (1981) test-bed engine with approximately 40% efficiency. This, of course, meant that advanced technology components would have to be replaced with components that could be installed with confidence in a 1981 Stirling engine. Design layouts and engineering specifications based on the exercise of the appropriate engine optimization codes were to result from this task. Because this design would serve as the basis for the 15-kWe solar Stirling engine to be executed in the follow-on program, the design would include an auxiliary heat pipe input source for engine checkout prior to its mating with the solar receiver/heat pipe.

Engine-System Interface Requirements: The engine and solar receiver designs are significantly interdependent. In close coupled systems, the engine heater tubes may be buried in the receiver. Other areas of interdependence are the insolation profile and the control modes. This task

was specifically set aside for all work that required close liaison and two-way feedback between the engine and the system designs.

At the end of this program phase, a reasonably clear choice would be available with respect to a single configuration Stirling engine development -- either kinematic or free piston.

(1) Design Study of a 15-kWe Free-Piston Stirling Engine/Linear Alternator for Distributed Receivers.

A contract with Mechanical Technology, Inc. (MTI) was initiated by LeRC on August 29, 1978, to study both the free-piston and kinematic Stirling engines. USAB was engaged by MTI to work on the kinematic engine study while Sunpower, Minneapolis-Honeywell, Dynatherm, Masco, and MTI worked on the free-piston engine study.

This later study resulted in a conceptual design of a free-piston solar Stirling engine/linear alternator (Figure 7-10), which could be designed and developed to meet the requirements of a near-term solar test-bed engine with minimum risks. The conceptual design was calculated to have an overall system efficiency of 38% and provide 15-kW electric output. The free-piston engine design incorporated features such as gas bearings, close clearance seals, and gas springs. This design was hermetically sealed to provide long life, reliability, and maintenance-free operation. An implementation assessment study performed as part of this study indicated that the free-piston solar Stirling engine/linear alternator could be manufactured at a reasonable cost (direct labor plus material) of $3450 per engine in production quantities of 25,000 units per year. Opportunities for significant cost reduction were also identified (Reference 13).

(2) Design Study of a Kinematic Stirling Engine for Distributed Receiver Solar Electric Power Systems.

A contract awarded to MTI in FY 1978 included a study of a conceptual design of a nominal 15-kW electric solar Stirling engine. A conceptual design was evaluated and developed by USAB (Reference 14) for a kinematic-type Stirling engine for small, dispersed solar power applications.

The study performed configuration definition studies, including a detailed parametric evaluation of the selected concepts, with a final ranking of all attractive configurations. These included single- and multiple-cylinder engines with rhombic and crankshaft drive, different seal systems, and heat exchanger arrangements. For the conceptual design, a four-cylinder double crankshaft engine with annular regenerators, with the power level increased to 20-kWe output from the alternator, was selected.

The study also addressed the interface between the engine heater head and the solar receiver and collector. Cases for solar radiation directly impinging on the heater tubes and condensing sodium heat transfer via heat pipe transport were considered.

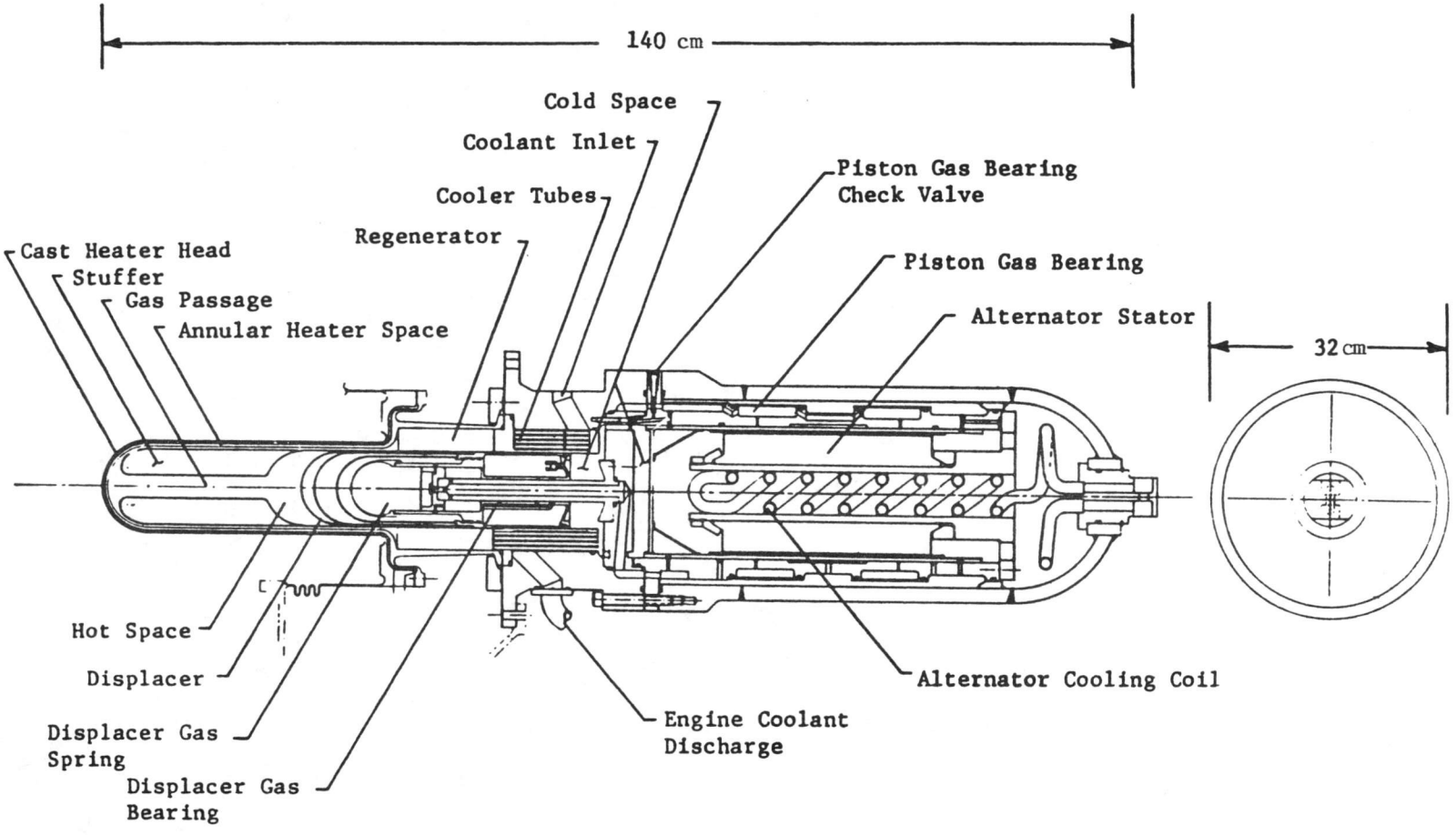

Figure 7-10. 15-kWe Free-Piston Stirling Engine/Alternator Conceptual Design

The USAB report describes the study processes and the results leading the way to the detailed design of an efficient Stirling engine/generator with concentrated solar radiation heat input.

The concept evaluation shows that the four-cylinder, double-acting, U-type Stirling engine with annular regenerators is the most suitable engine type for the 15-kWe solar application with respect to design, performance, and cost. (See Figure 7-11.)

Results show that the near-term performance efficiency for a metallic Stirling engine is 42%. Further improved components would produce an efficiency of 45% for the future metallic engine. Increase of heater temperature through the introduction of ceramic components contributes the greatest amount toward achievement of high efficiency, eventually around 50%.

Conceptual Design and Cost Analysis of Hydraulic Output Unit for a 15-kWe Free-Piston Stirling Engine. The primary objective of this joint study by the University of Washington/Joint Center for Graduate Study and Flow Industries, Inc., was to develop a preliminary design for a long-life hydraulic converter capable of interfacing with the free-piston Stirling engine designed by MTI as described in Item (1) above. The engine/converter system (Figure 7-12) interfaces directly with a heat receiver suspended at the focus of a parabolic dish solar collector. The hydraulic converter produces hydraulic flow at pressures suitable for operating a ground-based commercial hydraulic motor, which in turn drives a commercial rotary alternator to produce 15 kW of electric power output (Reference 15).

Hydraulic fluid at 34.5 MPa (5000 psi) is produced to drive a conventional hydraulic motor and rotary alternator. Efficiency of the low-maintenance converter design was calculated at 93.5% for a counterbalanced version and 97.0% without the counterbalance feature. If the converter were coupled to a Stirling engine with design parameters more typical of high-technology Stirling engines, counterbalanced converter efficiency could be increased to 99.6%. Dynamic computer simulation studies were conducted to evaluate performance and system sensitivities. Production costs of the complete Stirling hydraulic/electric power system were estimated to cost 17% less than an alternative Stirling engine/linear alternator system.

The hydraulic system is concluded to be a very attractive alternative to the linear alternator system, offering some cost advantages and requiring less development of new technology. Maintenance-free lifetime of both systems should be much longer than for any kinematic Stirling engine, and elimination of costly mechanical linkages and dynamic seals also offer other significant advantages.

Advanced Free-Piston Stirling Engine Driven 15-kWe Linear Alternator Study. The advanced free-piston Stirling engine driven 15-kWe linear alternator study award to Energy Research and Generation, Inc. (ERG) was directed toward incorporating ERG's technologies into a solar-energized electric power plant.

The objectives of this phase of the program were to (1) design and analyze critical components and subassemblies, (2) assess and optimize the

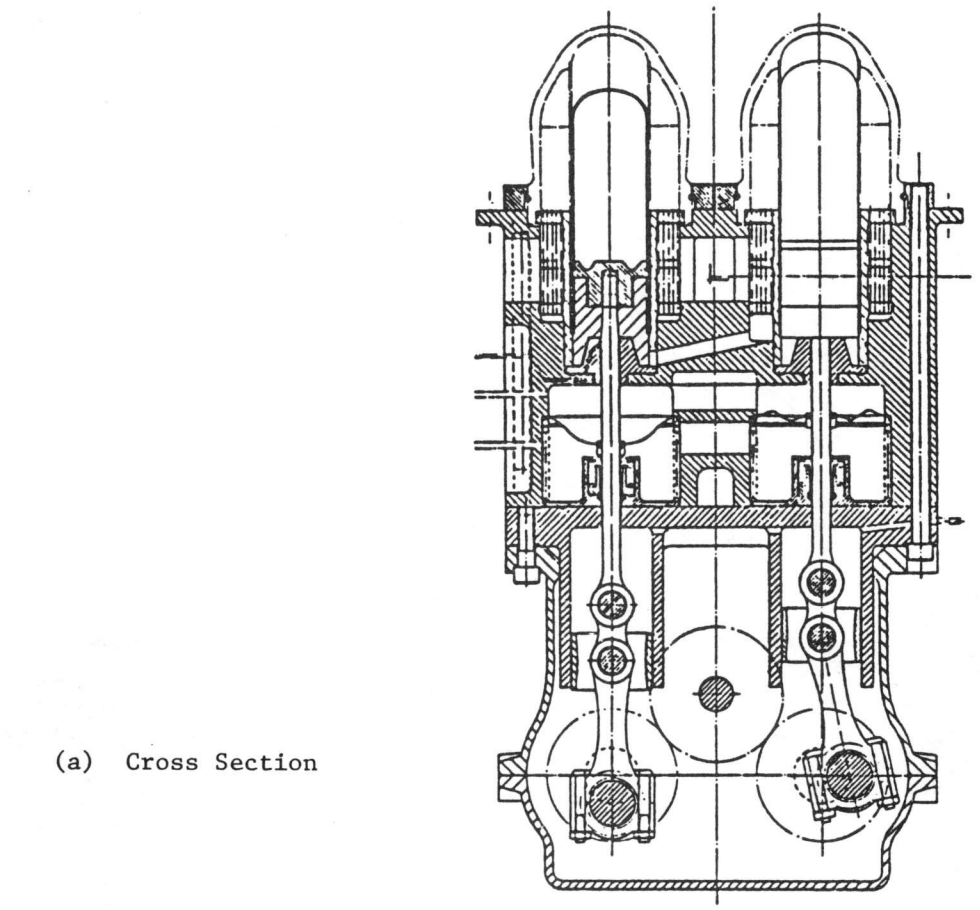

(a) Cross Section

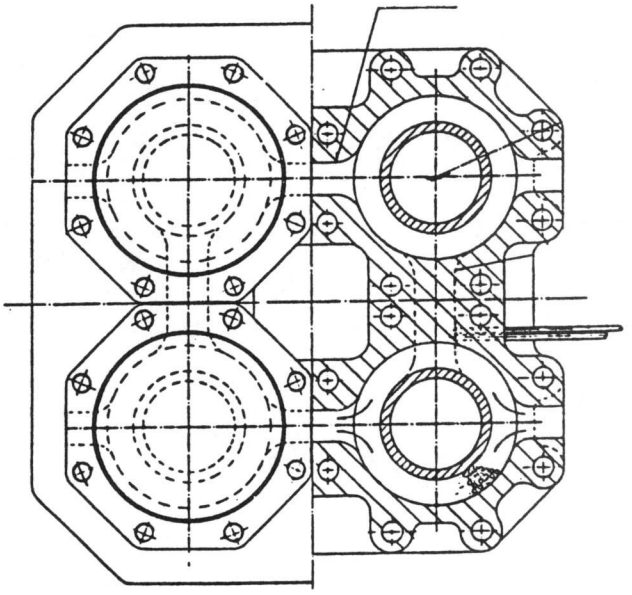

(b) Top View

Figure 7-11. Advanced Kinematic Stirling Engine

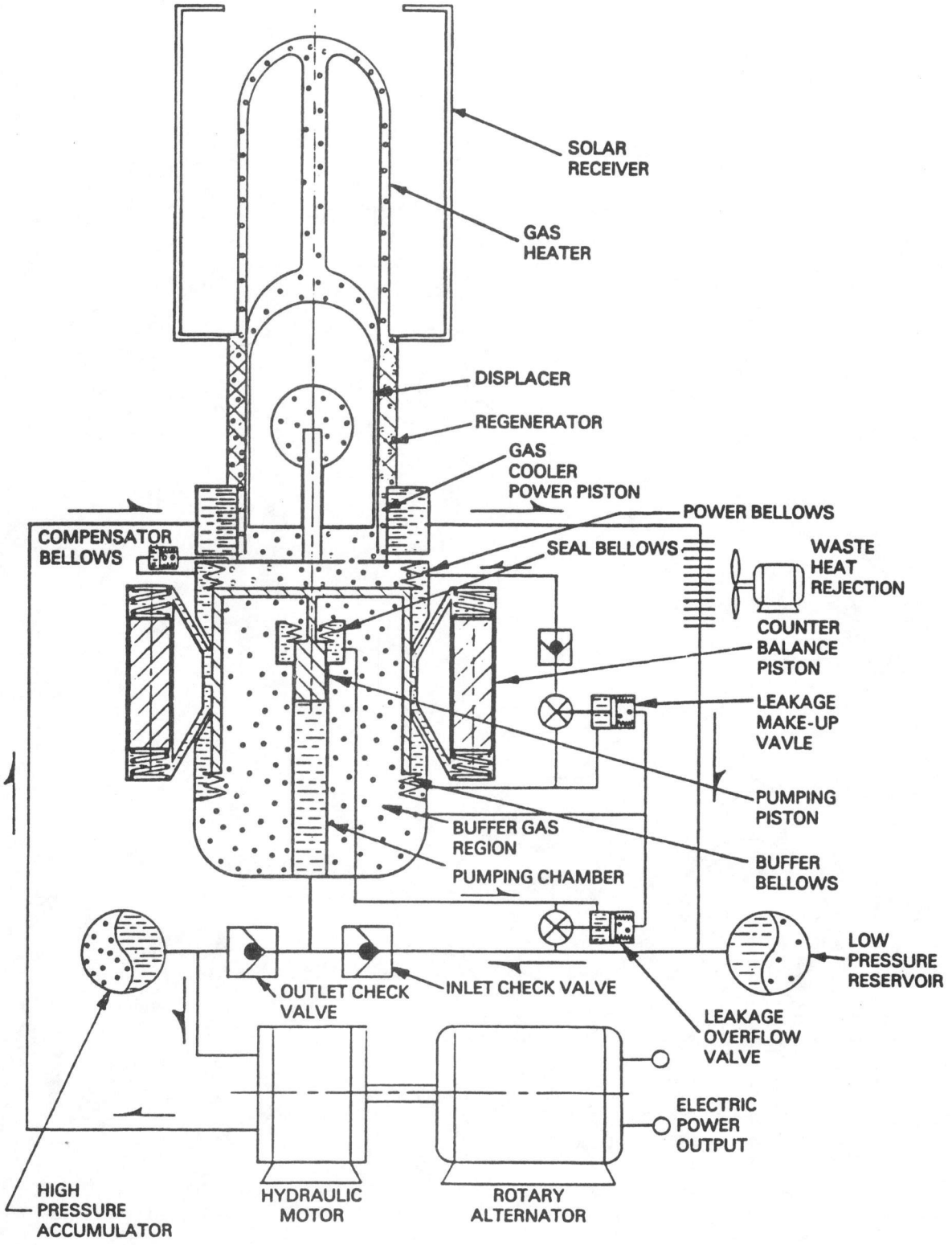

Figure 7-12. Stirling Hydraulic System Schematic

thermodynamic and dynamic performance through computer simulation, and (3) perform a preliminary design of a resonant free-piston Stirling engine (RFPSE) driven 15-kWe linear alternator. Particular emphasis was on heat exchanger matrices, gas bearings, narrow-clearance seals, control and stability, manufacturability, reliability, and production cost of a solar-energized electric power plant employing non-strategic materials. The results obtained in the study indicated the goals of 60% power conversion efficiency, $76/kWe engine/alternator cost, absence of strategic materials, high reliability, and lifetime. Features of the proposed design included a high-efficiency engine over the load range, lightweight, inexpensive engine and alternator, opposed pistons, isothermalized engine and gas spring chambers, foil-fin regenerator, self-pressurized gas bearings, and terminal voltage and frequency load independent. The results of this study were reported by G. M. Benson.[4]

Heat Pipe Solar Receiver with Thermal Energy Storage Power Conversion Unit. A General Electric Company heat pipe solar receiver (HPSR) Stirling engine generator PCU featuring latent heat thermal energy storage (TES), excellent thermal stability, and self-regulating, effective thermal transport has been described in References 16 and 17. The PCU has been supported by component technology testing of heat pipes and of thermal storage and energy transport models that define the expected performance of the PCU. Preliminary and detailed design efforts were completed, and manufacturing of HPSR components had begun. The modification of a Stirling engine for operation on condensing sodium vapor would have been required during 1981 in order for the PCU to be committed to a solar test at an early date. Additional developments would include the design, construction, and test of a flame impingement combustor that could be directly added to the existing PCU without major modifications. Progressive development of this first prototype toward low-cost, mass-production hardware was expected for wide solar application.

PCU Description. The heat pipe solar receiver with TES is a high-efficiency solar receiver and thermal storage assembly for use as part of a self-contained 15-to-25-kWe Stirling engine power conversion unit located at the focal point of a parabolic dish concentrator and operating at an engine temperature of 827°C (1520°F). Its unique feature is the efficient collection, transport, storage, and retrieval of solar energy through the use of high-temperature sodium heat pipes and $NaF-MgF_2$ latent heat storage.

The concept of heat flow in the PCU and a conceptual design of an advanced PCU are shown in Figures 7-13 and 7-14, respectively. The fourteen primary heat pipes in the receiver deliver heat through a bulkhead into a large secondary heat pipe containing (1) 73 capsules, each 2 in. in diameter and 33 in. in length and containing the eutectic fluoride TES salt, (2) a shell-side heat exchanger surface to accept heat from an efficient flame impingement combustor, and (3) the heat exchanger tubes of a Stirling engine assembly. The primary heat pipes transfer heat in one direction only to prevent heat loss from the TES. Heat transfer in the secondary heat pipe is effected in a near-isothermal manner by sodium vapor thermal transport without

[4]Benson, Glendon M., et al, "An Advanced 15 kW Solar Powered Free-Piston Stirling Engine," Paper No. 809414, 15th Intersociety Energy Conversion Engineering Conference, Seattle, Washington, August 18-22, 1980.

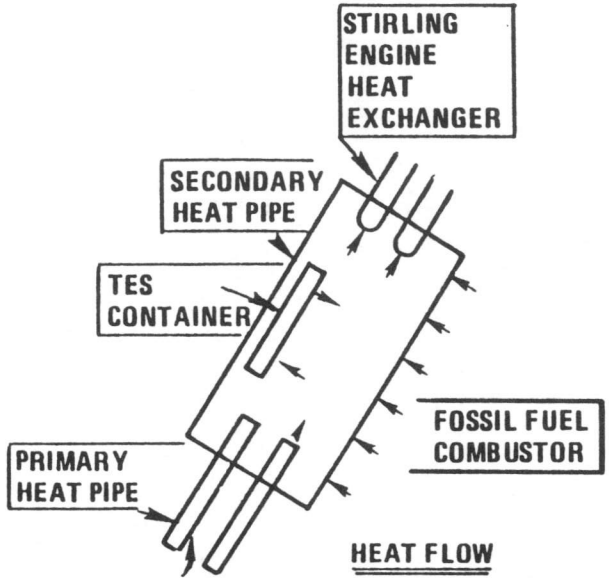

Figure 7-13. Schematic Diagram of Heat Flow in the HPSR

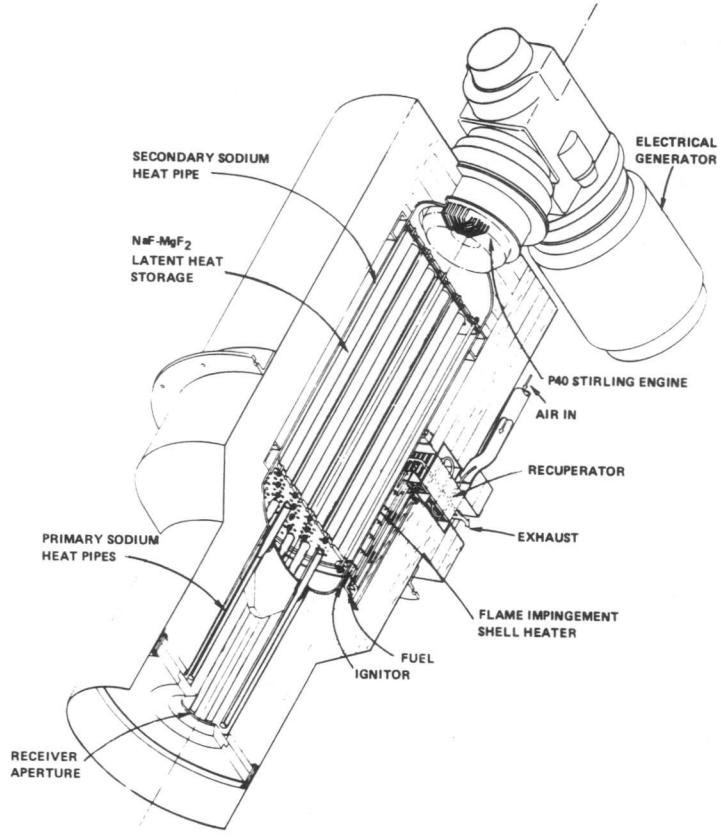

Figure 7-14. Heat Pipe Solar Receiver with Flame Impingement Fossil-Fuel Combustor

pumps, valves, controls or flow sensors. The hotter surfaces, such as the primary heat pipe, condensers, or the combustor heat exchanger reject heat, and the colder surfaces (where heat is being extracted) accept heat at near-isothermal temperatures. Differences in equilibrium vapor pressure within the assembly provide the driving force. Thus, the assembly is self-regulating in that the heat flow into and out of the assembly, the storage of energy in the latent heat salt, and the providing of heat to the engine are based upon minor temperature differentials occasioned by the operation of the assembly itself. Simple temperature instrumentation within the isothermal secondary heat pipe can indicate the subcooling or superheating of the TES. The temperature source for operation of the engine remains relatively stable varying only with the ΔT required to extract heat from the large surface area of TES material at low heat flux levels.

The small aperture of the receiver reduces convection and reradiation losses that results in high receiver efficiency. The proposed flame impingement combustor subassembly on the TES shell (providing for hybrid operation) features a high gas-side heat transfer coefficient approaching 681 W/m^2K (120 $Btu/h\text{-}ft^2\text{-}^oF$); sodium-side heat transfer coefficients are, of course, orders of magnitude higher. The technology of flame impingement combustors has been well advanced through the development of large thermionic converters and through demonstrated improvements in combustors for Stirling engines using silicon carbide ceramic materials and advanced impingement combustor design techniques.

Other features of the advanced HPSR concept include the following: (1) the all-stainless-steel construction made possible by the use of dished heads on the secondary heat pipes to minimize the stresses from very low differential pressure within and outside this heat pipe and by the use of sectioned-stiffened stainless steel forward and aft salt capsule support plates to carry axial loads from the salt capsules, (2) the development of reduced wicking requirements for supplying sodium with TES, and (3) improvement in Stirling engine efficiency from 39.6% to about 43% by engine heater head redesign to take advantage of improved sodium heat transfer coefficients at the heater tubes. This latter improvement in turn, decreases solar collection costs, improves TES storage time for equivalent weight and cost, and results in less sensitivity of the coefficient of thermal expansion to increases in fuel cost for the combustor-assisted PCU. The general effects of these expected changes in efficiency and of the value of TES in increasing the ratio of solar-to-fossil fuel utilization are shown in Figure 7-15; results are based upon system performance and economic analysis over a one-year period of simulated solar operation of hybrid Stirling solar systems.

Proof-of-Concept Experiments. The technology of the HPSR is based upon well-founded heat pipe and latent heat storage data and experience, and upon related heat pipe and latent heat storage developments for space applications. In addition, the primary heat pipes were experimentally tested (References 18 and 19) in all operating attitudes as indicated in Figures 7-16 and 7-17.

A modular TES experiment featuring a single primary heat pipe and a secondary heat pipe containing three standard salt containers and a heat extraction coil to simulate the Stirling engine was designed, built, and tested at initial design heat flux conditions on the TES salt containers.

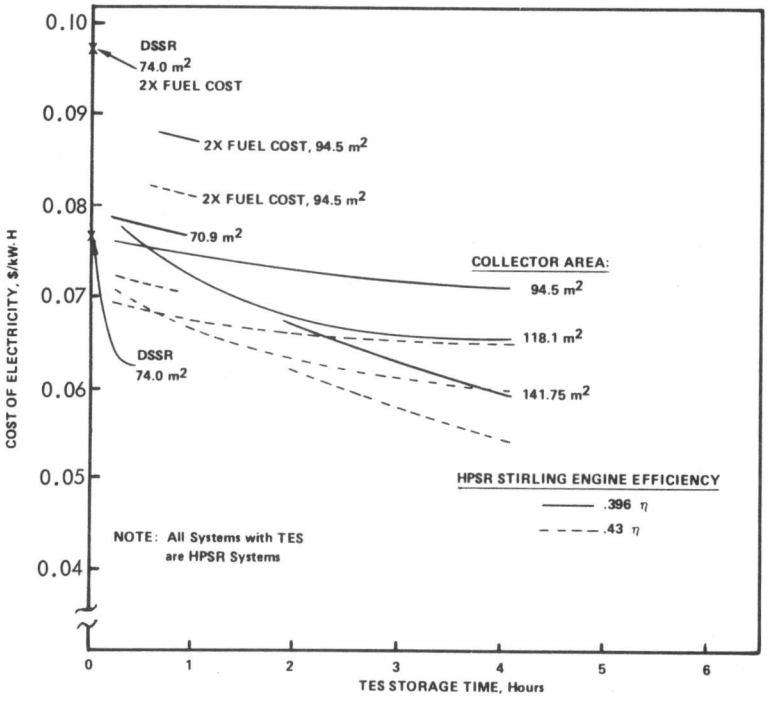

*30 Year Levelized Costs are Higher by a Factor of 2.66

Figure 7-15. Cost of Electricity versus TES Storage Time for Systems with Combustors

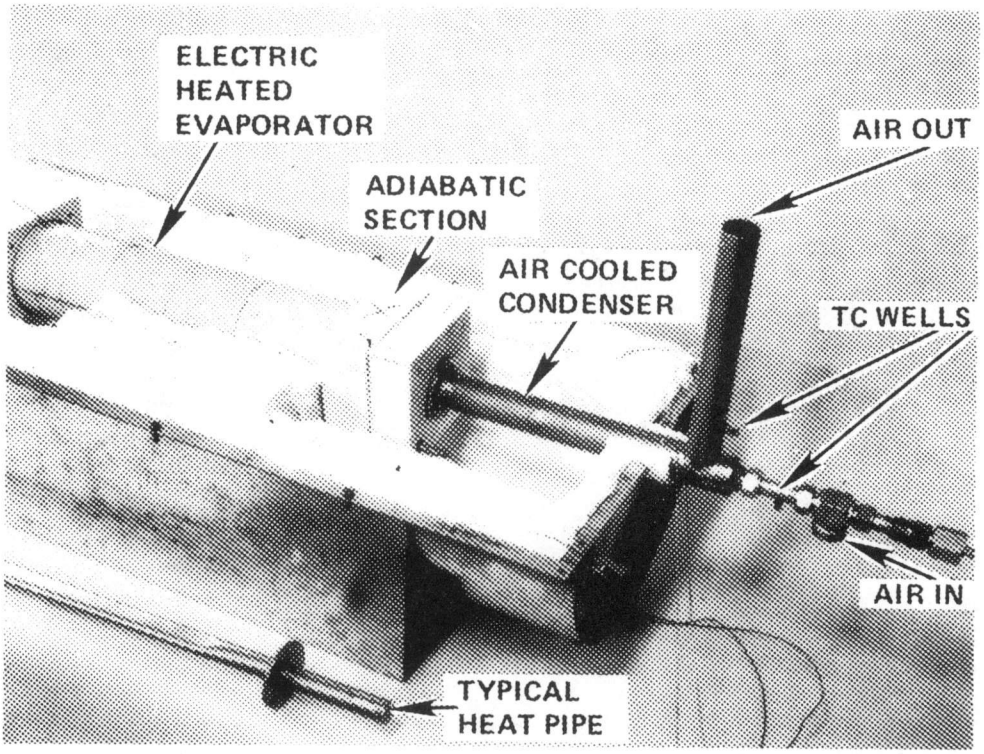

Figure 7-16. Heat Pipe Test Facility

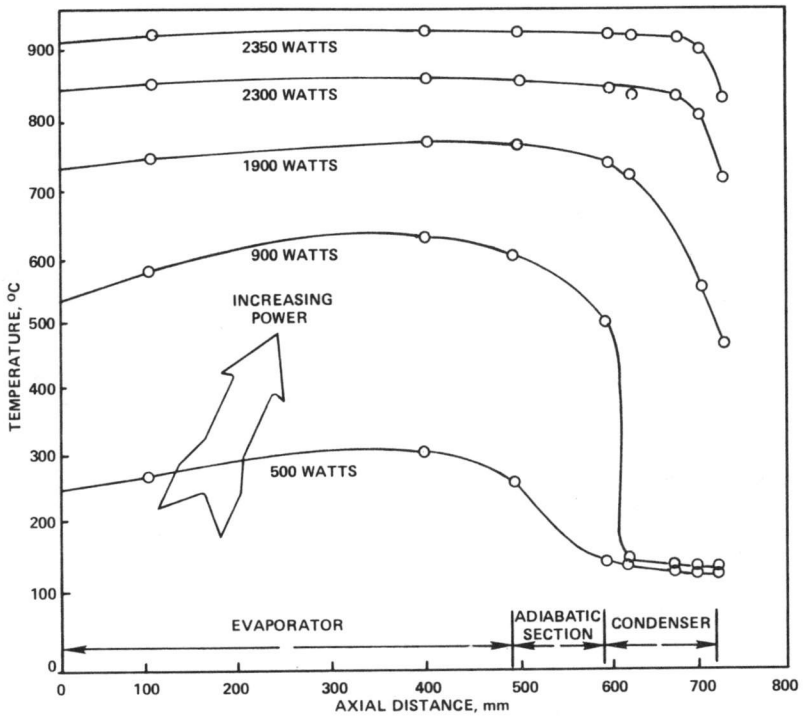

Figure 7-17. Operating Characteristics of Heat Pipe No. 1 at a 10-deg Inclination

This modular test apparatus was operated successfully at all operating angles in various modes of charging, discharging, direct heat throughput, and mixed modes of operation. The test indicated the excellent thermal inertia of the system (less than 2°F/min outside the latent heat range), low ΔT across heat pipes, and isothermal operation of the secondary heat pipe. The components of the system and a typical TES charging curve are shown in Figures 7-18 and 7-19.

The above experimental effort has contributed significantly to the demonstration of the validity and expected performance of the thermal transport and storage concept.

Final Design Activity. During the later months of 1980, a preliminary design was submitted; modifications to that preliminary design were made to accommodate, at a later date, the addition of the flame impingement combustor to the TES shell; and a final detailed design was prepared. This final design of a PCU using a United Stirling P-40 engine and a 25-kWe induction generator is shown in Figure 7-20. Sodium wicking is included inside the TES shell to permit internal heat transfer from the flame impingement combustor, which can be added at a later date. Other TES wicking includes arterial wicks that provide liquid sodium from a pool in the lower forward part of this large heat pipe; these wicks feed wire wicks on the surfaces of the primary heat pipe condensers and on the lower half of the TES salt containers. The upper half of the salt containers are supplied with sodium by gravity return from the engine through a diffusion-bonded arterial wick at the rear salt container support plate and, thence, along wire wicks on the salt containers. Figure 7-21 shows these details.

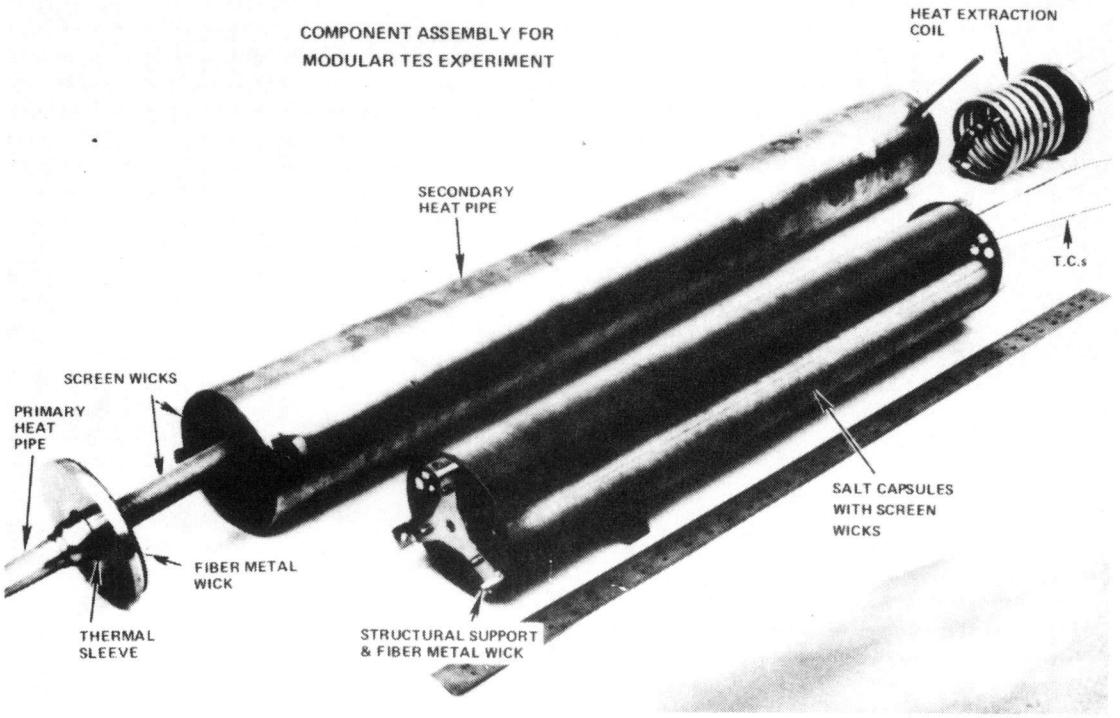

Figure 7-18. TES Modular Experiment Components

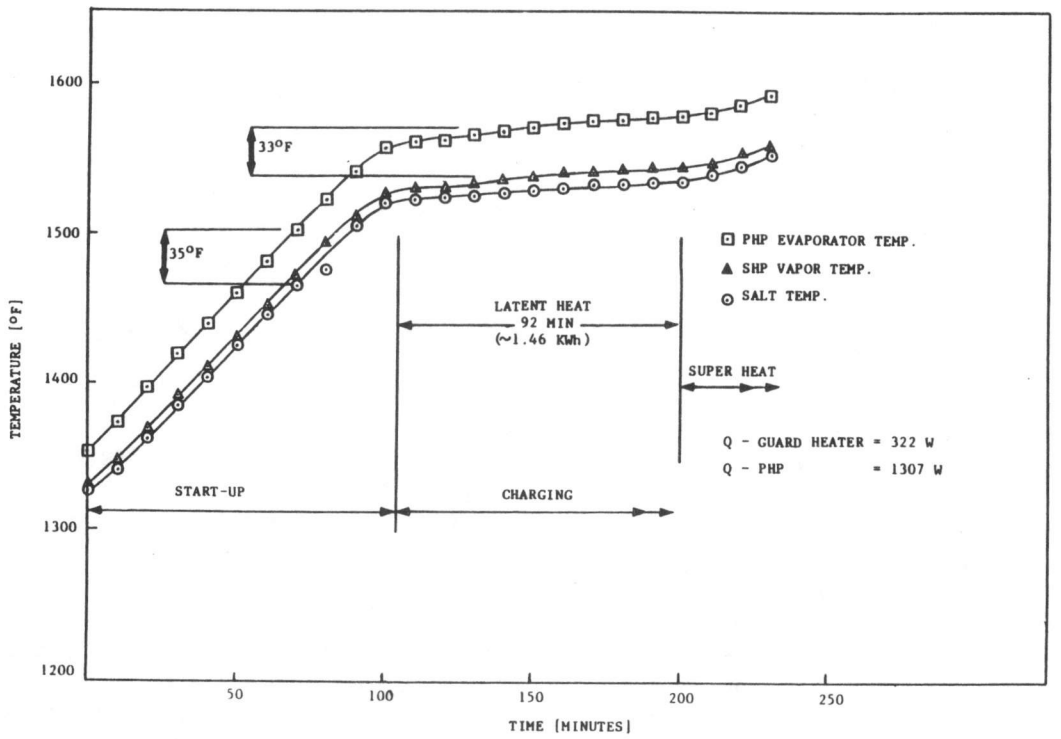

Figure 7-19. Typical TES Charging Curve for the Modular Experiment

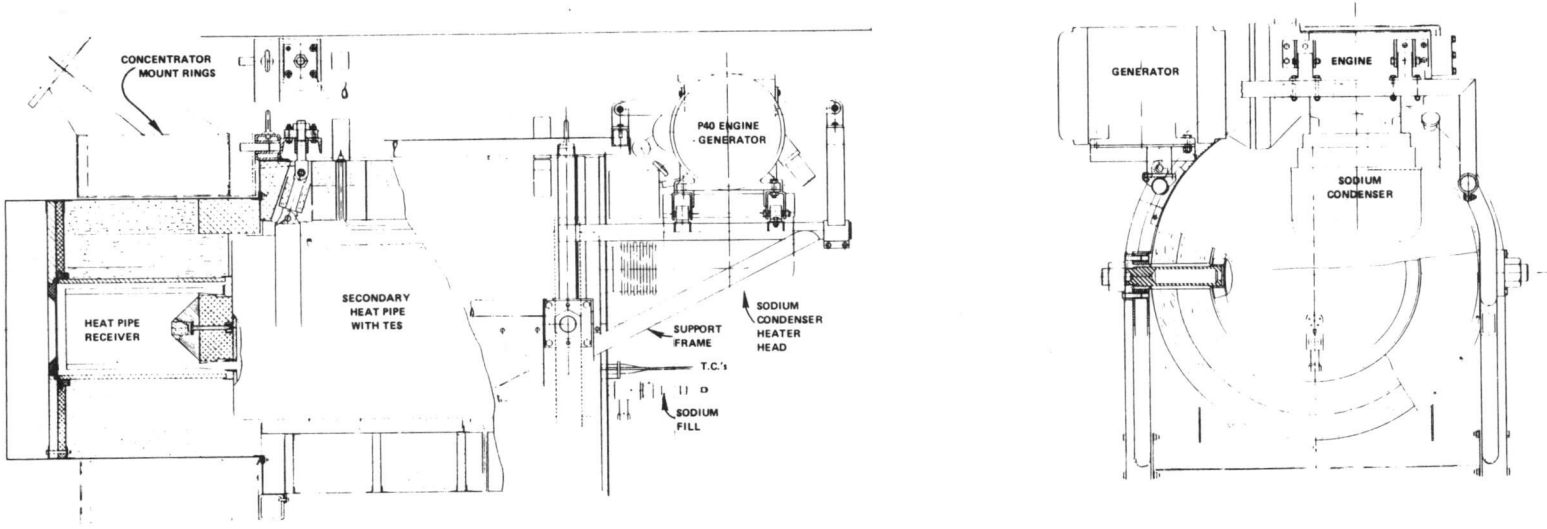

(a) Side View

(b) Rear View

Figure 7-20. 25-kWe Prototype HPSR/Engine/Generator System

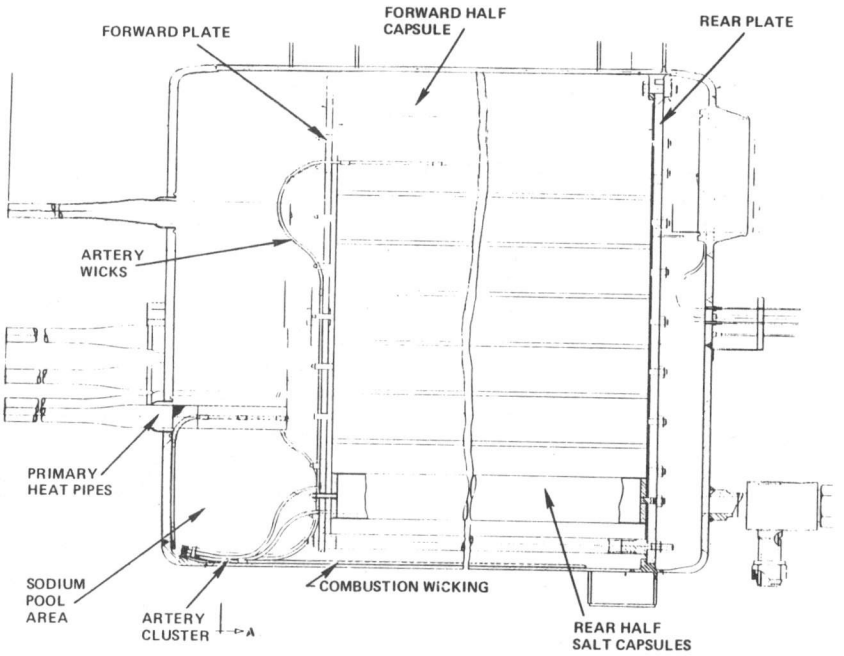

Figure 7-21. Secondary Heat Pipe Wicking

Key characteristics of the prototype design, on which manufacturing work was begun in early 1981, is shown in Table 7-2. With about 0.8 hours of latent and sensible heat storage,[5] the entire system should weigh about 1315 kg (2900 lb). Higher engine and system efficiencies than those shown could be achieved with the modification of the P-40 engine heater head for operation on condensing sodium vapor.

Prototype PCU Fabrication. During the early months of 1981, the first prototype PCU was fabricated, prepared for filling with sodium, and thermally conditioned to assure that all the arterial wicks would be filled and that the capillary wicks would be saturated with liquid sodium. The PCU was to be shipped to the PDTS in late summer 1981 for installation and solar test on a test bed concentrator. A key element in the assembly and operation of this system was the availability of a sodium heater head version of the P-40 Stirling engine, which was to be supplied by JPL for assembly with the HPSR prior to sodium filling. However, work to modify the engine was not started because of reduced funding, and General Electric Company's fabrication work was ended in early 1981.

Future Activity. Future thermal performance testing of the HPSR prior to solar operation would be desirable to check out the thermal transport and integrated operation of the receiver, TES, and engine/generator. The development of the flame impingement combustor could be carried out

[5] 0.8 hours is adequate to eliminate a large portion of solar insolation transients caused by variable cloud cover.

Table 7-2. Key Characteristics of the HPSR System

Test Bed Concentrator:	
Concentrator Diameter	11 m
Geometric Concentration Ratio	2000
Overall Concentrator Efficiency	0.9259
Shaded Concentrator Focal Plane Power	77.0 kWt
Solar Receiver:	
Aperture Diameter	16.5 cm (6.5 in.)
Intercept Factor	98%
Receiver Efficiency	91%
Power Output	68.5 kWt
TES Heat Pipe:	
TES Material	$67NaF-33MgF_2$
Storage Time (latent plus sensible at 66.2 kWt)	0.8 h
TES Efficiency	97%
TES Operating Temperature Range	804-835°C (1480-1535°F)
Power Output	66.2 kWt
P-40 Stirling Engine/Generator:	
Nominal Heat Exchanger Temperature	827°C (1520°F)
Engine Performance (15.1 MPa He, 1800 rev/min)	
Efficiency	0.396[a]
Power	26.2 kWe
Generator Efficiency	93%
Generator Output	24.4 kWe
Overall System Efficiency (solar to electric)	32%

[a]Conservative estimate is 43% with engine heat exchanger design for sodium condenser. Overall system efficiency is estimated to be 35% with sodium heat exchanger.

separately, and that combustor could be mated later to the prototype HPSR without modification to the interior of the secondary TES heat pipe. The test of the combustor on the HPSR could then be performed in either a factory test or a test on a solar concentrator. Finally, future design modifications and improvements would be required to minimize redundant wicking requirements and to introduce, in subsequent test hardware, lower cost components such as dished heads and alternative design support plates.

The advantages of the excellent thermal transport, stable operating temperature, and stored energy inherent in the HPSR are worthy of continued evaluation and improvement, not only as these concepts apply to dish/Stirling systems, but for the benefit of other high-temperature solar energy systems as well.

SECTION VIII

FIRST DISH/STIRLING POWER SUBSYSTEM MODULE DEVELOPMENT

A. SELECTION OF FIRST DISH/STIRLING POWER SUBSYSTEM MODULE FOR DEMONSTRATION

Because the ultimate system performance requirements could only be achieved through a combined DOE subsystem development program followed by a solar thermal industry advancement in conversion efficiency, component reliability, and manufacturing costs, the DOE Solar Thermal Technology Program in FY 1979 elected to demonstrate a system solar-to-electric conversion efficiency of 24% by pursuing an interim experiment to be demonstrated by FY 1981. The experiment would consist of a dish/Stirling power subsystem module composed of

(1) A solar concentrator (i.e., a PDTS test bed concentrator) for supporting a 500 kg (1100 lb) power conversion unit near the principal focus.

(2) A power conversion unit consisting of a modified USAB Model 4-95 Stirling engine, and/or a modified (scaled-up) Philips 1-98 Stirling engine assembly with an electrical generator assembly and a hybrid advanced receiver assembly. The interim solar Stirling engine assembly would have an actual thermal efficiency of from 38 to 43% at a nominal power of 20 kWe and would cost under $5500 per assembly at a production rate of 10,000 engines per year in order to demonstrate the system performance requirement potential.

The electrical generator assembly would be an off-the-shelf 25-kWe induction alternator with an efficiency of 93%, or a synchronous alternator with an efficiency of 87.5%. An advanced solar receiver assembly with both solar- and gas-fired capability would have to be implemented with industry. The hybrid advanced solar receiver characteristic would satisfy both the system performance requirement of meeting the demand load and the engine thermal cycling requirement. The maximum temperature of the pressurized engine hot parts would not exceed 816°C (1500°F) with the hybrid advanced solar receiver, which in production would cost less than $1035 for each assembly in order to meet the system performance requirements. Fairchild Industries was selected to design and fabricate such a hybrid receiver.

In order to demonstrate a solar concentrator unit capable of meeting the system performance requirements, parallel development of a conceptual solar concentrator unit was managed by JPL. Acurex Corporation was contracted to design, fabricate, assemble, test, and evaluate the likelihood of attaining a production cost of below $\$138/m^2$ while achieving a clear surface specular reflectivity of 94%.

After considering the alternative engines in the conceptual design stage, the choice of an advanced Stirling engine narrowed to modified versions of the Philips Model 1-98 engine and the USAB Model 4-95 (P-40) engine. The free-piston Stirling engine would require several more years of intense

development to reach the level of function, performance, and endurance of the kinematic-type Stirling engine, and resources were not available to the STT Program to pursue the free-piston option.

The USAB Model 4-95 was chosen for solar modification over the Philips Model 1-98 engine for two reasons. The conclusion reached by Fairchild Industries was that the very high operating pressure required by the Philips Model 1-98 engine to achieve the output (25 kWe) would result in unacceptable short creep life of the heater tubes. Also, the required heat transfer area of the receiver in the solar mode, as well as in the combustion mode, could not be attained with an acceptable degree of certainty.

On the other hand, the USAB Model 4-95 (P-40) engine with a relatively large heat transfer surface heater head could, with some modification, accommodate the required heat transfer in both the combustion mode and the solar mode.

The conclusion of the Fairchild Industries preliminary design activity was to proceed with a dish/Stirling solar thermal electric system, using a modified USAB Model 4-95 (P-40) engine with a direct-driven induction alternator and a test bed concentrator (TBC) with masked or removed facets to provide a suitably sized and configured concentrator. This configuration provided a narrow flux pattern inside the receiver cavity suitable for a direct-heated Stirling engine and a small diameter aperture required for high thermal receiver efficiency.

B. TEST BED CONCENTRATOR

1. Design Requirements

In order to rapidly obtain a solar concentrator unit for test and evaluation of power conversion units (including the Stirling) and solar receiver assemblies, two test bed concentrator units were designed, fabricated, assembled, and installed at the Parabolic Dish Test Site (PDTS), Edwards Air Force Base, California, by E-Systems, Inc. The reflector surface facets were designed and fabricated by JPL. The risk associated with the development of the test bed concentrator unit was minimized by specifying a modification of an existing proven antenna structure in the technical requirements. Key design requirements given in Table 8-1 (from Reference 20) define a full motion structure capable of boresight pointing anywhere within a hemispherical envelope at rates consistent with defocusing needs. The key design requirements agree with normal design criteria for antenna structures with only a few exceptions: (1) the focal point load is about ten times that of a subreflector or feedhorn on a comparably sized antenna; (2) the ratio of focal length to dish diameter (f/D) is about double that of microwave dishes; (3) the 61-by-71-cm (24-by-28-in.) reflector panels supplied by JPL represent only a small fraction of the reflector panel size on a comparable radio antenna.

2. Design Characteristics

A 13-m-diameter communication antenna was selected for the TBC application. The antenna was originally designed for the RCA Domestic

Table 8-1. Key TBC Design Requirements

Physical	
Aperture Diameter	11 m (35 ft)
Rim Angle	45 deg
f/D Ratio	0.6
Focal Point Load	500 kg (1100 lb)
Receiver Mounting	76 cm (30 in.) inside diameter ring
Tracking Control	
Azimuth	
Travel	178 deg
Slew Rate (13 m/s wind)	2028 deg/h
Elevation	
Travel	0 to 90 deg
Slew Rate (27 m/s wind)	168 deg/h
Tracking Accuracy (operating wind)	0.05 deg
Pointing Accuracy	1.0 deg
Environmental	
Operating Wind	13 m/s (30 mi/h) gusting
Survival Wind	45 m/s (100 mi/h)
Seismic	0.25 g, any direction
Ice	0.4 cm (1 in.) radial
Snow	0.4 kg/m^2 (10 lb/ft^2)

Satellite System, and five units were subsequently constructed in the continental U.S. Only the reflector structure was used for the TBC because the antenna was a limited motion satellite tracker with a maximum of 60 deg of azimuth coverage. Therefore, an entirely new pedestal was designed for the TBC to enable full sky coverage. Figure 8-1 shows the completed test bed concentrator.

The reflector support structure is a structural steel space frame consisting of eight truss beams radiating from a central hub, all interconnected with appropriate diagonal and intercostal members. The hub, which employs shear webs, is unusually large (it is unchanged from its 13-m configuration), and exhibits exceptionally high stiffness characteristics. The only major modification required to adapt this structure to the TBC was an increase in the section modulus of the members comprising the two vertical radial beams that form the primary load path for the focal point mass. A parallel tube matrix serves as the interface structure for mounting the rectangular mirror panels on the radial reflector structure. Mirror attachment is effected by specially designed clamps that provide maximum adjustability for panel gapping and alignment.

The receiver support structure is a tubular bipod interfacing the toroidal receiver ring at the focal plane with the periphery of the reflector support structure. It is stabilized laterally and torsionally by adjustable rods that also attach at the periphery of the dish. The total structure thus minimizes the amount of surface blockage as compared to the more conventional, quadripod mount, and is as stable.

The pedestal is an elevation over azimuth, wheel and track alidade. It is a fully triangulated, structural steel space frame, designed to transmit all loads from the elevation axis to ground in tension or compresson. The azimuth axis is defined by the pintle bearing, which is bolted to the foundation and reacts all radial and uplift loads. Gravity loads are reacted by the three railroad-type wheels that ride on a 9-m (29-ft)-diameter track bolted and grouted permanently to the foundation.

A weight summary of the system is shown in Table 8-2. It is important to recognize that no attempt was made to optimize the design of the TBC. The design employed was expedient and achieved the primary purposes of stiffness, timely delivery, and adaptability required for testing.

The structure was comprehensively analyzed using both computer and manual methods. Several proprietary and library programs were employed of which the principal one was SPACE. This is a finite element program that relates applied loads to displacement and rotation at the joints, which in turn are used to calculate internal loads and stresses in the structural elements.

The system design was predicated on a consideration of stiffness rather than on stress. Thus, as a result of maintaining deflections within specified limits, the members are relatively lightly loaded.

In Table 8-3, the calculated system error analysis is compared to the specified requirements. The predicted combined system error is thus only

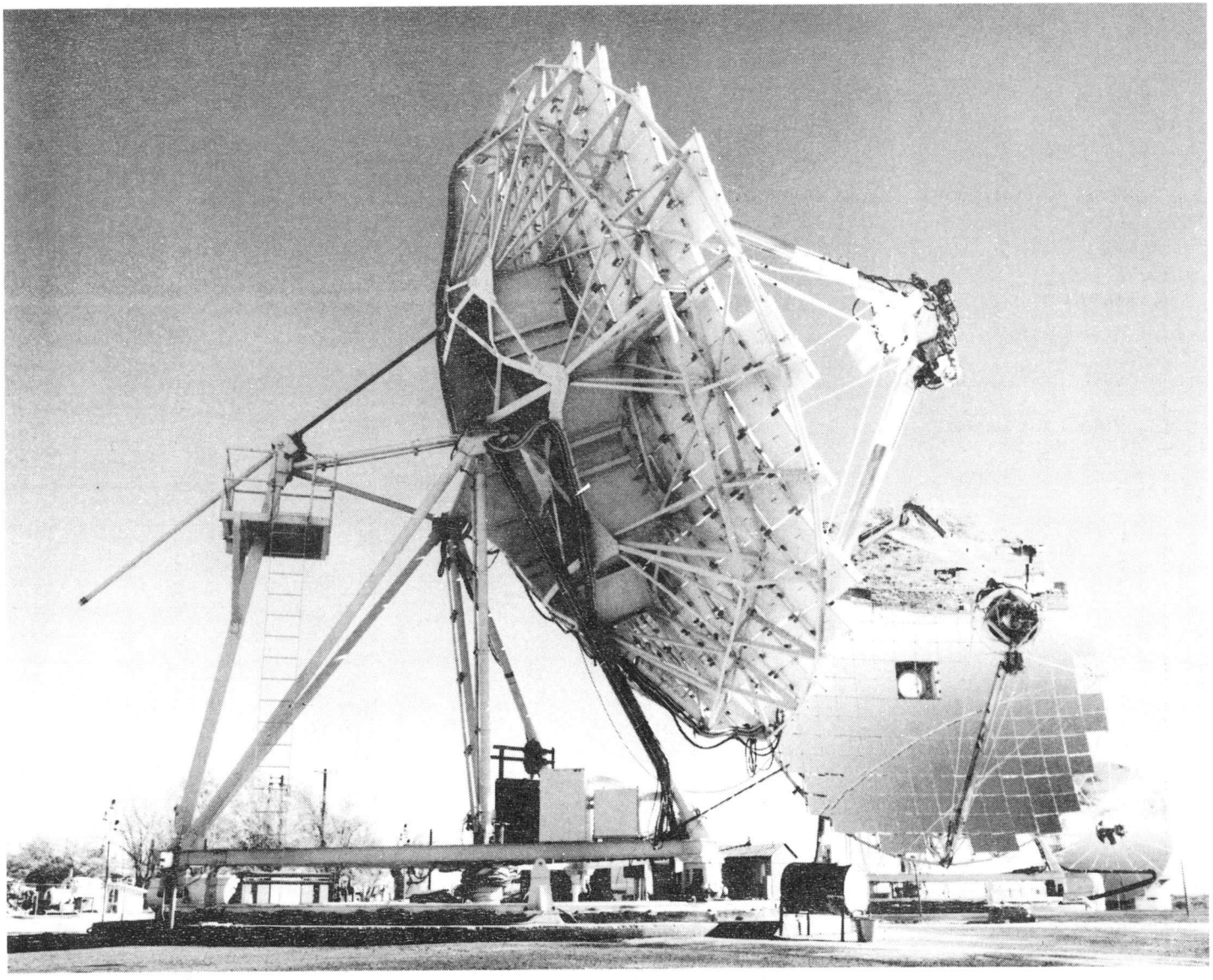

Figure 8-1. Two Test Bed Concentrator Units with PCUs Mounted at the Focus

Table 8-2. TBC Structure Weight Summary

Assembly	Weight, kg (lb)
Reflector Support Structure	5,443 (12,000)
Receiver Support	590 (1,300)
Panel Support Tube Matrix and Clamps	363 (800)
Alidade	4,309 (9,500)
Track	1,134 (2,500)
Ancillary Equipment/Hardware	2,041 (4,500)
Mirror Panels and Brackets	1,633 (3,600)
Focal Point Package	499 (1,100)
Total Weight on Concrete	16,012 (35,300)

about one third of that specified. As a result of this increased accuracy, improved performance of the TBC in the form of higher concentration ratios was realized.

In azimuth, a 3-hp dc servo motor drives one of the three alidade wheels through a 740 to 1 gear reducer. Because the wheel-to-track ratio is 23 to 1, the overall speed reduction is over 17,000 to 1. An identical 3-hp motor is used in elevation to drive a 20-ton screw-type linear actuator through a single helical gear box. The total speed reduction in this axis is 160,000 to 1.

The control system provides for active sun tracking as well as program tracking. Active tracking (auto tracking) is accommodated via two photocell sensors, one for each axis, which generate error voltages as a function of position error. The auto tracking mode is used only after the concentrator has been positioned by program (or manually) to within 2.5 deg of the sun.

Program tracking (Memtrack) employs the closed-loop position control method, implemented through the use of a microprocessor. Azimuth and elevation angle data may be entered into memory as a function of time by recording actual sun position when in the autotrack mode. Ephemeris data may also be entered manually.

3. Installation

The design, as well as the program plan for the TBC, gave major consideration to minimizing on-site installation time. To accomplish this objective, it was necessary to ensure that all parts fit properly prior to

Table 8-3. Results of Pointing Angular Error Analysis

	Specification,[a] deg	Predicted,[a] deg
Reflector Assembly		
Reflector Support Structure	-	0.0070
Panel Support Tube Matrix	-	0.0248
Receiver Support Structure	-	0.0019
Total Structural Error	0.02	0.0258
Control System		
Servo Limit Cycle	-	0.0001
Servo Angular Error	-	0.0001
Servo Wind Gust	-	0.0003
Servo Bias	-	0.0010
Sensor Error	-	0.0067
Total Control Error	0.05	0.0068
Combined System Error	0.07	0.0267

[a]Standard deviation.

arrival on site. Thus, the key acceptance criteria for the steel fabrication phase was trial assembly of the reflector structures and pedestals at the fabricator's facility in Birmingham, Alabama.

The reflector structure was designed so that it could be completely constructed at ground level, including mirror panels, and placed on the pedestal in a single lift. A 45-ton, 100-ft boom hydraulic crane was employed for a total of three days to place both reflector assemblies. This served the dual purposes of minimizing both assembly time (construction directly on the pedestal is commonplace in antennas) and costly large crane expenses. For the remainder of the installation, an inexpensive 7-ton crane served adequately. It is noteworthy that the E-System's installation team consisted of one supervisor and three ironworkers full time, supported part time by the control system subcontractor. Installation of the TBCs, including tracking and

control system operational checkout, required a total of two months. Acceptance of the installation by JPL on October 17, 1979, represented completion of the entire contract one month ahead of schedule.

4. Reflector Surface Alignment

The reflector surface assembly consists of 224 individual reflector facets with three tabs fastened to a parallel tube matrix on the reflector backup support structure. Each reflector facet -- composed of a fusion glass superstrate silvered mirror bonded to a spherically contoured cellular glass substrate -- has an experimentally measured focal length and standard slope error (Reference 21). The alignment of one entire concentrator (224 mirrors) took about two weeks of night work.

A light source was located at a NASA facility atop a hill 5.8 km (3.6 mi) southwest of the test site. Once the light source was aimed, the TBC was boresighted to it. This was done using two sets of cross hairs and two disks that were replaced by a series of disks with successively smaller apertures. The cross hairs were placed at the front (outer end) of the receiver mounting ring and at the rear of the concentrator dish structural hub on the geometrical center. The disks with variable size circular apertures were placed at the mirror surface plane and at the focal plane of the receiver. By moving the concentrator while sighting along the cross hairs and through the disk apertures to the light source, the concentrator was boresighted to the light. The final aperture size in the two disks was 1.27 cm (0.5 in.) in diameter, resulting in the maximum pointing error being within $\pm$0.05 deg. The control system position repeatability for the concentrator system was designed to be $\pm$0.01 deg. When programmed to move the concentrator to the boresighted position of the light source, a visual alignment check always verified an image centered at the focal plane target location.

Only one TBC mirror facet could be aligned at a time, making necessary individual mirror covers that could be removed and reinstalled easily. An opaque plastic cover with Velcro fasteners was chosen. Mirror alignment is implemented by using a three-point adjustment system. Each mirror facet is attached to the concentrator structure with three flexures. The three flexure halves bonded to the mirror facet are bolted to a matching bracket on the concentrator structure. Both halves of the joint have slotted holes to allow for adjustment or movement. One at a time, each of the 224 mirror facets was loosened at the flexure joint and adjusted to center its image on the focal target. When the image was centered, the three flexure joints were tightened in place.

Additional alignment verification checks were made periodically by removing a cover from a previously aligned mirror and reverifying its light image position. No displacement was evident in these checks. After all the mirrors were aligned, the opaque target at the focal plane was replaced with a translucent target, and a picture was taken of each individual mirror image. All mirror covers were then removed and the resulting image was recorded on film. A further alignment check was made by pointing the concentrator at the moon and imaging the moon on the target; this image was also recorded on

film. The moon's image was approximately 20 cm (8 in.) in diameter. This matched the predicted image size and further verified that the mirrors were aligned satisfactorily. On several occasions, one edge mirror was uncovered while the concentrator was pointing at the sun. This provided increased confidence in mirror alignment because the sun produced an elliptical image from these edge mirrors of approximately 20 cm (8 in.) maximum dimension, as determined by eye observation from the ground. The edge mirrors produce the maximum elliptical image size because they are the farthest off axis (Reference 22).

5. Test and Evaluation

a. Focal Zone Radiative Energy Flux Distribution. TBC focal zone radiative energy flux distribution was measured with a "flux mapper" described in Reference 23. It consists of a radiometer that is moved through the concentrated sunlight in a series of planes perpendicular to the optical axis by means of a mechanical rastering device. Various radiometer probes can be utilized, depending on the time and accuracy requirements of the program. Energy flux is recorded as a function of location. Reduction of these data can be in various formats, e.g., contour maps, digital arrays, isometric visualizations, and other displays as the user requires.

A complete set of energy flux mapping data was recorded using a Kendall radiometer for each step in the mirror uncovering process. A set of data included a minimum of three rasters. Each raster consisted of 1056 discrete data points. For several of the mirror configurations, rasters were taken 1 in. in front of and behind the nominal focal plane and then every 2 in. along the Z direction thereafter (concentrator axis). Each raster took approximately 45 minutes to complete if everything performed smoothly. When this time is added to the TBCs' sun acquisition and normal operational sequence time, one complete raster consumed at least one and a half hours. A close-up of the flux mapper from the outer end is shown in Figure 8-2.

The initial energy flux mapping results (Reference 24) indicated that the TBCs, with the initial mirror alignment where all the mirror facets were focused on the center of the target at the nominal focal plane, produced a peak flux of 1500 W/cm^2 when the insolation was normalized to 1000 W/m^2 (Figure 8-3). It should be noted from the figure that 98% of the energy is within a 20.3-cm (8-in.)-diameter aperture. Flux mapper results also indicated that the majority of the peak flux was being produced by the center mirror section, which totaled 68 facets. In addition to being nearly on axis, these 68 mirror facets had focal lengths very close to their geometric nominal requirement. It was concluded that by readjusting these center mirror facets, the peak flux could be reduced, thereby reducing the possible thermal damage to the TBC structure and the receiver cavities. During the second mirror alignment, all the images from the center 68 mirrors were centered on a 51-mm (2-in.)-diameter circle on the target at the nominal focal plane. This produced a slightly reduced peak flux of approximately 1250 W/cm^2; therefore, mirror alignment was undertaken a third time. The center mirrors were realigned so that their image was geometrically on the opposite side of the target as compared to their physical location on the dish. Their images were centered on a 102-mm (4-in.)-diameter circle across the center of the

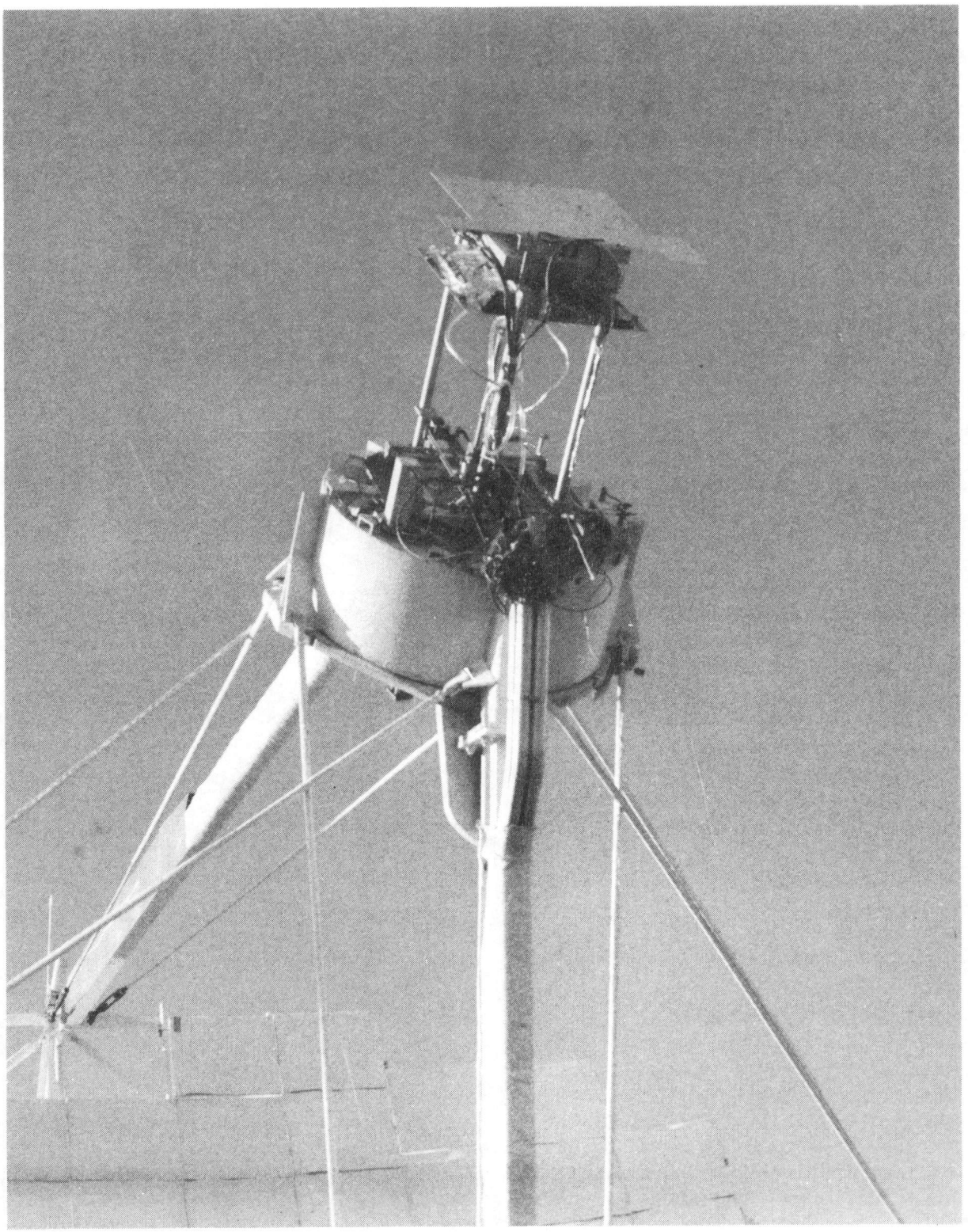

Figure 8-2. Close-Up of Flux Mapper from Outer End

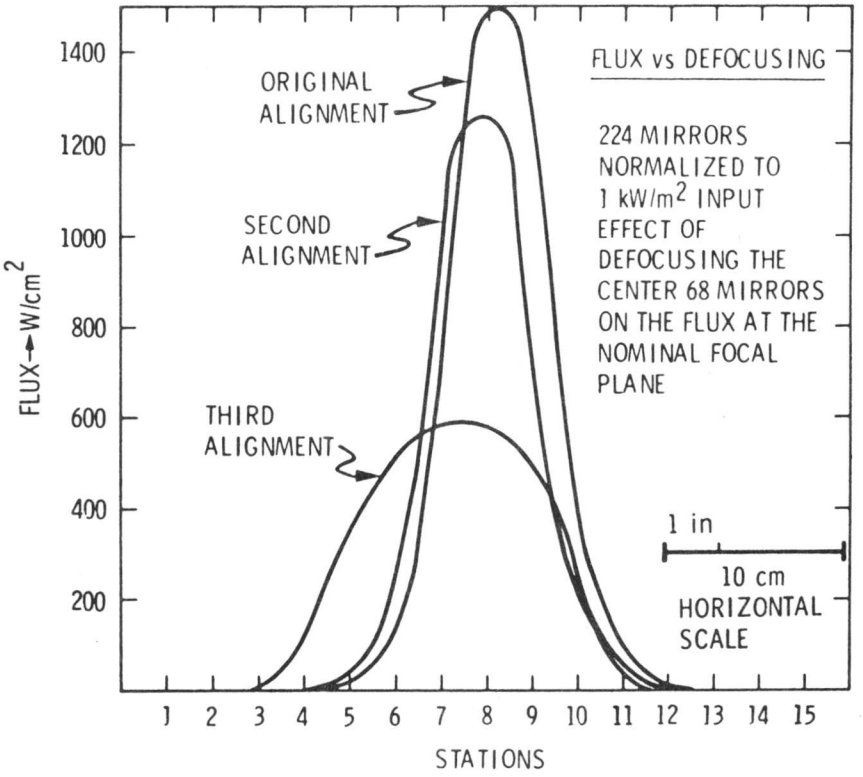

Figure 8-3. Solar Flux Measurements on Test Bed Concentrators

550-W/cm^2 range, but kept the total energy through the 20.3-cm (8-in.) aperture essentially constant.

For the first dish/Stirling subsystem PCU tests, the test bed concentrator unit was realigned in May 1981 in order to be compatible with the Fairchild Industries, Stratos Division (FSD) solar receiver focal plane location and energy flux requirements. All of the TBC's 220 reflector facets (four center facets having been removed because of shadowing) were adjusted to concentrate solar energy at the aperture of the PCU. The Stirling engine Inconel heater head cone had been designed for an evenly distributed energy flux of less than 55 W/cm^2 magnitude, and the aperture cone zirconia petals had been designed to withstand no more than a peak energy flux of 600 W/m^2.

In these energy flux-mapping tests, data were obtained and recorded at a 0.5-in. spacing. Direct insolation was measured with several instruments, compiled, and written on computer tapes for processing. Four utility computer programs were developed to display and to integrate the energy flux measurements (Reference 25). Among all the flux mapper data, only results of measurements at the solar receiver aperture plane are shown. Figure 8-4 shows the three-dimensional energy flux distribution at the solar receiver aperture plane for a superimposed 220-reflector facet configuration. For probe

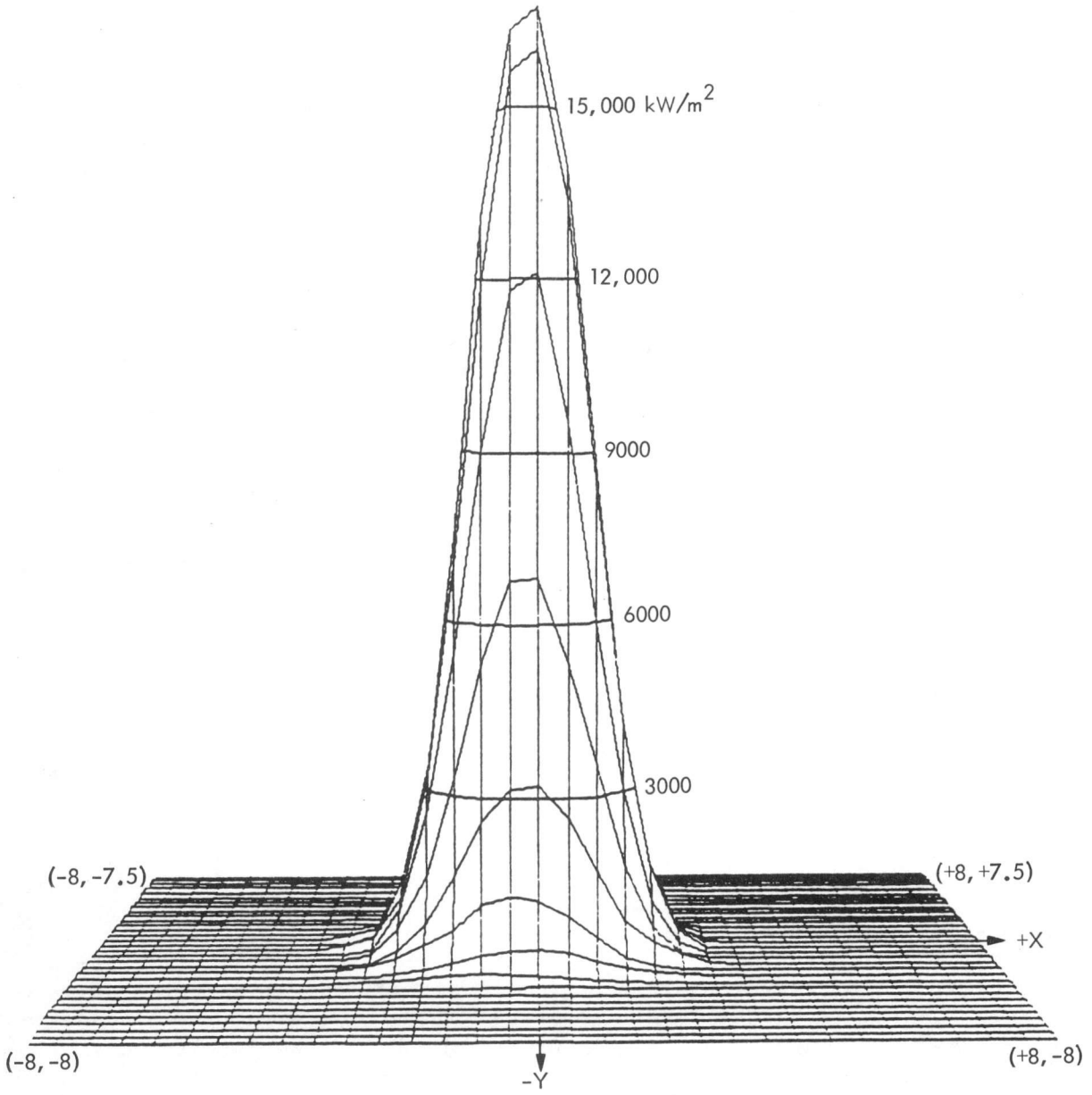

Figure 8-4. Superimposed Focal Plane Flux Distribution Based on Flux Mapper Data

survival, only 110 reflector facets could be simultaneously uncovered. Because the concentrator unit pointing may not be perfect due to bias in the sun sensor alignment, the solar image does not always coincide with the optical axis. Figure 8-5 shows the flux profile at the power conversion unit aperture plane for the superimposed 220-reflector facet configuration. The flux mapper data were shifted 5 cm (0.2 in.) to compensate for a center off-set. An analytical flux profile computed by Dr. L. Wen (Reference 26) -- based on experimental reflector facet radius of curvature and standard slope error -- agrees closely with the flux mapper profile. Cumulative solar power interception measured from the energy flux distribution is shown in Figure 8-6 as a function of PCU aperture radius. Calorimetric data obtained in the test to be described later are presented for comparison.

The intercept factor, as a function of PCU aperture radius, is shown in Figure 8-7 for the analytical model, the flux mapper data, and the calorimeter data with excellent agreement. This agreement confirms the analytical flux profile model ability to accurately compute the intercept factor with experimentally obtained reflector facet radius of curvature and standard slope error. The equal intensity contour shown in Figure 8-8 computed with the analytical flux profile model has proven valuable in the design of solar Stirling engine heater heads.

b. Focal Plane Radiative Energy Rate. The objective of the focal plane radiative energy rate tests conducted on the test bed concentrator (No. 2) was to provide thermal energy rate characteristics for the planned Stirling engine PCU tests based on a 20.3-cm-diameter receiver aperture. The focal plane radiative energy rate would be required for several TBC-2 mirror patterns representing differing thermal power levels as described in Reference 27. Also, the focal plane radiative energy rate would be obtained for alternative aperture sizes.

Apparatus. The cold-water cavity calorimeter (CWCC) was developed to characterize the power available in and around the focal plane for several aperture sizes for point-focusing parabolic dish solar collectors. The CWCC device determines this power through the measurement of water flow rate and its temperature increase under solar input. Water-cooled aperture plates screen the calorimeter cavity from solar input except for the desired aperture size. Flow rates through the calorimeter and aperture plates are sufficiently high to maintain near-ambient temperatures throughout the hardware. This minimizes error due to heat transfer with the ambient environment.

The CWCC was mounted on TBC-2 on July 16, 1981, spaced back from the mounting ring zero plane by 19.05 cm. With the arrangement of the aperture plates as shown in Figure 8-9, the aperture plate front plane is 45.24 cm in front (toward the concentrator) of the mounting plane zero. The 20.32- and 25.40-cm-diameter aperture plates are water-cooled through a coiled tube brazed to the front surface. The 15.24-cm-diameter aperture plate has a water cavity flow passage behind the aperture plate as shown in Figure 8-10. The 10.16-cm aperture is made by placing a pyrolytic graphite insert into the 15.24-cm aperture plate.

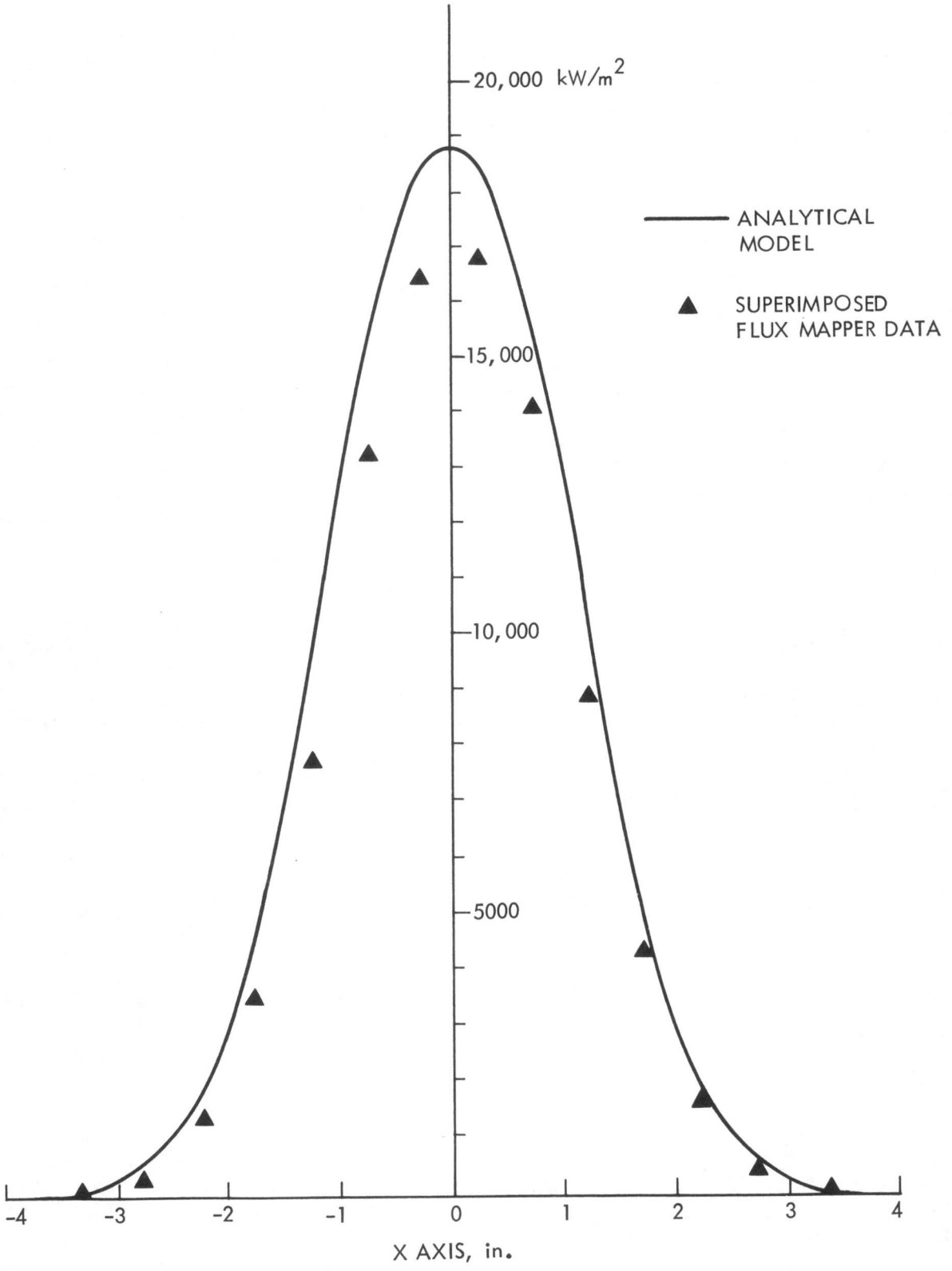

Figure 8-5. Aperture Plane Flux Profiles (100% Mirror Configuration)

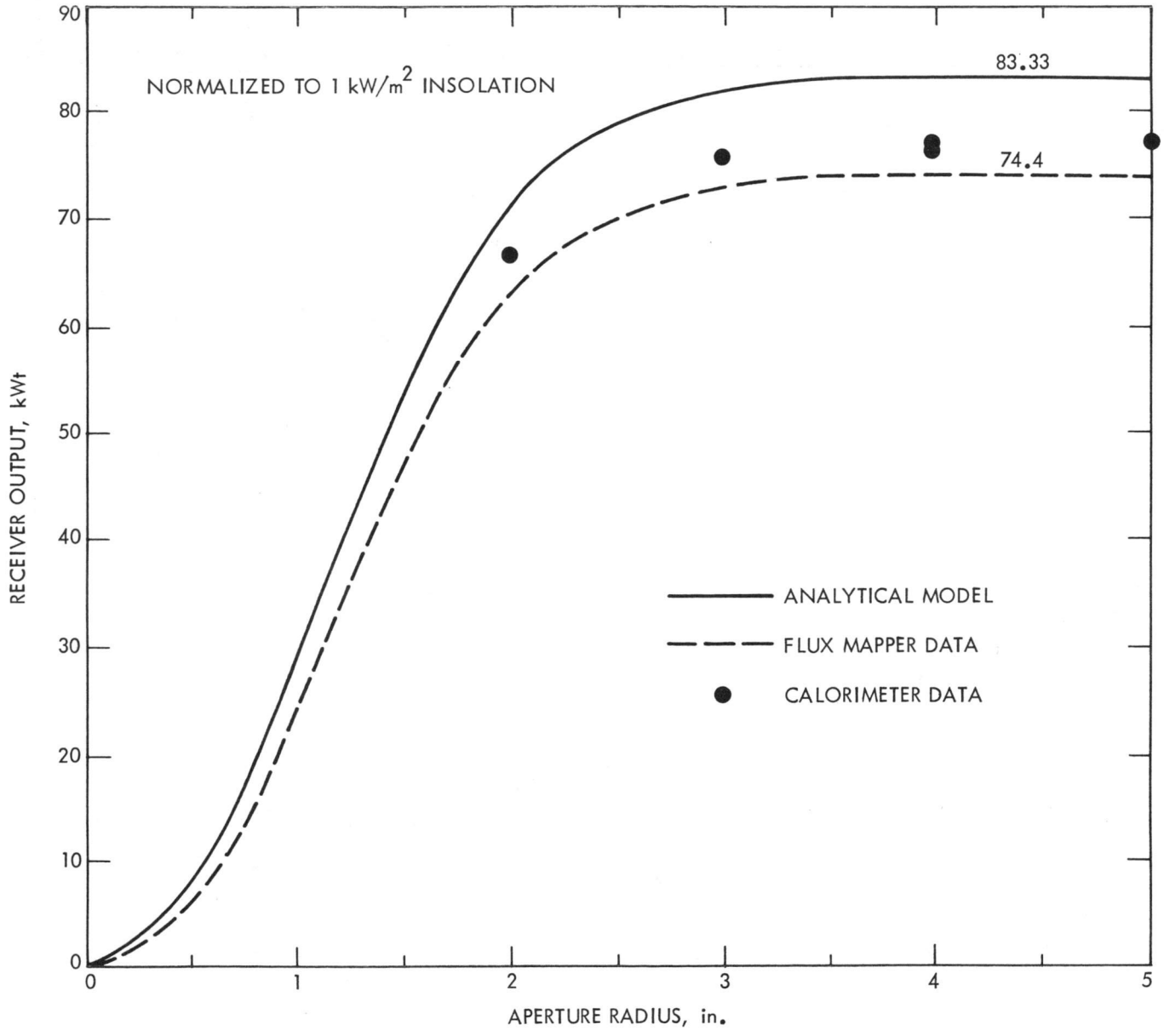

Figure 8-6. Accumulative Energy Distribution (100% Mirror Configuration)

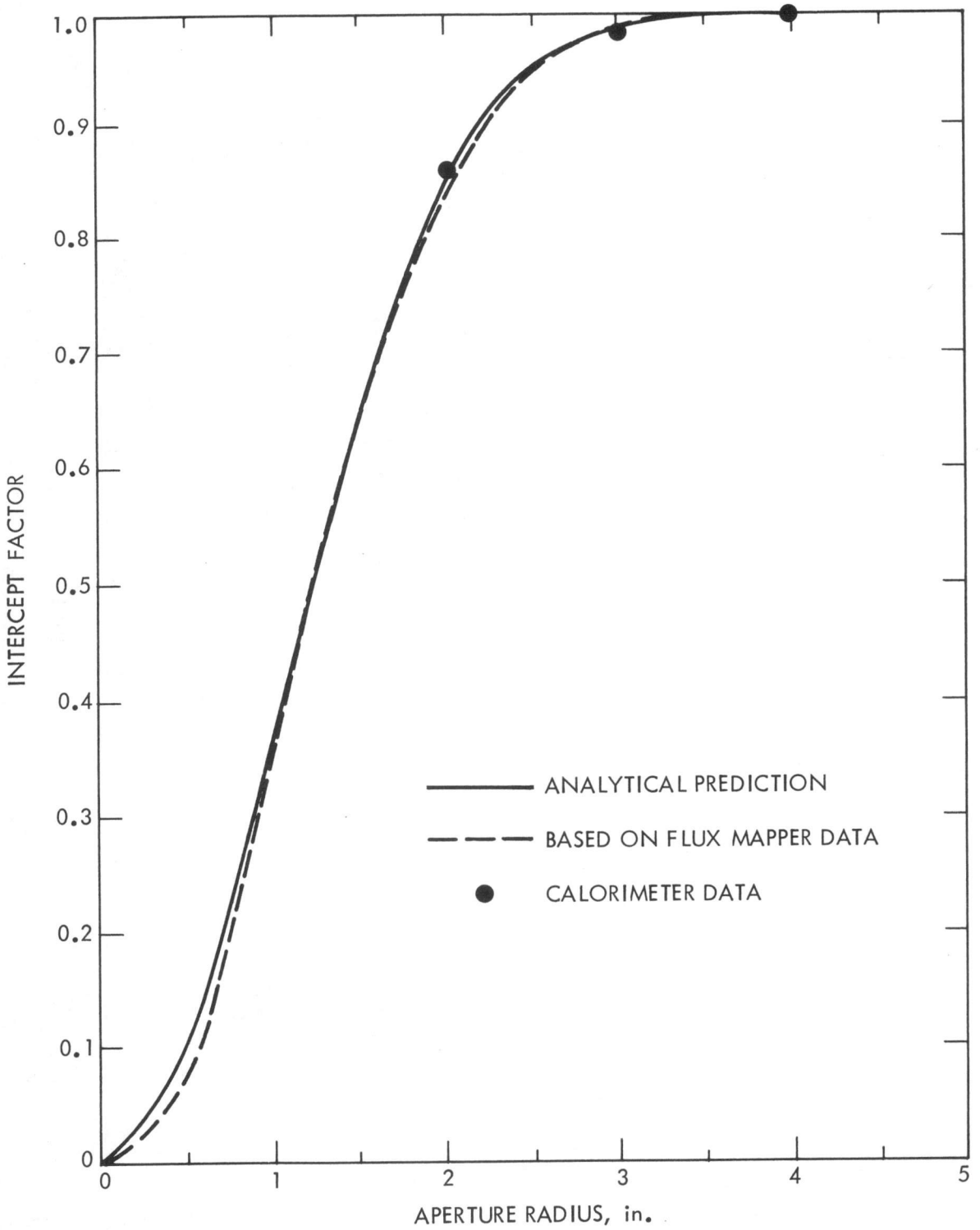

Figure 8-7. Intercept Factor Distribution (100% Mirror Configuration)

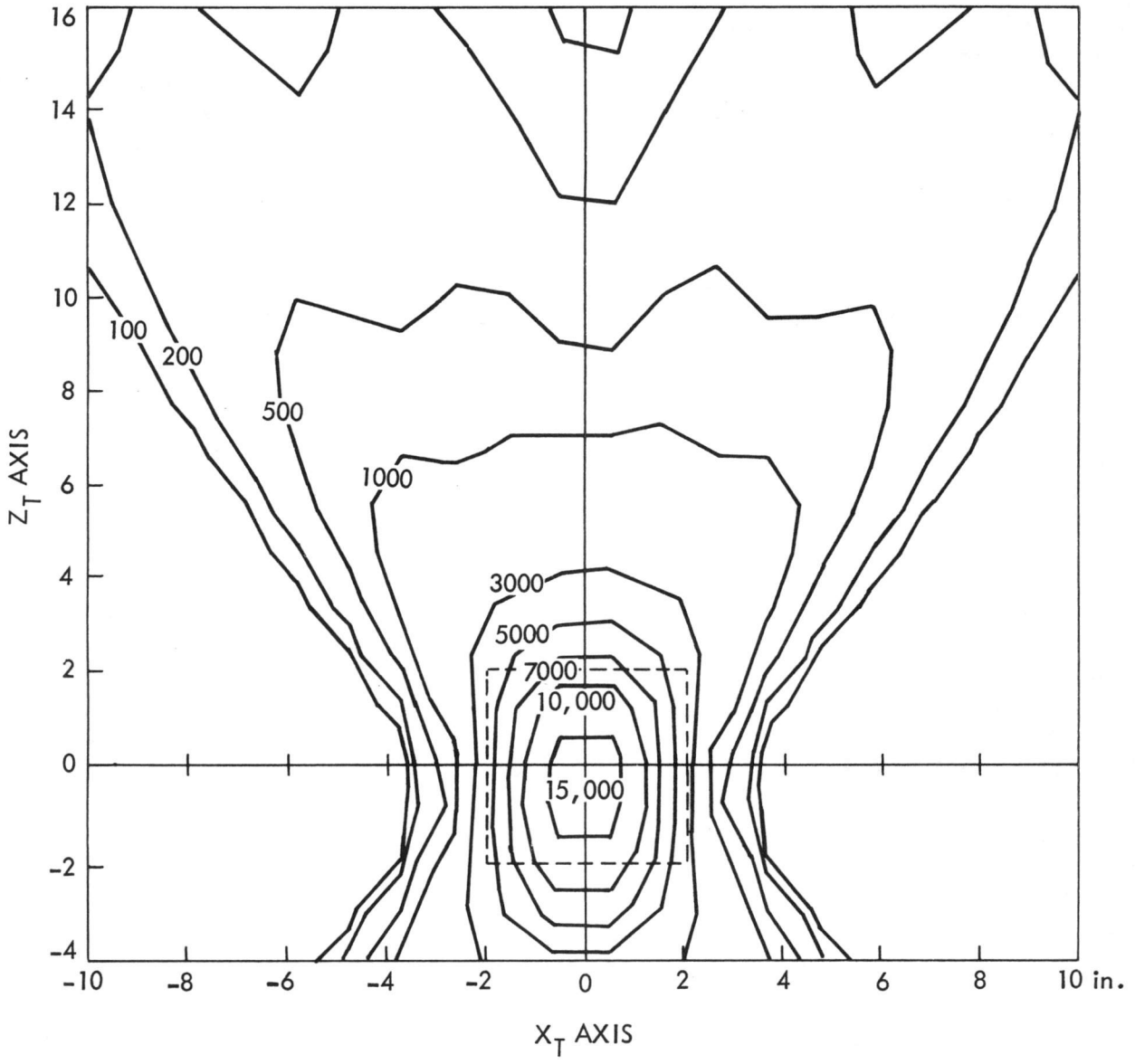

Figure 8-8. Equal Intensity Contour in X_T-Z_T Plane

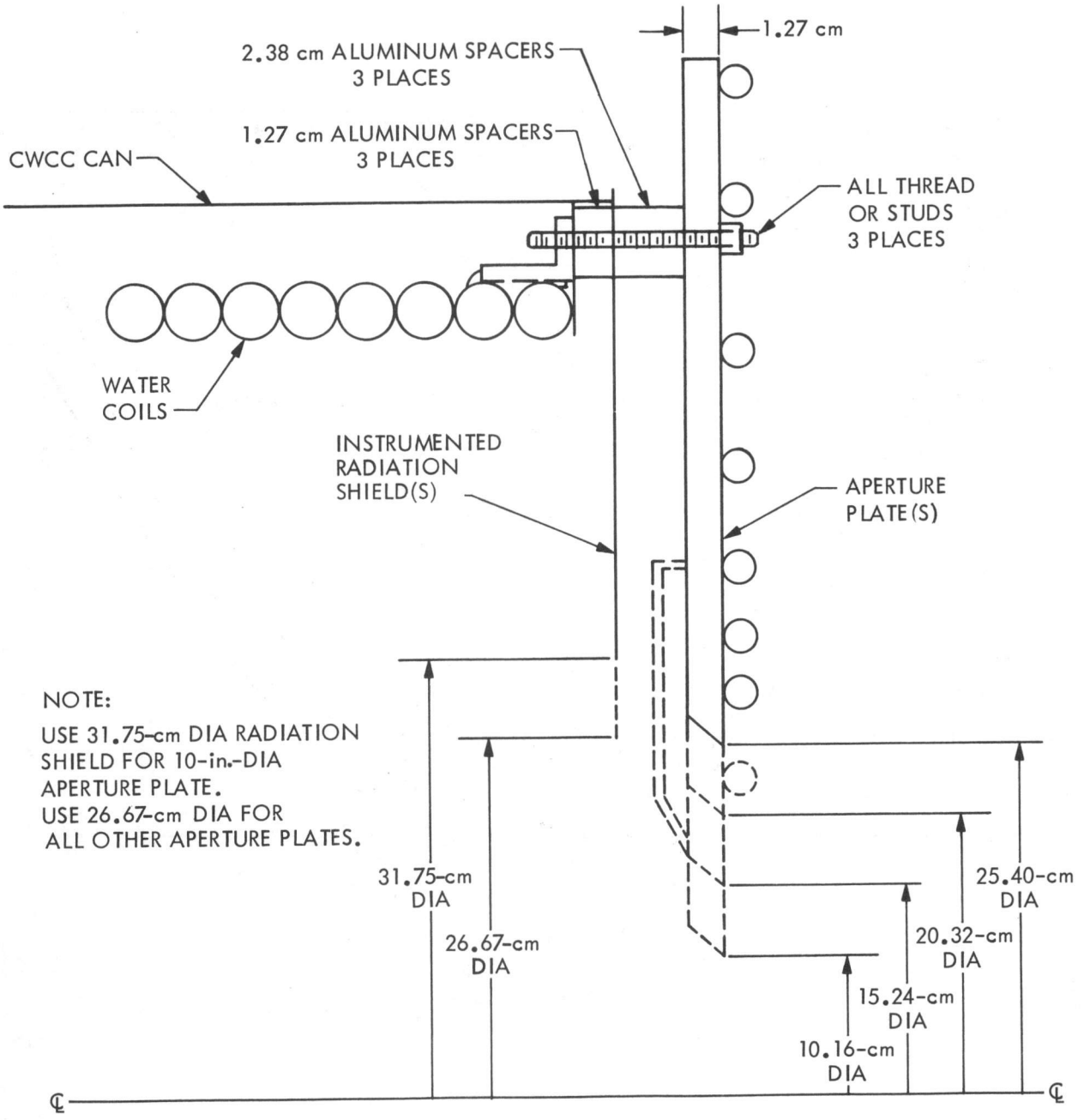

Figure 8-9. CWCC Radiation Shield and Aperture Mounting Assembly

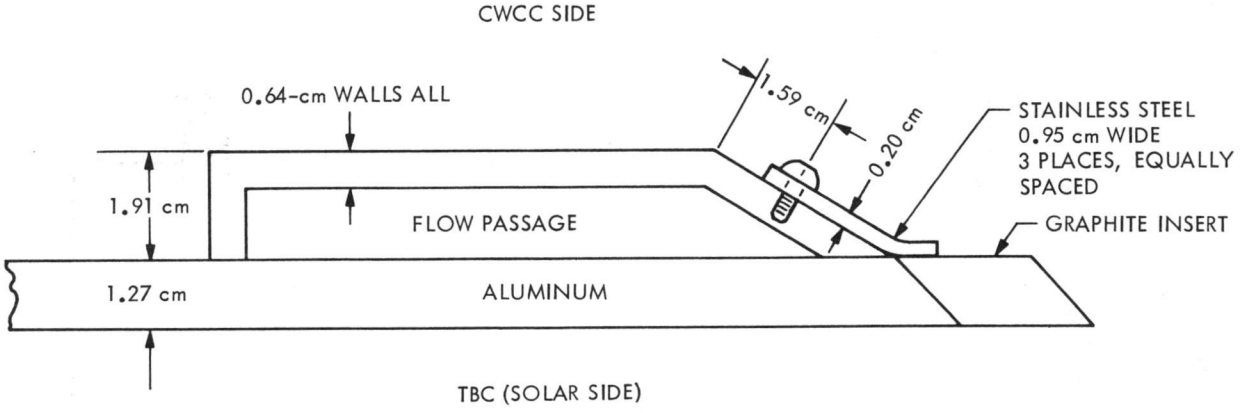

Figure 8-10. CWCC Graphite 10.16-cm-Diameter Insert Retainment

A schematic of the flow and instrumentation diagram is shown in Figure 8-11. Water flow rate, inlet temperature, inlet pressure, exit pressure, and inlet to exit temperature differential were recorded for both the cavity calorimeter and aperture plate. Cavity temperatures and various exterior temperatures of the hardware were also recorded.

Procedure. Testing was conducted by first recording calibration data and then establishing flow based upon mirror configuration and insolation to obtain a 6.7°C temperature differential across the calorimeter. Flows were adjusted using the pump bypass and exit valving on the calorimeter and aperture. Minimum flow through the aperture was 0.378 kg/s (6 gal/min) for the coiled tube apertures and 0.560 kg/s (9 gal/min) for the 15.24-cm cavity flow passage aperture. The concentrator was instructed to acquire sun; upon reaching steady conditions, minor calorimeter flow corrections were made by adjusting the pump bypass to achieve close to a 6.7°C calorimeter temperature differential. Upon reaching an acceptable condition, data were acquired for 20 to 30 minutes. If uneven solar flux spillage was observed on the aperture plate, tracking offset adjustments were made to correct the condition and another 20-to-30-minute run was recorded. Only elevation tracking corrections were made, always to the same value [from elevation offset (ESO) = +0.21 to ESO = +0.01]. At the conclusion of solar testing, water flows were maintained and data were recorded for a non-solar period of about 10 minutes.

Sixteen tests were conducted from July 22 to August 5, 1981, for 15.24- and 20.32-cm-aperture diameters with 56 ("25%"), 112 ("50%"), 176 ("80%") and 220 ("100%") mirrors uncovered, and additional runs were performed at 100% with 10.16- and 25.40-cm aperture diameters. Partial power mirror configurations

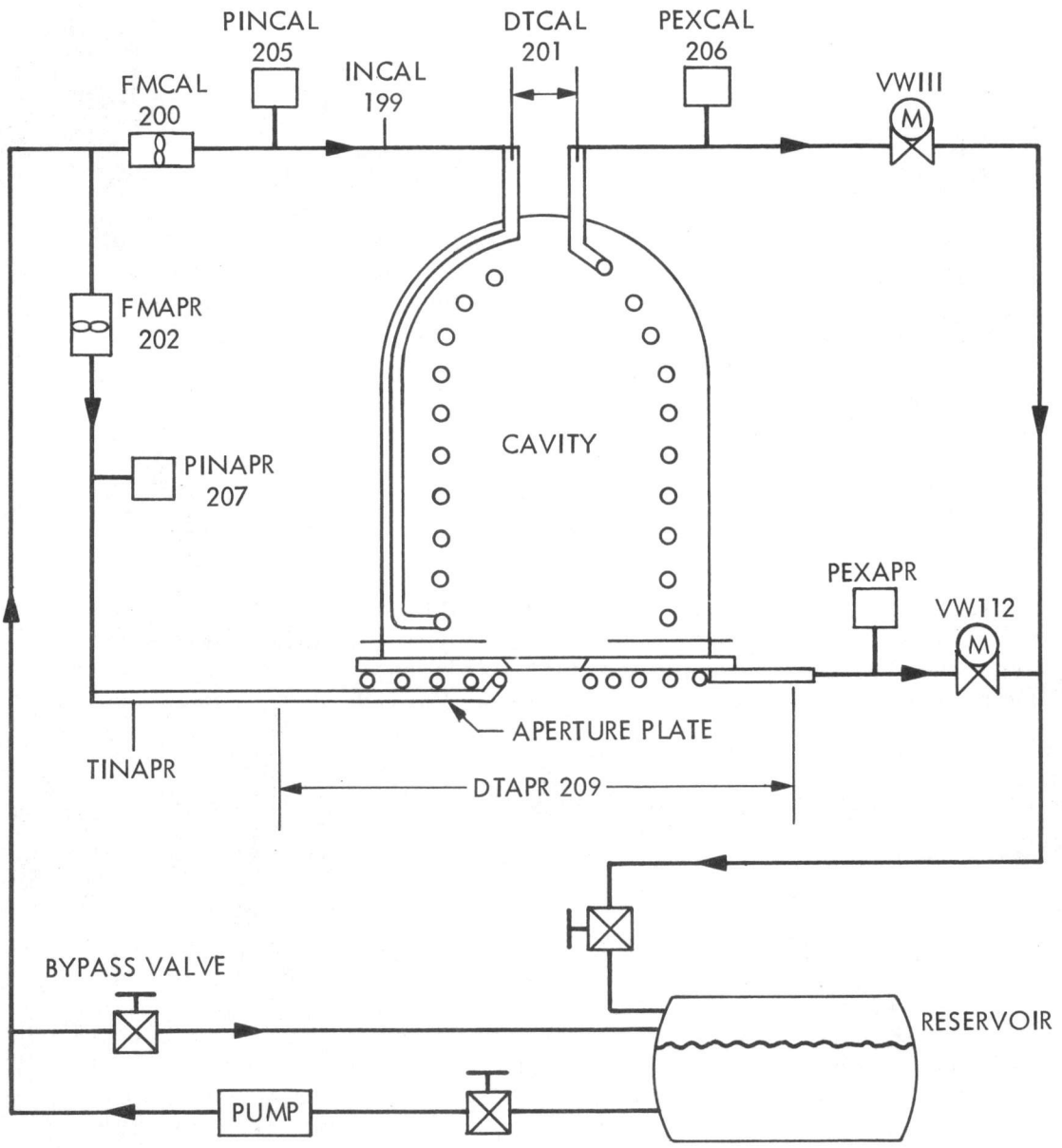

Figure 8-11. CWCC Flow Instrumentation Diagram

are shown in Figure 8-12. Percentage power values are shown in quotes because they are not all exact percentages and depend upon the total number of mirrors being either 220 or 224.

Data Reduction. Data were reduced using algorithms designed for use on the PDP 11 data acquisition/recording computer. Based upon inlet and exit water temperatures, the enthalpy, specific volume, and saturation pressure for saturated liquid water were evaluated from polynomial curve fits to tabular data. Assuming incompressible fluid assumption, sub-cooled state water enthalpies were extrapolated by:

$$h_{act} = h_f + v_f(P_{act} - P_f)$$

where the subscript "act" means actual value and "f" means saturated fluid value. Power from exterior sources (including solar) was determined from energy balance by m (h_{out} - h_{in}). This method should correct for "flow work" due to pressure loss; however, residual power was observed under no solar input. This residual amount was considered the result of small error due to incompressible flow assumption, pressure and temperature difference calibration, and heat transfer with the ambient. To determine solar power, observed power under solar test was reduced by this non-solar amount. This corrected value was then normalized to 1000 W/m^2 from the Eppley pyrheliometer data.

Results. Final results of testing are shown in Table 8-4 for the various aperture sizes and power levels. TBC-2 was tested for power delivered within 10.16, 15.24, 20.32 and 25.40-cm-diameter apertures at the focal point with the cold-water cavity calorimeter. For a 20.32-cm-diameter aperture, power delivered normalized to 1000 W/m^2 insolation was 77.3, 64.7, 42.4, and 19.5 kWt for 220 ("100%"), 176 ("80%"), 112 ("50%"), and 56 ("25%") mirrors uncovered (percentage power), respectively. From the table, it is evident that a concentrator tracking ESO of +0.01 deg is slightly better than the original tracking of +0.21 deg. This was also the consensus from visual observation of spot on the aperture.

C. POWER CONVERSION UNIT DEVELOPMENT

Fairchild Industries, Stratos Division, was awarded a contract by JPL in FY 1979 to develop a hybrid solar/natural gas combustor receiver (Reference 28). FSD also studied the alternative kinematic-type Stirling engines and selected USAB to modify their existing Model 4-95 (P-40) Stirling engine for use with a developmental dish/Stirling power system composed of an FSD/USAB power conversion unit mounted on an 11-m-diameter E-Systems/JPL test bed concentrator unit. FSD awarded a contract to USAB, who redesigned the Model 4-95 (P-40) for this developmental application (Reference 29).

1. Design Modification of the USAB Model 4-95 (P-40) Stirling Engine

While the concentrator is tracking the sun, the engine assumes an inclination varying between 90 and 180 deg relative to its normal upright position. This required changing to a "dry-sump" engine lubrication system

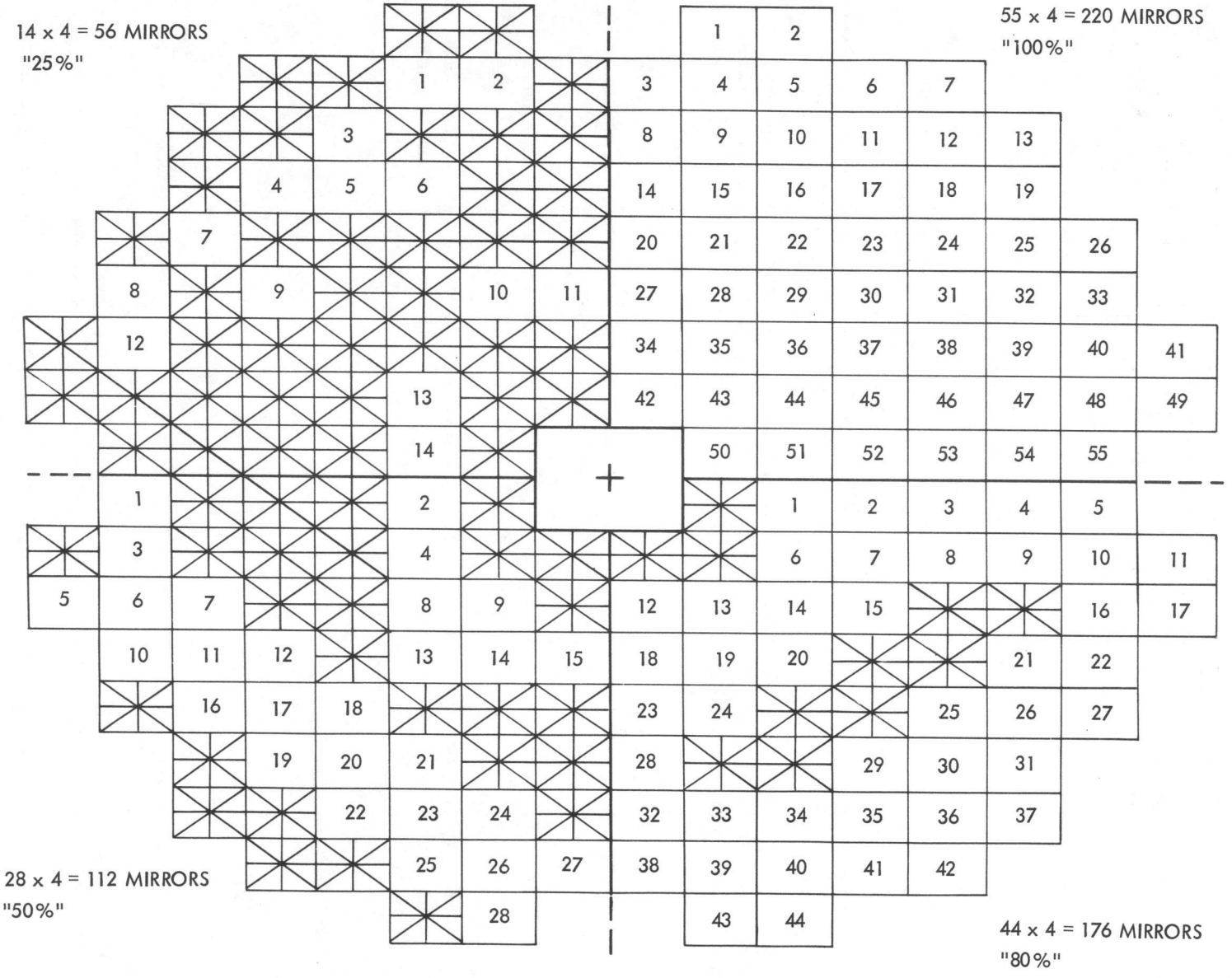

Figure 8-12. TBC Mirror Configurations

Table 8-4. TBC-2 Power Input versus Aperture Diameter and Mirror Configuration (Corrected to 1000 W/m^2 Insolation)[a]

Mirror Configuration, %	Tracking Offset, deg	Aperture Diameter, cm			
		10.16	15.24	20.32	25.40
25	ESO = +0.21	-	20.2 kWt	19.5 kWt	-
	ESO = +0.01	-	20.6	-	-
50	ESO = +0.21	-	40.1	42.4[b]	-
80	ESO = +0.21	-	60.1[b]	64.7[b]	-
	ESO = +0.01	-	60.4[b]	64.7[b]	-
100	ESO = +0.21	-	76.2[b]	76.8	77.8 kWt[c]
	ESO = +0.01	67.1 kWt[c]	-	77.3	-

[a]Azimuth offset (ASO) = -0.20 deg for all tests.

[b]Corrected with calculated estimate of Eppley pyrheliometer insolation.

[c]Location of calorimeter to TBC mount ring changed by removing 0.95 cm of mount spacers from lower right (looking at concentrator mirror surface) mounting leg.

and modification of the engine cooling system. The changes to the lubrication system involved replacing the internal oil pump by an external pump, and the existing oil sump by a separate oil tank. The engine and the tank are connected by nine drainage lines. Two of these, which carry a major part of the oil flow, are routed to a separate scavenge pump that keeps oil from accumulating inside the engine and interfering with the movements of the cross heads. The remaining lines, one of which drains the working gas compressor, work by gravity forces alone. As these lines carry a much smaller flow, there is ample capacity. The main oil pump and the scavenge pump are stacked on the front of the engine and driven by an extension of one of the two crankshafts.

The major purpose of the work was to perform a module systems-level test with the engine and associated equipment including a test bed concentrator, hybrid receiver, and alternator. Specifically, the engine and a GE alternator type No. 193B4014AD were interfaced using a specially designed intercasing, containing a Layrub coupling. This coupling is capable of absorbing all kinds of minor misalignments and of damping torsional vibrations.

The engine and alternator were supported in a main frame by six flexible mounts. Four of these were connected to the engine by individual brackets. The two legs on each side of the alternator were joined with a beam, and the remaining flexible mounts were centrally located on these beams. The flexible element in the mount consisted of two concentric cylinders with the annular space between filled with rubber.

The hybrid receiver, designed and manufactured by FSD, was supported entirely by the engine and replaced the standard combustion system and heater of the P-40 engine. The standard P-40 cylinder and regenerator tops were brazed to the receiver cone, and the whole assembly was bolted to the cylinder block in the normal way. The bolt holes, by which the standard external heat system was fastened to the engine, were used to keep the receiver casing and the natural gas combustion system in position. Some of the receiver auxiliaries were mounted on one of the engine brackets inside the flexible mounts to prevent relative motion between receiver and auxiliaries.

The main frame, finally, was bolted to the test bed concentrator mounting ring at four locations. This main frame was rigid enough to distribute the load uniformly inside the mounting ring and prevent distortion of the ring itself.

The engine electronic control unit interfaced with the system electronic control unit. The power output of the engine was controlled by varying the internal gas pressure of the engine. In this application, the power output was held constant by manually setting the gas pressure at a fixed level and keeping the temperature of the receiver constant. This was done by a separate temperature control system that controlled the firing rate of the natural gas combustion system so that the total amount of heat absorbed from solar insolation and hot combustion products remained constant. This temperature control system was part of the receiver package.

The most complicated part of the control was the start-up sequence. In a simplified way, the engine-related part of the sequence may be described as follows: (Note that in this particular test series the engine was always started in the combustion-only mode, i.e., with the concentrator not tracking the sun.)

(1) Prepare engine for start with working gas pressure at low level (4.5 MPa) and cooling water pump in operation.

(2) Fire combustion system at 50% of full load.

(3) Simultaneously with firing the combustion system, start cranking the engine by connecting alternator to grid. To prevent excessive bearing loads, the time to speed the engine up to 1800 rev/min is limited to 3 to 5 seconds by use of starting resistors.

(4) When the receiver tube temperature has reached 700°C, which should take about one minute, the engine is ready for full power operation. The combustion control system is now switched to constant temperature control and the engine working gas pressure raised to a level determined by the preset power output.

(5) The concentrator may now start tracking the sun.

Any stop sequence (normal or emergency) was initiated by turning the concentrator away from the sun and shutting off the fuel supply. The normal stop routine continues as follows:

(1) Reduce working gas pressure to a low level. When engine ceases to produce power, disconnect the engine from grid.

(2) After a predetermined soaking time (10 minutes) or when cooling-water temperature has dropped to a safe level, the cooling-water pump may be switched off.

The output power from the engine could be reduced almost instantaneously by short-circuiting the engine, i.e., interconnecting the four normally independent Stirling cycles in the engine. The same heat flux was drawn from the receiver, but more heat was then rejected to the cooling water. This feature was used, for example, to protect the engine from overspeeding should the grid suddenly be disconnected. As this maximum speed was on the order of 5000 to 6000 rev/min with hydrogen as the working fluid, the short-circuiting function was useful to protect the alternator. The same function was capable of forcing the engine to a complete stop within a few seconds after disconnection from grid in an emergency.

The necessary control signals to and from the engine electronics are summarized in Figure 8-13. This figure also contains a recommended set of engine-related indication lamps and continuous displays for the instrument panel.

As the Stirling cycle computer codes have been extensively calibrated and validated against numerous laboratory tests with several individual P-40 engines and because the gas passages in the hybrid receiver are reasonably similar to the passages in the standard P-40 heater, it was possible to predict the performance of the solar engine with reasonable accuracy.

The nominal efficiency at 15 MPa working gas pressure and 710^{o}C heater tube outer wall temperature is 35% as expressed by the ratio of engine shaft power to heat absorbed by the working gas. Shaft power is 22.5 kW. This is 1.5 percentage units (or about 4%) and 2 kW lower, respectively, than consistently predicted for a P-40 with a standard heater. This small discrepancy is due to the fact that the receiver had to be designed for an existing engine and an existing concentrator and that the hybrid mode requires the heater tubes in the receiver to be capable of absorbing solar as well as combustion gas heat.

2. Assembly and Factory Testing of the USAB Model 4-95 (P-40) Stirling Engine

Procurement of components for the baseline 4-95 Stirling solar engine (No. 21 in series) began September 1, 1980, with engine assembly later that month. Acceptance testing was to be done at the USAB facility in Malmo, Sweden, using a conventional fossil-fuel combustion system and with the engine upright rather than inverted (Reference 30).

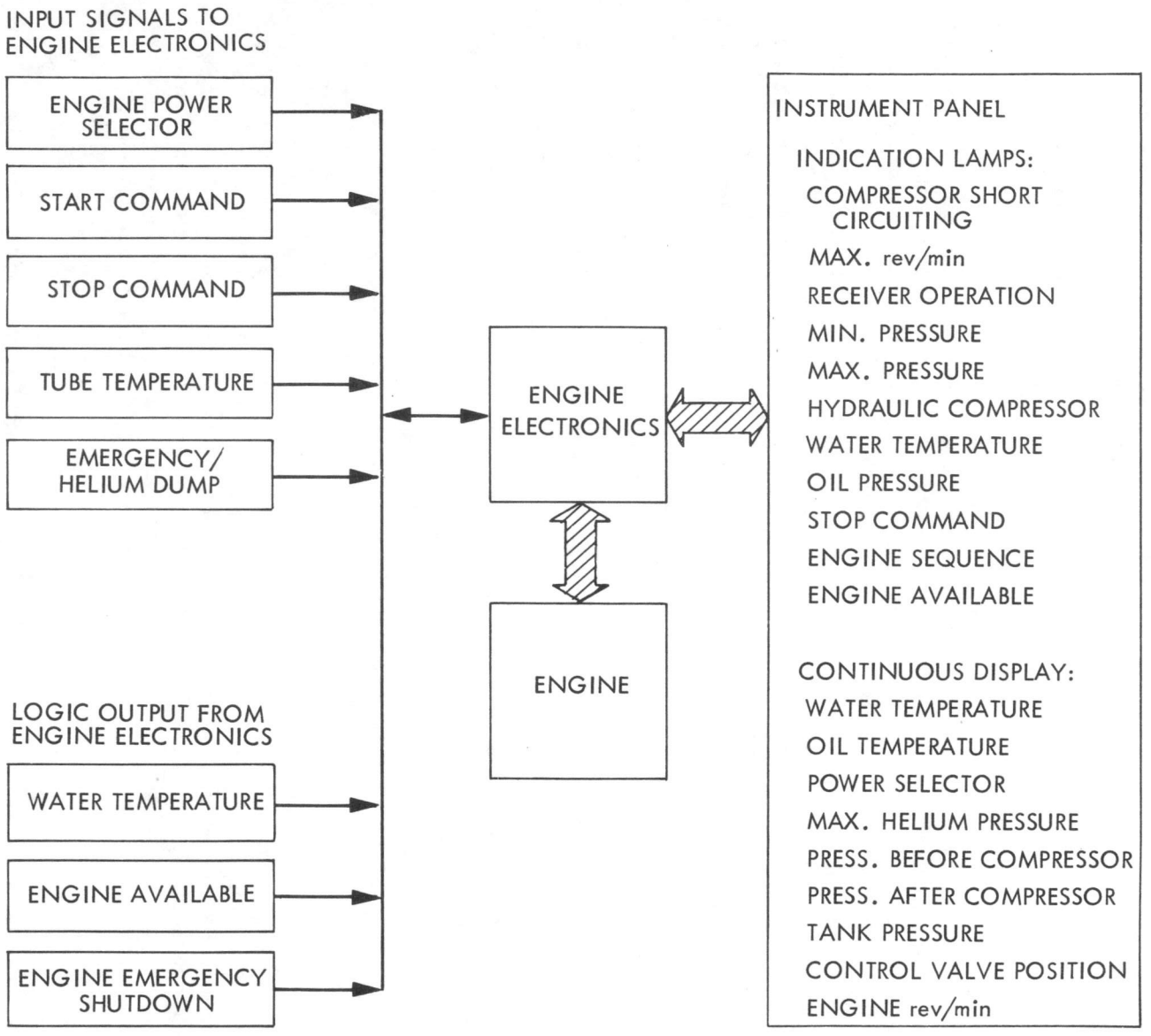

Figure 8-13. Engine Electronic Control Unit Input and Output Signals

The engine began its initial dynamometer "run-in" for checking out engine functions on November 13. The test included constant speed operation, with helium as the working fluid, at 1800 rev/min and half load for about 11 hours. Following this, acceptance tests requiring about 12 hours were run between idle and full load (3 to 15 MPa mean pressure) and between 600 and 4000 rev/min at 720°C nominal tube temperature and 50°C coolant temperature. Data logging included usual temperatures and pressures and all parameters required to determine power and thermal efficiency over the load and speed range. Final tests included control system measurements, requiring 8 hours.

During the acceptance and control tests, check out of data indicated higher than normal friction, especially at the lower speeds. At the end of 31 hours, the engine was disassembled for inspection. One cross head and its cylinder liner were found scuffed as the result of improper clearance and, possibly, as a result of lube oil contamination with machining residues from fabrication. After cleaning and replacing the parts, a second run-in test was made for 11 hours, followed by 6 hours of acceptance testing between 1000 and 4000 rev/min under all load conditions. Data indicated no further problems, and the tests were completed after a total of 48 hours running time on December 8, 1980 -- ahead of schedule.

Results of testing engine 4-95 No. 21 with a standard involute heater showed that the engine power at 1800 rev/min ranges from 20 kWe at 11 MPa to 27 kWe at 15 MPa. Auxiliaries include the lube oil pump and the helium pump, which were the only ones to be engine-driven at the PDTS. (The water pump would be at ground level.) The solar thermal efficiency ranged from 37% at 11 MPa to 39% at 15 MPa, on helium. On hydrogen, the efficiency at 15 MPa was estimated to be 40%.

After completion of the dynamometer testing, modifications to the lubrication system for inverted operation were started (Reference 31). Design and fabrication were accomplished in cooperation with Ricardo of England, with whom USAB had a cooperative agreement. Modifications included machining numerous holes and slots to form oil drain passages in the crankcase bulkheads and in the gas compressor housing. The goal was to provide adequate oil drainage by gravity alone. This was achieved in static tests made at Ricardo with the crankcase inverted as well as horizontal. To further assure "dry-sump" operation under dynamic conditions, an external scavenging pump was installed, driven from one of the crankshafts. The external pressure lubrication pump was fitted adjacent to the scavenge pump. An external oil drain tank was installed below the lowest (under all orientations) drainage point and connected to seven crankcase outlets by short pipes.

The principal unknown during the design phase was the effect of oil flooding on the piston rod sliding seals (termed by USAB, the "PL seals"). Because the PL seals are normally in the "upper" part of the crankcase and, therefore, continuously drained, it was believed they might be incapable of pumping outward against the additional head of oil that might occur with the engine inverted, thereby contaminating the engine working spaces with lubricant.

Integration of the engine/alternator unit to the TBC-2 mounting ring was made by fabricating a steel frame of square tubes that forms the interface between the mounting ring bolt circle and the engine/alternator mounts. For

testing at USAB's laboratory, the main frame was attached to a secondary mounting frame having a horizontal axis to allow rotation of the engine for inverted operation. The engine and frame assemblies can be seen in Figure 8-14.

Engine testing was done with helium working gas, as specified by JPL. At all times, the load was carried by the alternator connected to the local grid. Because Swedish frequency is 50 Hz, the engine was run at 1500 rev/min under all load conditions. The engine was started by running the alternator as an induction motor using a tapped transformer at reduced voltage to increase the time to reach 1500 rev/min to about 7 seconds in order to moderate bearing loading at low speeds. The engine was initially tested in the inverted position with the combustor in place to study the oil flow distribution and the PL seal operation. Minor problems with oil flow were solved by increasing the drainage pipe area. Initial running while inverted gave some indication of a PL seal problem, with oil contamination occurring in one cylinder. However, upon examination of the seal, it was found to be improperly manufactured. After replacing it, no further oil problems were encountered during the entire laboratory test program, with the engine operating between horizontal and inverted positions.

After 130 hours of initial testing, the engine was performance tested for 25 hours, followed by 175 hours of endurance running. The engine was disassembled for inspection at 100 hours and after the endurance run. No problems were encountered. Further checkout tests and demonstration runs resulted in a total of 350 hours of successful operation under simulated solar dish orientation. The gasoline combustion system appeared to function

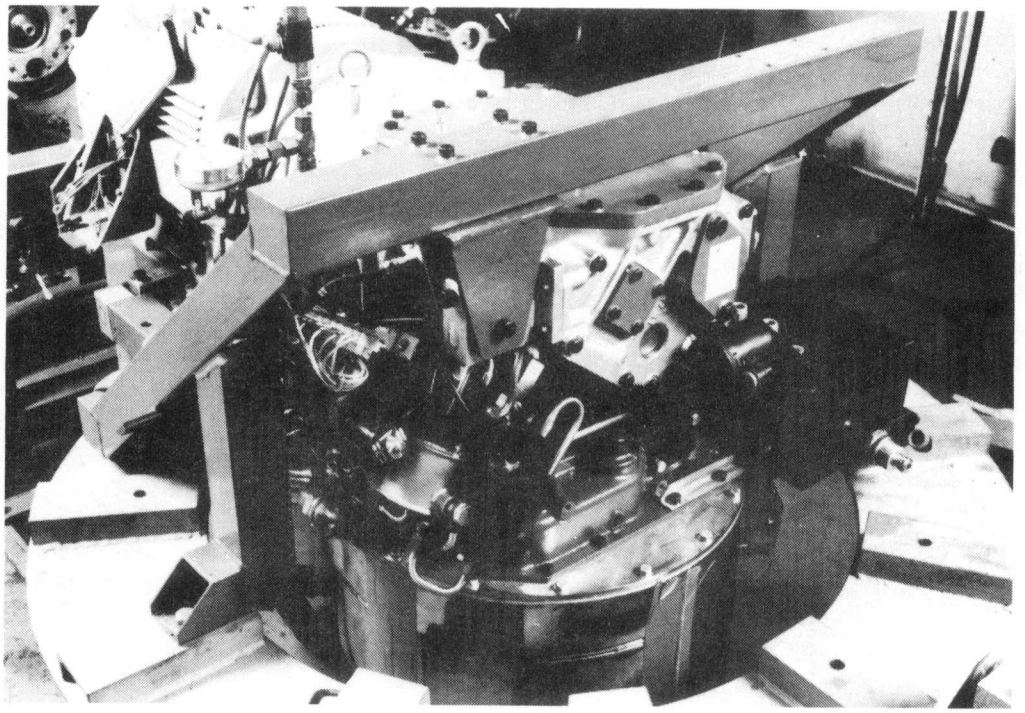

Figure 8-14. 4-95 Engine Inverted with Combustor and TBC Mounting Ring

properly in all positions, and the induction alternator operated as expected. Alternator efficiency was outstanding -- 92 to 93%. USAB has learned that near future designs could be expected to approach 95%.

The measured performance at 1500 rev/min for various levels of working gas mean pressure, which is proportional to load, was obtained. Maximum power was 22 kWe output, at an overall efficiency of 31.5%. The average temperature of the involute heater tubes (outer wall) was 720°C, and average cooling water temperature was 50°C. Auxiliaries driven by the engine included the lubricant and scavenge pumps and the helium compressor. Based on an alternator efficiency of 93% and a burner efficiency of 89%, the "solar" thermal efficiency is calculated to equal 38% (net heat to solar heat exchanger and shaft power output).

It is estimated that efficiency at 1800 rev/min is nearly identical to that at 1500 rev/min, and the maximum power is 20% higher. Performance in the inverted position was found to be the same as measured when running upright, as was expected.

After completion of testing in Sweden, the engine was shipped to the PDTS in June 1981 for integration with the DSSR (described below) and installation on a test bed concentrator (Figure 8-15).

3. Design, Construction, and Factory Test of the Solar/Gas-Fired Receiver Assembly

This section describes the design and development effort of a gas-fired, combustion-augmented dish/Stirling solar receiver (DSSR) assembly, which was specifically designed to operate with a modified USAB P-40 engine/alternator and a test bed concentrator. This PCU has a design output of 25 kWe at an overall conversion efficiency (sunlight to electric output) of approximately 30%. The DSSR and P-40 engine/alternator mounted on the test bed concentrator is shown artistically in Figure 8-16.

The principal function of the DSSR is to convert concentrated sunlight to heat and to supply this heat directly, efficiently, and uniformly to the Stirling engine hot end without intermediate heat transfer devices, such as heat pipes or thermal buffer storage.

The gas-fired combustion augmentation, which uses natural gas as fuel (but could be designed to use a variety of gaseous and liquid fuels), provides the capability to supplement the heat available from the sun with heat from another source on cloudy days or at night, so that the system can provide a controlled electrical output at all times. The available solar energy is always used first and then augmented with combustion heat, as necessary.

a. Design Requirements. The solar/gas-fired receiver assembly would intercept a continuous peak of 76.5 kW radiative energy rate from a paraboloidal solar concentrator unit with optical parameters of focal length to diameter ratio of 0.6 and a 3-mrad standard reflector slope error. The dish/Stirling solar receiver assembly would incorporate a solar to working gas heat exchanger with an even distribution of radiative energy flux of no more than 50 W/cm^2. The DSSR assembly included a gas-fired combustor

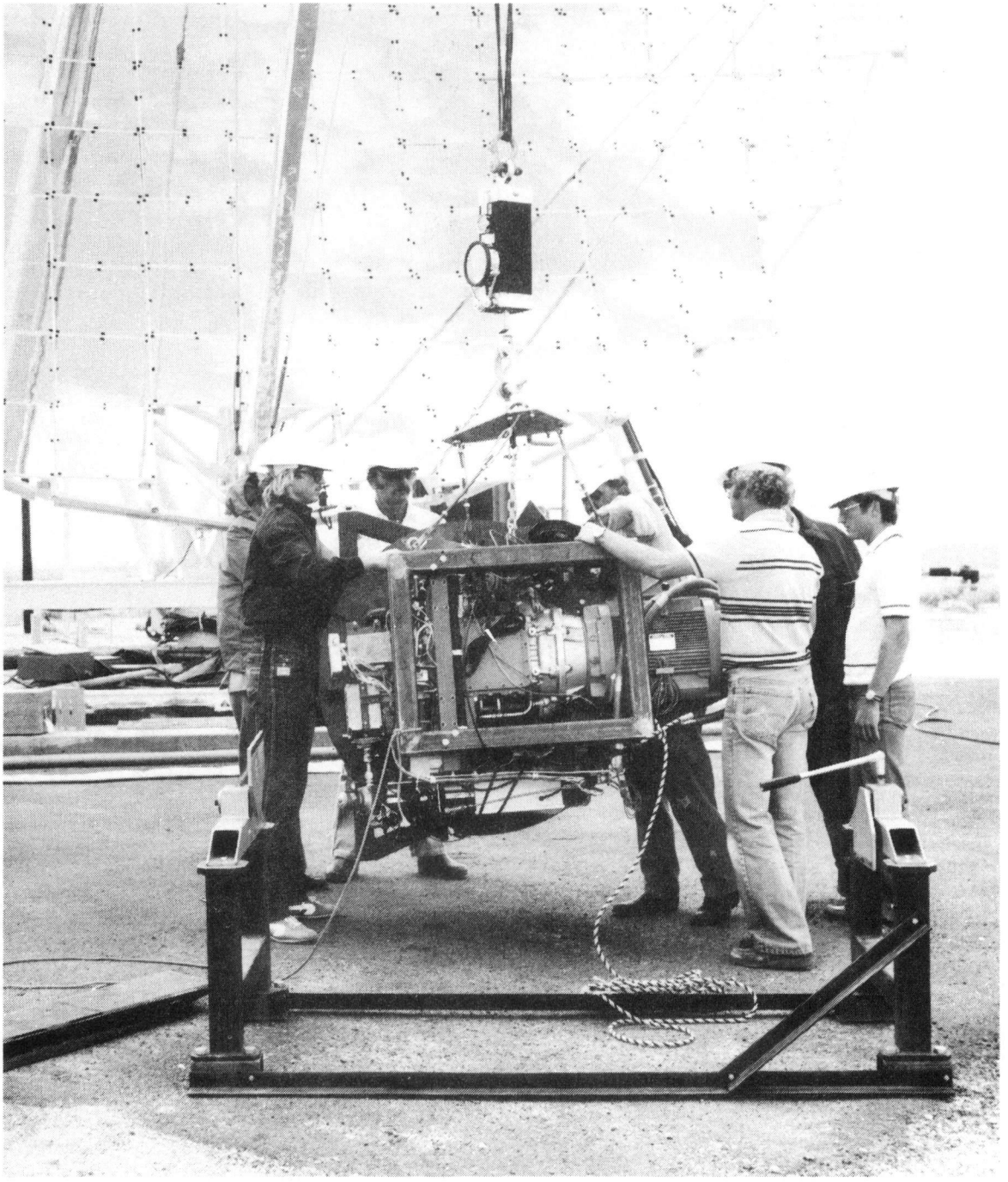

Figure 8-15. First Dish/Stirling Power Conversion Unit Being Mounted on TBC-2

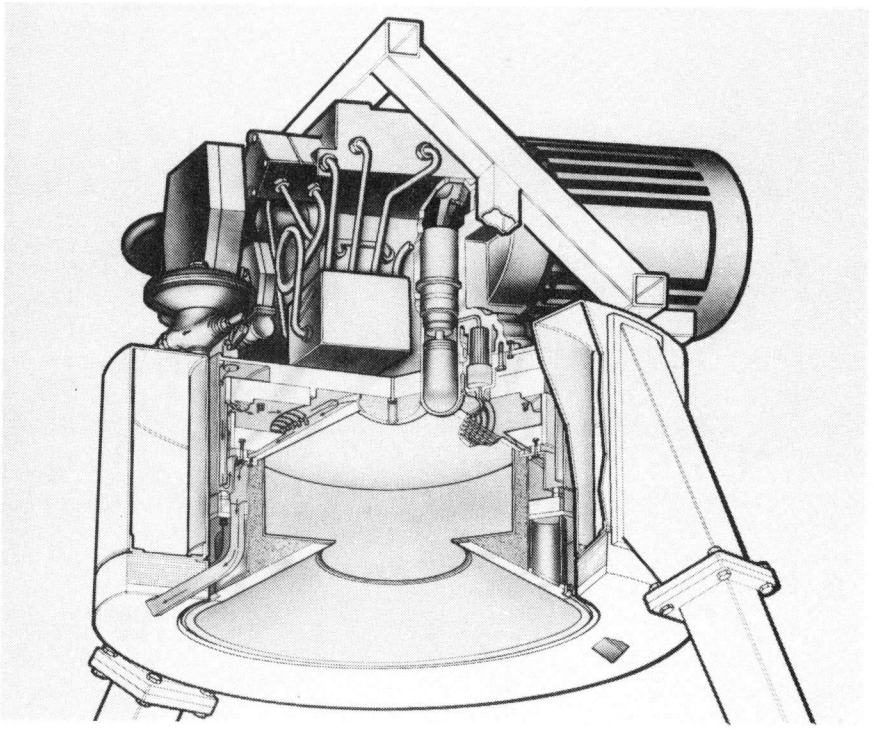

Figure 8-16. DSSR and P-40 Engine/Alternator

subassembly supplying up to 70 kWt to the helium working gas of a USAB Model 4-95 engine operating at 20 MPa maximum pressure and at temperatures ranging from 660 to 815°C. The gas-fired combustor assembly would have a turndown ratio of 10:1, thereby allowing a continual combustion flame. Total mass of the PCU with the DSSR could not exceed 750 kg.

In addition, certain important design constraints were imposed on the receiver design by the P-40 engine.

(1) The total flow area of all heater tubes must be the same as the area of the standard P-40 heater head.

(2) The L/D (L = tube length, D = inside tube diameter) must be as close to 100:1 as possible.

(3) The orientation and location of cylinders and regenerators and their manifolds (including their offset in the horizontal plane, as shown in Figure 8-17) must remain unchanged.

b. Receiver Design. The basic design of the receiver and the analytical substantiation of its design and performance has been reported in Reference 28. The general arrangement of the receiver is shown in Figure 8-18.

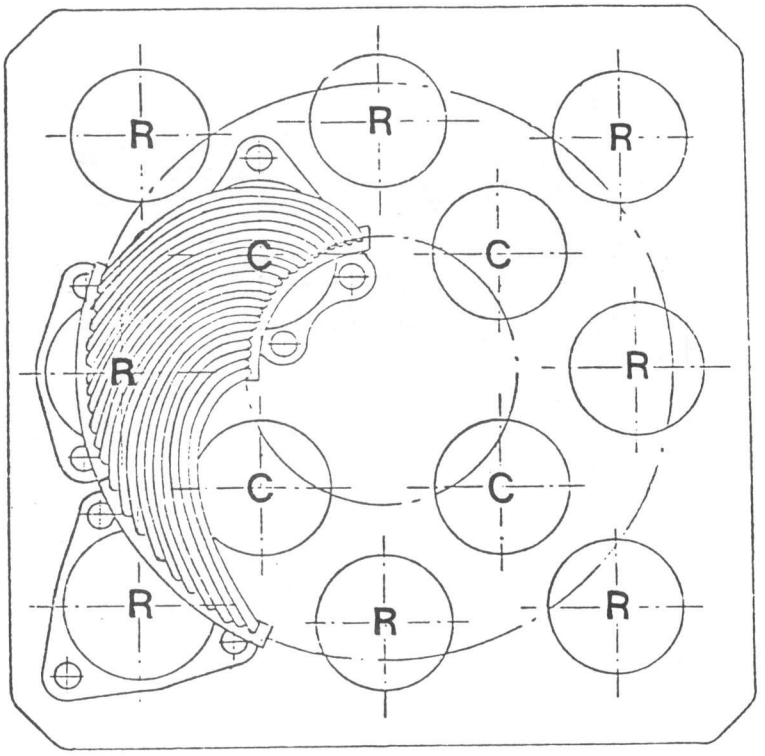

Figure 8-17. P-40 Cylinder and Regenerator Arrangement

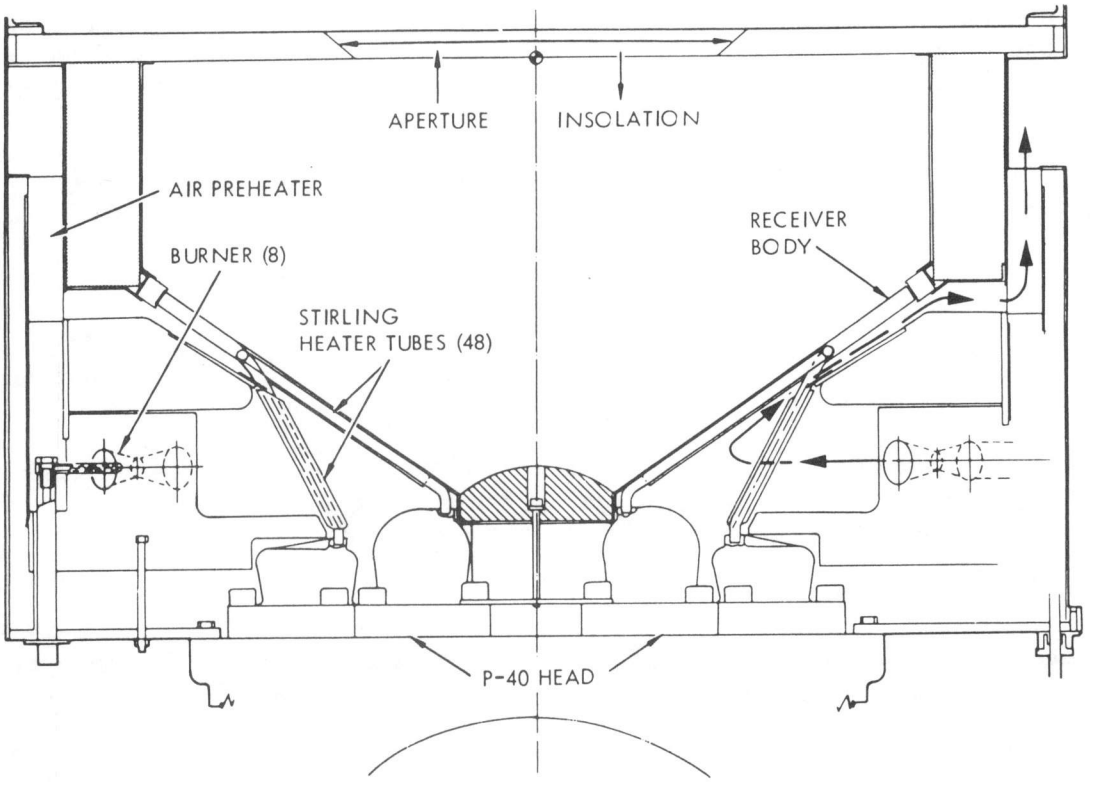

Figure 8-18. Dish/Stirling Solar Receiver

The receiver was divided into two sections: an upper section that contained the optical receiver cavity covered by a conical ceramic aperture plate and a lower section that contained the combustion system. The two cavities were separated by a conical receiver body made of copper encapsulated in Inconel 617 for oxidation protection and structural rigidity at elevated temperatures. Forty-eight equally spaced Inconel 617 engine heater tubes were embedded in the copper in such a manner that a near-uniform temperature was maintained around and along the heater tubes, despite the non-uniform solar flux impinging on the surface of the cone in the optical cavity. The embedded tubes were of sufficient length to transfer all thermal energy from the concentrator to the engine working fluid. Computations showed a uniform temperature distribution on the surface of the receiver cone and within the cavity at full solar flux with the engine working fluid at 649 and 816°C (1200 and 1500°F). The receiver thermal efficiency was calculated to be 87.5% and 82.5% at working fluid temperatures of 649 and 816°C, respectively.

The engine heater tubes, which extend from the bottom surface of the receiver cone to the engine regenerators, were designed with Inconel-clad copper sleeves to provide the necessary heat transfer area and spacing in the combustion mode while uniform heater tube surface temperatures were maintained for engine performance.

In the hybrid mode, the heater tube embedded in the receiver cone was primarily heated by the solar flux and, to a lesser degree, by combustion gases sweeping under the cone. The heater tubes extending from the underside of the receiver cone were heated entirely by combustion gases. Thermocouples attached to these tubes sensed the engine working gas temperature indirectly and provided signal inputs to the combustion system to increase or decrease the firing rate, as required, to maintain a given heater tube temperature. In this way, full utilization of all available solar heat was assured, and combustion heat was only supplied as necessary to provide constant heat input to the engine. This arrangement also allowed the receiver to be thermally stabilized with the engine running prior to focusing on the sun and after detracking, which would minimize thermal stresses and thermal shock and also increase receiver life.

The combustion chamber was designed with eight venturi-type mixing nozzles firing tangentially into the annular combustion chamber, as shown in Figure 8-19. The nozzles were arranged so that a high velocity rotating flow field is maintained in the combustion chamber, providing sufficient residence time to complete combustion while at the same time providing uniform combustion gas temperatures upstream of the heater tubes exposed to the combustion chamber. Ignition and flame safety was provided by a Fenwal spark igniter and flame sensing subsystem. The mixing venturis and fuel nozzles were sized to provide turndown capability in excess of 10 to 1.

A combustion air preheater of annular configuration (shown in Figure 8-20) was located above the combustion chamber around the outer edge of the receiver cone and was designed to preheat the combustion air up to a temperature of 760°C (1400°F). The cold combustion air (from the external electric-motor-driven constant-speed blower) was introduced at the bottom of the receiver housing and flowed in an annulus between the inside of the receiver housing and the preheater and combustion chamber to the top of the preheater. This flow pattern assured cooling of the outer receiver housing by

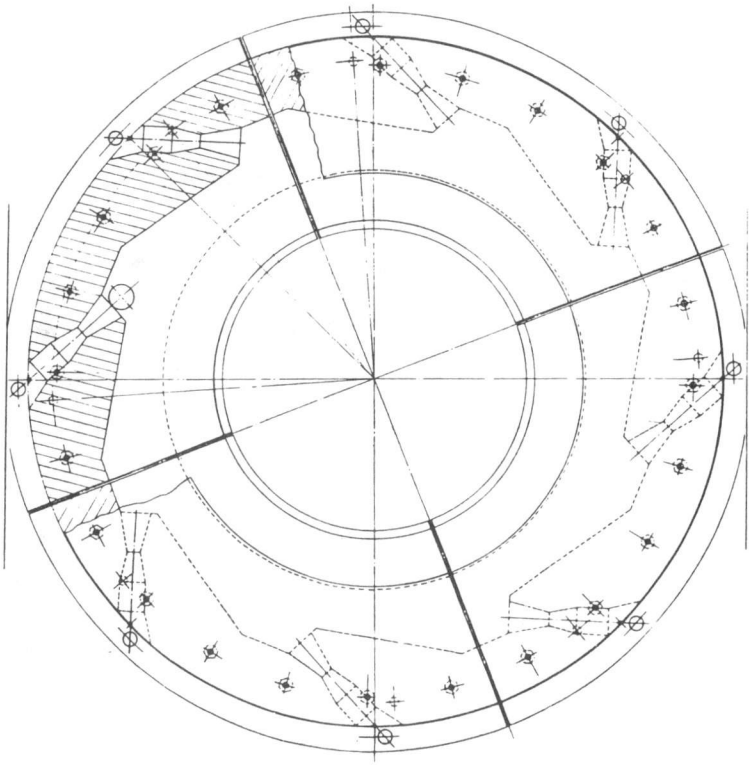

Figure 8-19. Refractory Combustion Chamber

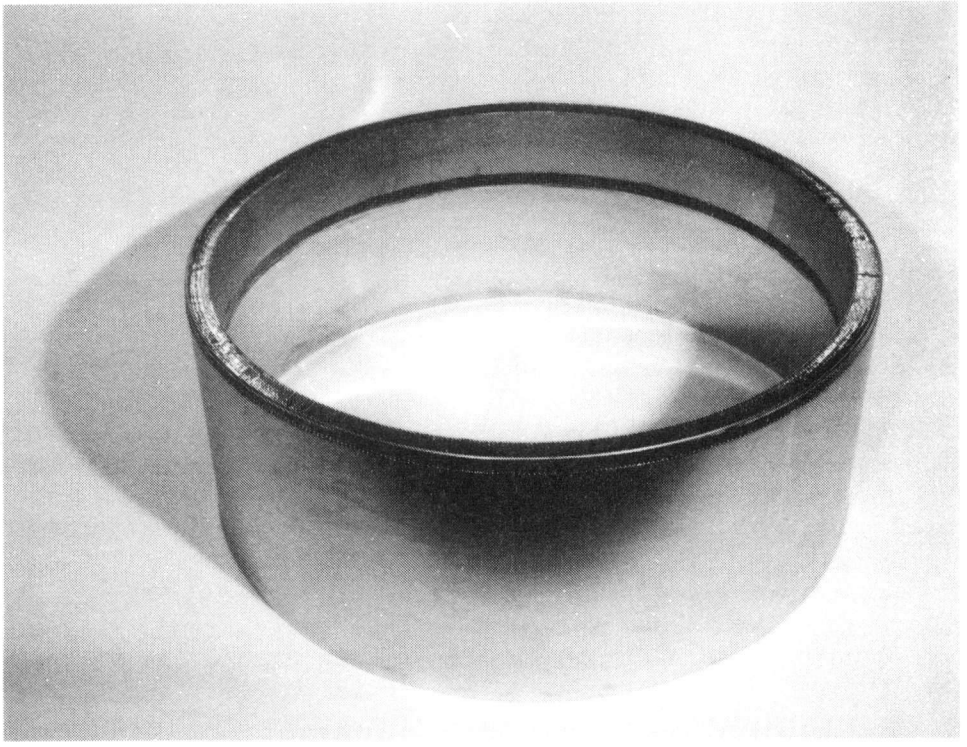

Figure 8-20. Combustion Air Preheater

the air so that the structural integrity of the receiver housing and the surrounding focal mount was maintained, while heat loss from the receiver was minimized. Particular care had been taken in the design to incorporate flexible Fiberfrax seals at critical locations to minimize thermal stresses and facilitate thermal expansion and contraction.

Two exhaust pipes in the front of the receiver, extending from an exhaust manifold behind the conical aperture, directed the exhaust away from the receiver mount and bipod in areas that would not be traversed by the "fireball" during focusing and defocusing of the concentrator.

The external configuration of the receiver is shown in Figure 8-21, which also shows the arrangement of the combustion air blower, a Siemens unit of the side-channel type that is driven by a 1.15-hp single-phase, 50/60-Hz, 115-V electric motor. This type of blower was selected for its high head and low flow characteristics. A commercial air filter (with replaceable filter cartridge) and silencer were installed on the blower intake. The air and fuel control valves were of the electrically operated industrial type by Honeywell, which had been modified at FSD to provide the desired control capability and characteristics.

c. Combustor Tests. An experimental program to evaluate and verify the operational and energy transfer characteristics of the DSSR combustor and heat exchanger system was conducted. The combustor/heat exchanger design was characterized by a single row of closely spaced curved tubes in a swirling cross flow of high-temperature combustion gases provided by eight burner jets. The results of the program verified the ability of the system to meet design specifications for the prototype DSSR. Specific conclusions are:

(1) Cold-start ignition can be achieved at 10% design maximum firing rate with non-preheated 10% excess combustion air.

(2) A two-igniter/probe fuel safety system was inadequate, and a three-igniter probe system was successfully incorporated.

(3) The combustor can be controlled adequately and safely, and operated at a constant air/fuel ratio (10% excess air) over the entire range of anticipated firing rates.

(4) Substantial combustor system air leakages were observed that must be minimized in the final DSSR prototype.

(5) Combustion gas temperatures were lower than expected. A reduction of system air leakages and installation of the air recuperator would provide improvement in this regard.

(6) Average gas-side heat transfer coefficients and semi-local heat transfer coefficients along the lengths of the tubes were obtained. The results showed significantly enhanced heat transfer characteristics for the DSSR heat exchanger when compared to similar data for closely spaced tubes perpendicular to cross

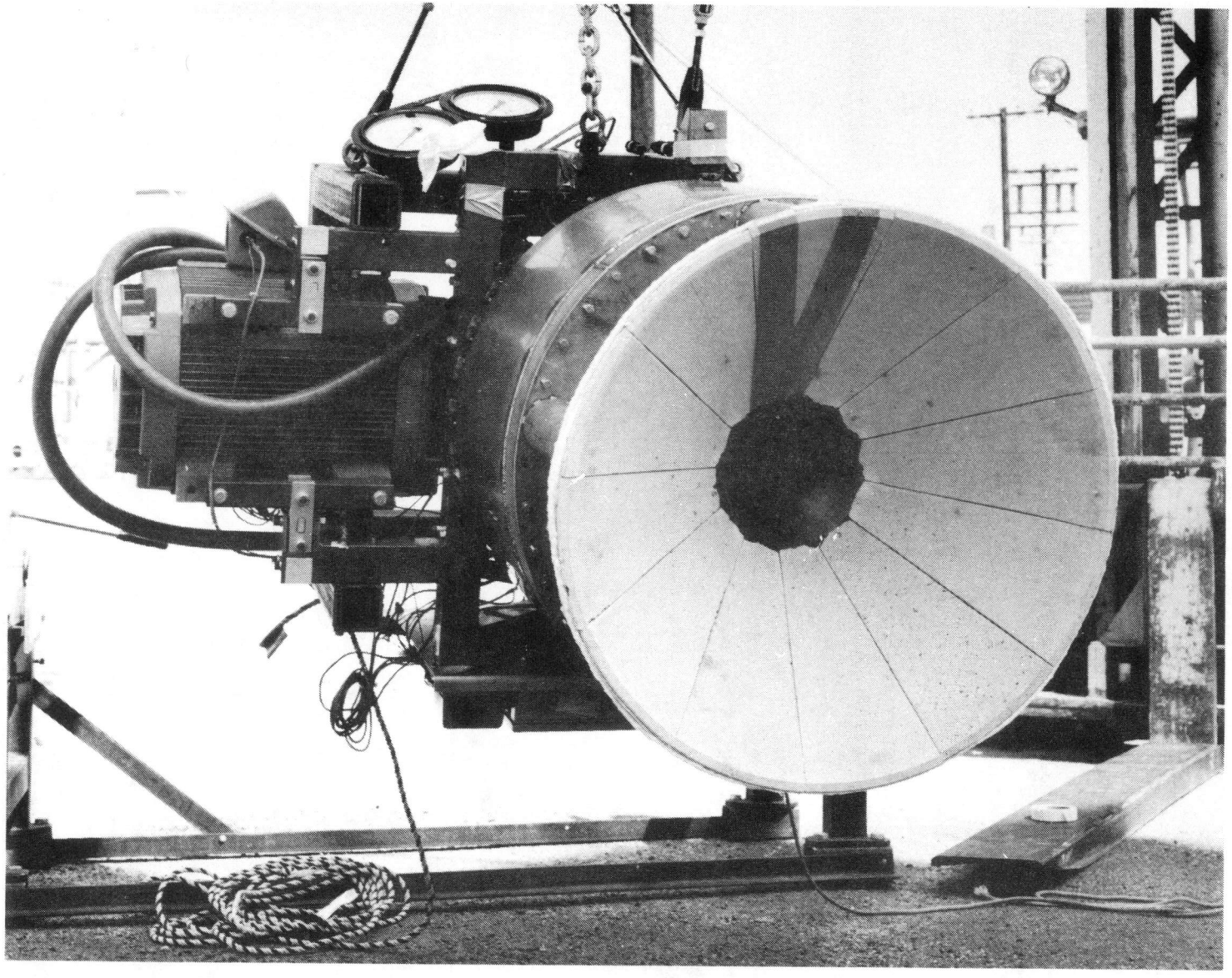

Figure 8-21. Hybrid Receiver, External Configuration

flow. These data provided new information on heat transfer to tubes in cross flow that can be achieved in a high-temperature combustion system when complex geometries such as the one described here are utilized. Furthermore, it was concluded that the present DSSR combustor/heat exchanger met design thermal requirements such that prototype fabrication could proceed (Reference 32).

4. Integration and Test of the USAB Model 4-95 (P-40) Stirling Engine with the FSD Solar/Gas-Fired Receiver

Initial testing by Advanco (Reference 33) of the hybrid receiver and 4-95 Stirling engine was conducted on the precursor pad at the PDTS on September 22, 1981. A heater tube temperature of 600°C was reached when an overheating condition in the GE interface unit triggered an alarm and initiated automatic shutdown.

A GE representative adjusted components of the electric power subsystem on September 23. Testing was then resumed, and the receiver was successfully brought up to its design operating temperature of 717°C as measured on the rear side of the heater tubes. A 4-95 Stirling engine operated smoothly and quietly; the alternator output was 10.2 kWe. The receiver aperture was not installed during this test to allow visual observation of the relative thermal expansion of the receiver quadrants, which causes the heat loss from the receiver cavity to be greater than normal. The receiver quadrant temperatures were 573°C on the rear side facing the combustion gases and 535°C on the front side normally facing the concentrated sunlight.

The combustion was excellent, and the control in a semi-automatic mode maintained proper excess air at all times; however, the fuel flow was difficult to control because of the nonlinear, unpredictable characteristics of the adjustable potentiometer.

The hybrid receiver and 4-95 Stirling engine power module was installed on TBC-2 on October 2, 1981. Following adjustment and checkout of controls and instrumentation and the readiness review on October 28, initial testing with 25% active mirror facets was accomplished on November 9.

Subsequent to the testing, a loss of helium pressure was noted, and the engine and receiver were removed from TBC-2 and inspected.

Quadrant 5 was found to have two heater tube braze joint leaks and was returned to Solar Turbines International (STI) for repair. Quadrant 7, which previously had been repaired by STI, was installed. The receiver was then installed on the 4-95 engine. The assembly and subsequent pressure/leak tests were successfully completed on November 19. Additional thermocouples were installed on the receiver quadrants to allow better monitoring in order to avoid local overheating, which was believed to be the cause of the failure of quadrant 5 on November 9. Improvements in the gas control potentiometer arrangement were incorporated together with an extension for the Corning O_2 probe to avoid direct exposure of the probe to the combustor flame.

The Thermox aspirator was connected in such a way as to draw combustion gases over the probe, which was relocated in a "well" below the bottom surface of the combustion chamber.

After completing 25% active mirror facet tests in early December 1981, testing with 50% active mirror facets was attempted on December 8; however, the test had to be terminated due to a sudden loss of helium pressure. Subsequent inspection revealed that the braze joint on the outermost heater tube on quadrant 7 had opened up, probably due to an over temperature condition resulting from an inability to adjust the combustor fuel flow down as required to maintain the intended level. Additional fuel flow adjustment capability was incorporated, and the ability of the engine to operate at 7 MPa with the 50% active mirror configuration was reviewed. There appeared to be an imbalance between the heat input (from the concentrator and combustor) and the heat absorption capability of the engine when operating at 7 MPa.

Using the remaining funds available for the FSD hybrid receiver test program, the helium leak was repaired and a test was made on TBC-2 on April 22, 1982; however, this test resulted in a new leak, which again was caused by hot spots on the heater due to an air leak between the combustion chamber and the preheater.

The feasibility of a natural gas-fired hybrid solar Stirling engine receiver was demonstrated even though considerable development will be required to attain proven technology. The USAB Model 4-95 Stirling engine performed without fault or failure during this test series.

D. TECHNOLOGY ASSESSMENT

1. Test Bed Concentrator

The test bed concentrator approach to power conversion unit demonstration was satisfactory although it added several problems. First, there was no specialized mounting capability. The existing mounting ring interfered with the induction generator and would not allow the Stirling engine and its receiver to mount at the geometric focus of the dish. Thus, the mirrors had to be realigned to focus 229 mm (9 in.) inside the mounting ring. Protection for the ring therefore required fabrication of an aperture cone rather than an aperture plate. Second, the design weight for equipment at the focal point of the dish was 500 kg (1100 lb), which was too low for the Stirling test system. The DSSR subsystem was 800 kg (1800 lb) and the ESOR subsystems were 650 to 700 kg. The larger mass could be accommodated by the structure, but the elevation jack screw was seriously overloaded. Also, cabling for each PCU under test was specialized. Thus, cables for every system had to be installed, overloading the conduits. Schedule interference between the different PCU tests, together with assigning priorities for test, maintenance, and data logging caused difficulties.

On the positive side, operation with the TBCs assured accurate, calibrated solar input. It was therefore possible to test the power conversion unit as a separate entity.

The TBCs at the PDTS showed relatively slow degradation in mirror reflectivity between washings. However, they were brush-scrubbed thoroughly when high-performance testing was scheduled. Even this frequent cleaning did not prevent a slight amount of long-term coating of the mirror surface that could only be removed by special treatment.

Interfaces between the PCU and the system can only be partially simulated with the TBCs. In practice, reflective surface accuracy and tracking accuracy may be greatly reduced. Dynamics of the system may be quite different. During PCU development, however, such questions are considered secondary.

2. Power Conversion Unit

After many hundreds of test hours on the solar-Stirling PCU, the unit is still considered experimental. Receiver performance was only partially identified; engine and alternator performances were determined with a standard combustor test prior to delivery to the solar test site. Concentrator performance was calibrated prior to installation of the PCU. Numerical differences during solar testing were attributed to receiver performance (Reference 34).

Over a range of operating power levels, combustor-only performance could be compared to combustor-plus-solar hybrid performance. If sufficient data can be taken for different ambient, wind, and insolation conditions and for different concentrator angles, very good characterization of the receiver is possible. However, only limited testing was completed (Reference 35), because of the poor reliability of the DSSR.

The hybrid receiver, although functional, was over designed. The exceptionally high heat transfer coefficient for oscillating gas flow in the Stirling engine heater tubes will allow direct solar flux levels of 60 to 80 W/cm^2 without embedding the tubes in copper. Thus, the receiver was far too heavy and complex. However, it was noted during solar test that the receiver convection losses were very low for this design. Because of the compact configuration of the engine head/heater tube area, it would be difficult to eliminate hot spots in a hybrid combustor operating with solar heating. Therefore, it has been recommended that a ceramic hybrid receiver/heater head be designed and tested with this engine. Technology is now available in silicon carbide materials for this application (Reference 36).

The DSSR had very low chamber pressure (less than 7 in. H_2O), and commercial combustion controls were found to be unavailable. Microprocessor development was considered too costly at that time. A set of standard temperature sensors with PID (proportional-integral-differential) controller were used to drive the natural gas supply valve. An oxygen sensor in the combustion chamber generated the control signal for the air supply valve. Phase lag in the controls was quite large although marginally usable. Development of a suitable, passive 10:1 air/fuel ratio value is highly desirable. The ceramic (zirconia) O_2 sensor in the combustion chamber proved to be unreliable because of the temperature cycling on the system.

Combustor preheater optimization was not completed. Further analysis is needed of preheater temperatures and efficiencies, duty cycle requirements, start-up lag, etc. The combustor ceramic was massive (100 kg), and start-up stabilization time was lengthy (~1 hour). Thermal warping and leakage introduced data inconsistencies. In the next iteration of hybrid combustor design, operational requirements, efficiency, and cost will need additional careful trade-off study. The addition of the hybrid combustor mode was found to permit system solar operation at a higher efficiency.

SECTION IX

IMPROVED DISH/STIRLING POWER CONVERSION UNIT DEVELOPMENT

A. DESIGN ACTIVITY

In 1978, United Stirling became a part of the "Advanced Year 1985 Dish/Stirling Electric Power System" conceptual design activity together with MTI through a DOE-funded design study. During the course of the kinematic Stirling engine conceptual design activity, United Stirling and MTI conceived five direct solar-only engine heater designs, one suitable for the existing Model 4-95 (P-40) Stirling engine with modified regenerator location as shown in Figures 9-1 and 9-2. This design incorporated the involute tubes covering most of the heater cage area. To obtain a wide outer diameter and at the same time have short tubes, the inner diameter would be rather wide and the involute tubes would span over an angle of 90 deg. The 4-95 engine (65.5-deg angle) regenerator location would have to be modified.

United Stirling recognized the heater to be the most critical component in the design of a solar Stirling engine. The direct solar-only heating concept could not meet the optimum cycle data, such as small dead volumes and uniform temperature distribution; however, its lower performance relative to indirect sodium heat-pipe heaters could be more than offset by the robust, low-risk design. The design of a heater for direct heating required a detailed

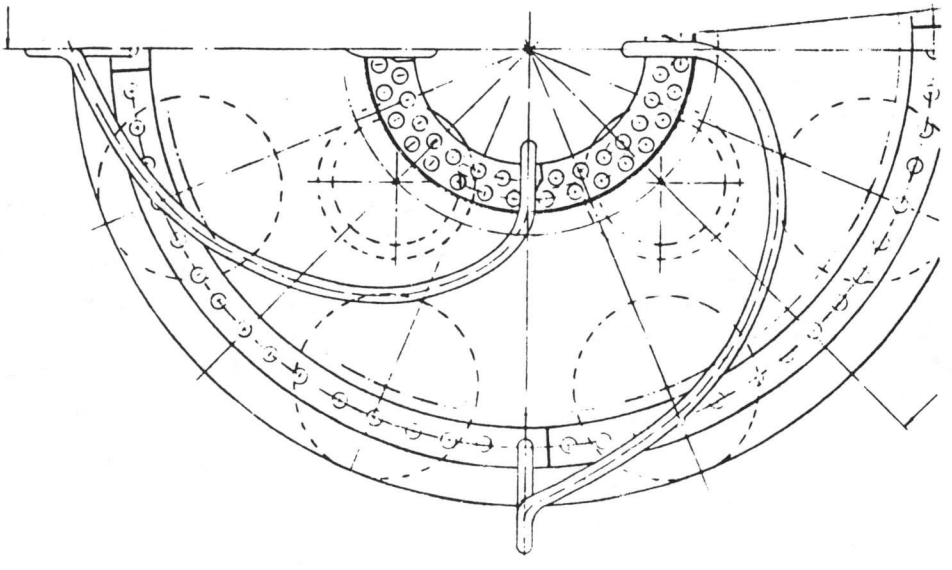

Figure 9-1. Heater Design for Direct Heating -- Top View, Modified P-40 Engine Heater Design

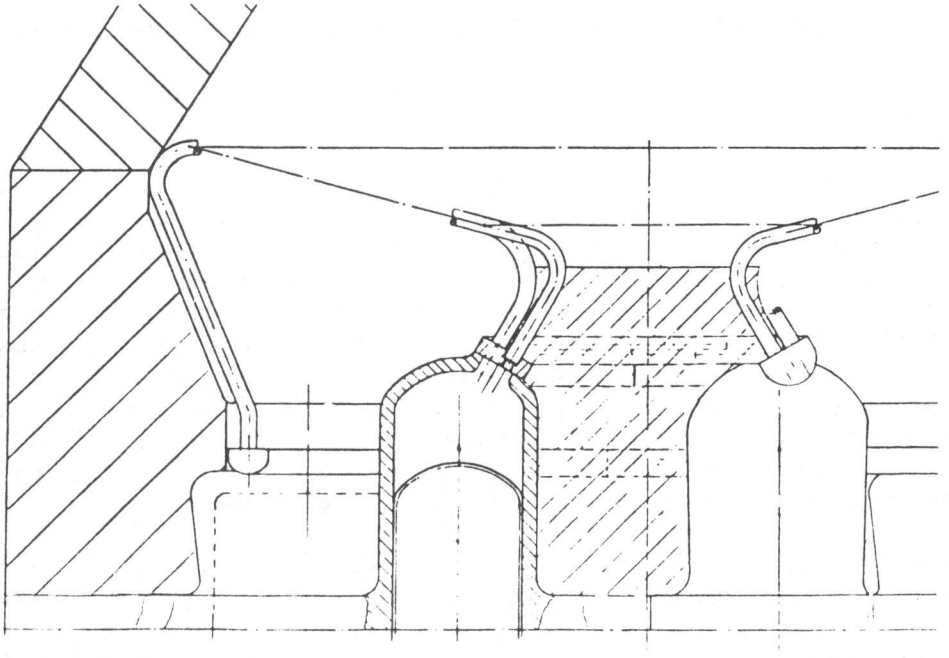

Figure 9-2. Heater Design for Direct Heating -- Cross Section

analysis of engine performance, including the heat flux distribution. The design of all of the other Stirling engine components are affected by specific design parameters of the heater. Two different design philosophies for the heater heads were (1) to arrange the gas passages to match the physical needs of the Stirling engine with the receiver radiative flux in order to achieve a uniform temperature distribution on the heater head and/or (2) to arrange the gas passages close to each other in a uniform way to completely cover the heater cage area so as to exclude the need for surface extension or buffer material. If the first design philosophy were to be followed, the heater would contain buffer material between the gas passages such as in the FSD design. With this design philosophy, heater tube length would increase modestly with heater cage diameter, resulting in less than optimum engine performance. In the second design philosophy, moderate heater tube length results in small heater cage diameters; however, the tube length increases very rapidly for increased outer heater cage diameter (or decreased inner heater cage diameter) and penalizes engine performance.

A parametric study of the heater that varied the total heater tube length, unheated tube length, dead volume between regenerator and heater, and dead volume between cylinder and heater resulted in the following observations:

(1) Tube length is not critical. For example, an increase in tube length of 50% will decrease efficiency approximately 0.5% and power approximately 1 kWe.

(2) Unheated tube length up to 25% and dead volumes up to 20 cm^3 at the regenerator will have a similar influence on performance as in (1) above.

(3) Dead volume at the cylinder up to 20 cm^3 will have a negative influence on power of approximately 0.5 kWe and cause a slight decrease in efficiency.

The temperature variation due to the uneven heat flux was calculated. With some parts of the tubes receiving no heat input due to design, the temperature variation would be 75°C between the maximum temperature and the minimum temperature (where the tube is unheated).

The variation caused by a solar concentrator heat flux distribution would be on the order of a maximum of 25°C. The different distributions according to the cone angles would, of course, influence the performance. The influence is rather small, and the difference between a 60- and 75-deg cone angle is so small that optimization was not performed. The results were based on a 60-deg cone angle.

The temperature drop through the heater tube wall was calculated, based on tube wall thickness. At the maximum tube wall thickness, the temperature drop was 75°C. The tube dimensions differ in the calculations, but the final design for the directly heated heater has a tube dimension of 4/7 mm [inner diameter (ID)/outer diameter (OD)]. If small tubes are used, wall thickness also can be smaller, and the temperature drop will be increased. The large (ID/OD) ratio was set because of lifetime requirements.

The variation in heat flux distribution around the tube would result in a temperature variation around the tube. This variation was indicated to be low because the working fluid would aid the thermal distribution in the tube walls.

Subsequent to the above conceptual design activity, USAB, using its own resources, continued a program of developing an improved dish/Stirling power conversion unit around the solar modified Model 4-95 engine with a direct heater. The development program included computer modeling and an optical analysis of several receiver designs. By definition, a Stirling receiver includes the engine heat exchanger (receiver body) and the optical cavity surrounding the receiver body. The cavity consisted of a sheet metal cylinder with internal insulation and ceramic aperture plate. Two different heat exchangers, somewhat resembling the standard 4-95 involute heater, were constructed, as well as several receiver cavities incorporating different types of insulation and reflecting surfaces. The heater cage diameter was 40 cm (15.75 in.) on the new involute heaters compared to the standard heater dimension of 28.6 cm (11.25 in.). The Experimental Solar-Only Receiver IIA (ESOR-IIA) is shown mounted on the improved power conversion unit in Figure 9-3 and is shown separately in Figure 9-4. ESOR-IIB, made without a circumferential manifold, is shown in Figure 9-5. Calculated power and efficiency (from Reference 37) of the engine with the two receivers are shown in Figures 9-6 and 9-7.

To control the PCU, a special USAB digital electronic control unit was designed. This control system for the solar Stirling engine was designed for

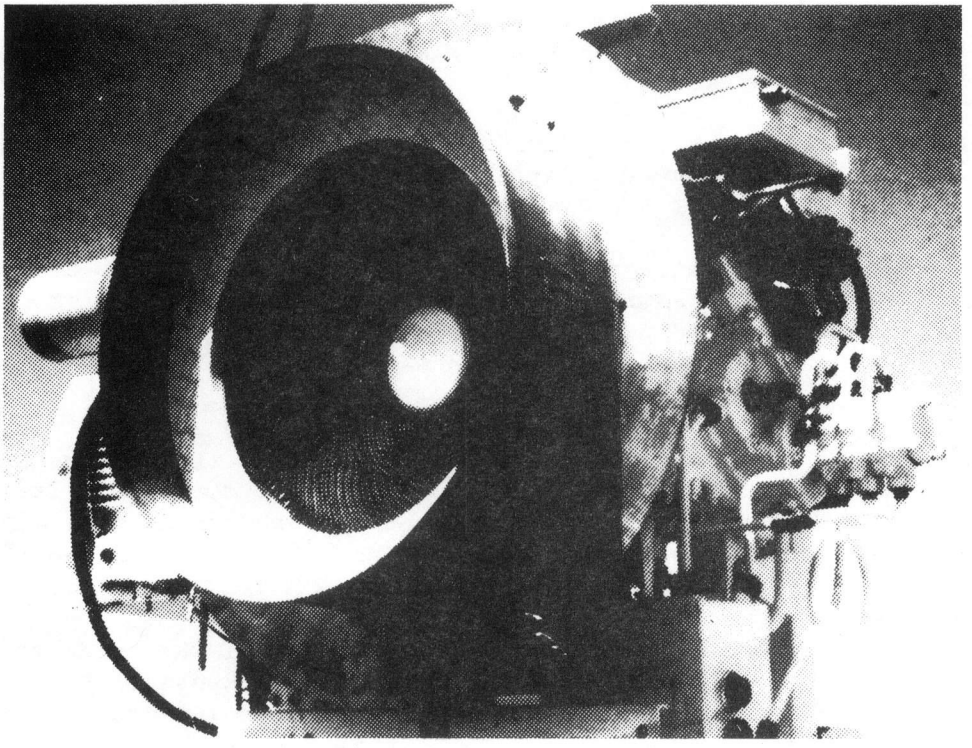

Figure 9-3. Power Conversion Unit Model 4-95 No. 2

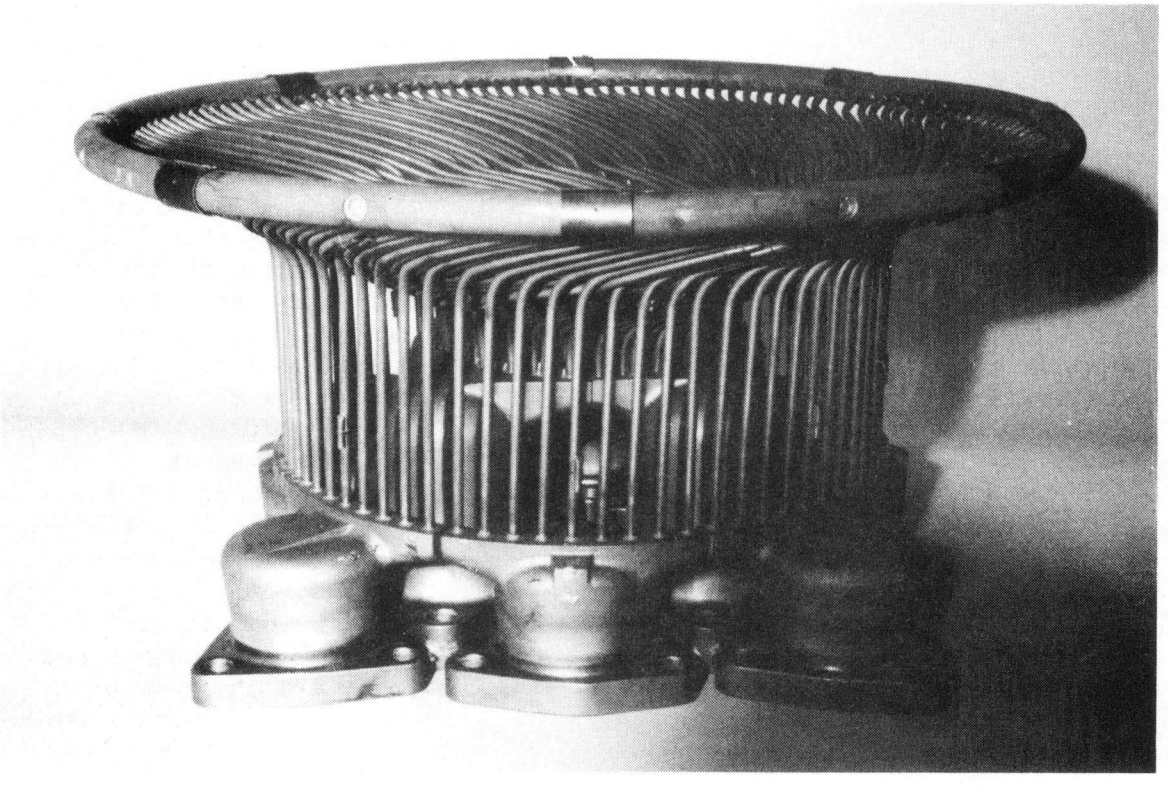

Figure 9-4. ESOR-IIA

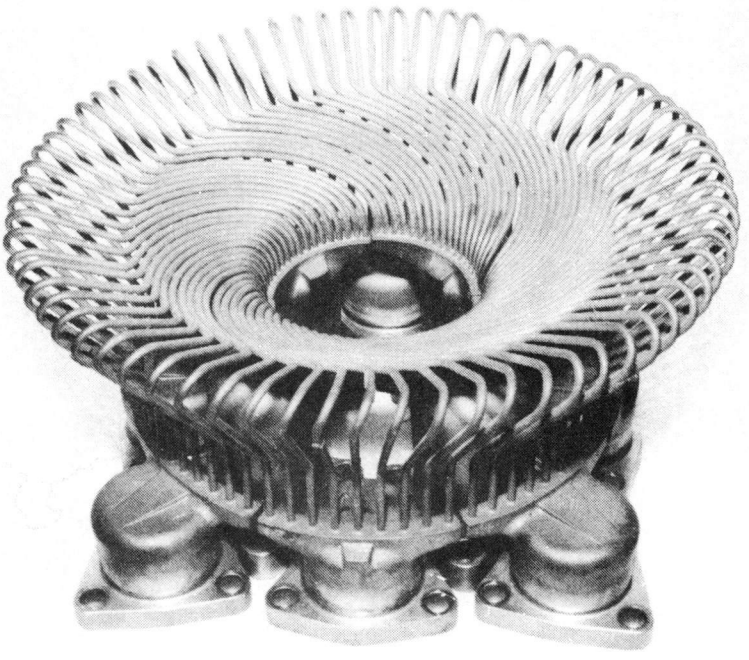

Figure 9-5. ESOR-IIB

automatic, totally remote, unattended operation. Manual control capability was provided for installation checkout, testing, and maintenance. The control equipment consisted of one unit located near the engine in the focal mount of the parabolic dish and one monitoring unit in the control room for the capability of start-up, shutdown, manual operation, and recording/display of data. The engine control unit consisted of both electronic (digital) control equipment and electric equipment, such as solenoid valves and high-voltage relays and meters for grid connection of the alternator. The digital control unit included all operational modes as well as guard and emergency functions. The monitoring unit for manual operation and recording and display of data included the same digital control unit for communication as a digital engine control unit. The monitor also included a cathode ray tube and meters for data display and a keyboard for manual operation, such as value change of a constant for different types of operations or control modes (Reference 38).

B. INTEGRATION AND TEST OF THE IMPROVED DISH/STIRLING POWER CONVERSION UNIT

Integration and test of the improved USAB dish/Stirling power conversion unit took place in three distinct phases: the first two phases were from August 1981 through March 1982, lasting less than four months each. The final phase extended from May 1982 through December 1983, a total of 20 months.

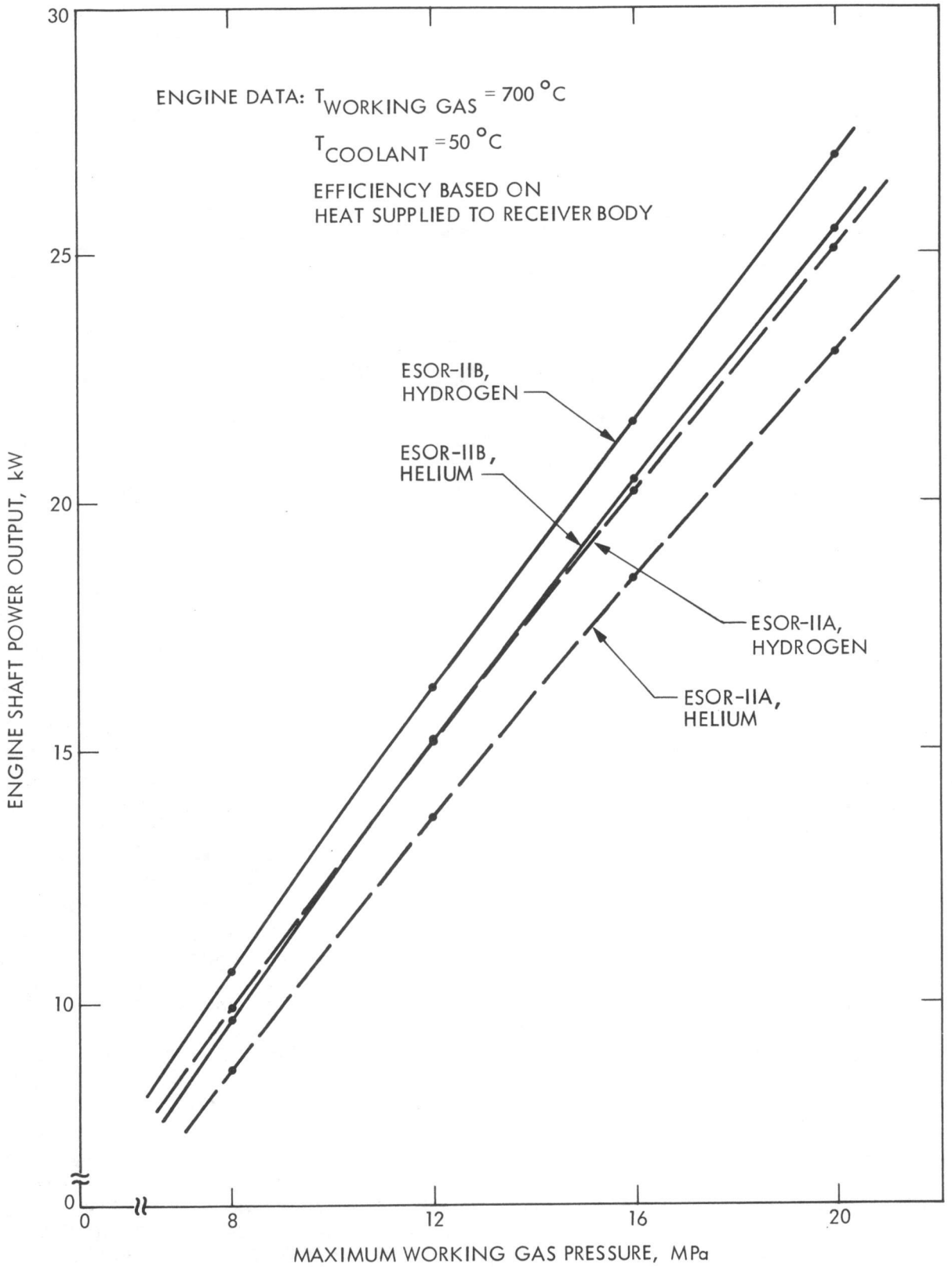

Figure 9-6. Calculated Performance of ESOR-IIA and ESOR-IIB, Power Output versus Maximum Working Gas Pressure

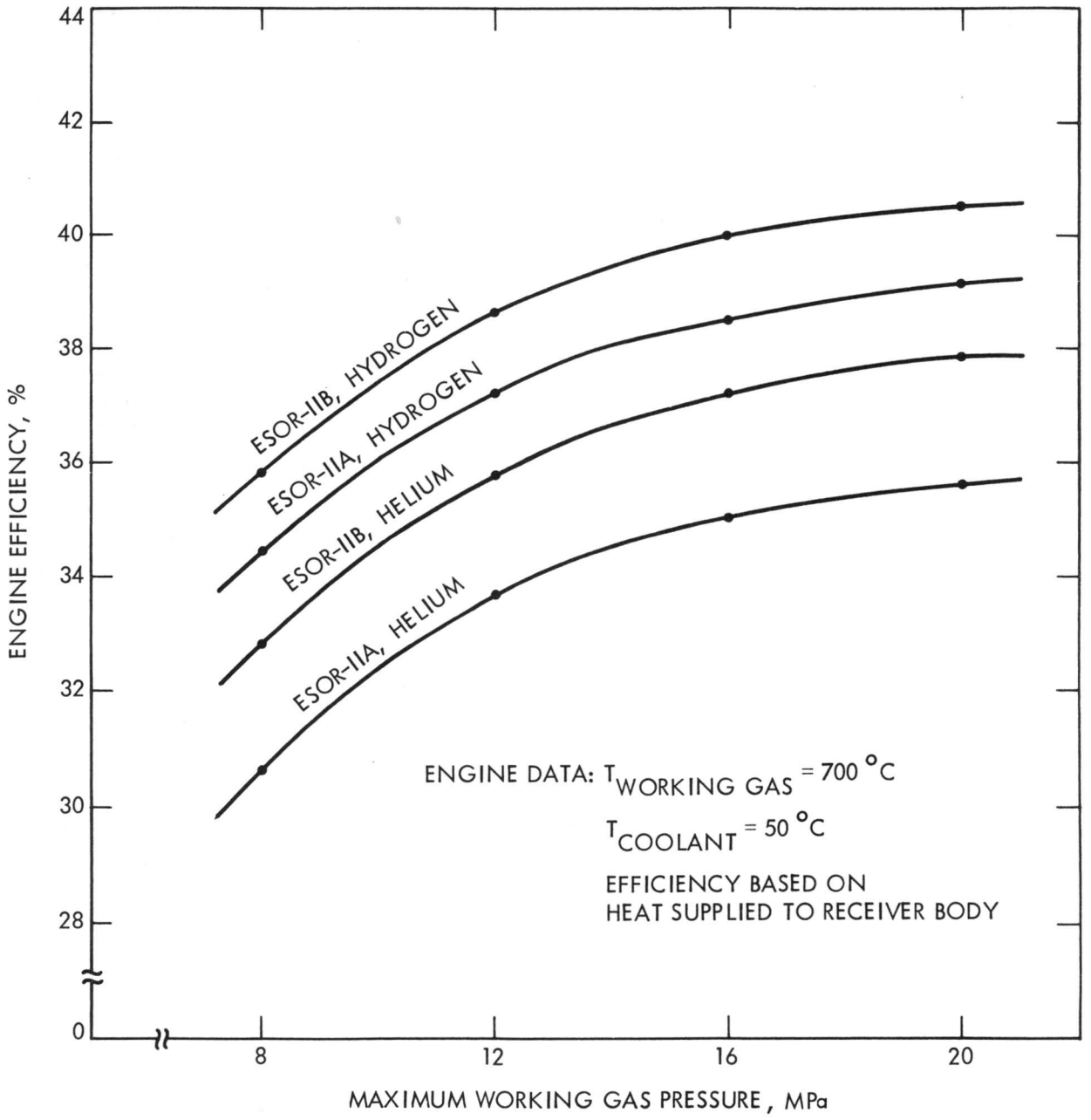

Figure 9-7. Calculated Performance of ESOR-IIA and ESOR-IIB, Efficiency versus Maximum Working Gas Pressure

1. United Stirling Testing at Georgia Tech Research Institute

On the campus of Georgia Tech is a solar installation known as the DOE Advanced Components Test Facility (ACTF), consisting of a field of 550, 0.9-m (3-ft)-diameter mirrors. By means of mechanical shaft and cable drives, the mirrors track the sun and focus concentrated solar flux at the lower level of a tower platform 21 m (70 ft) above the ground.

As a result of discussions, which began in January 1981 between United Stirling and ACTF management, USAB contracted to test a 4-95 engine/generator package nearly identical to the one at the JPL Parabolic Dish Test Site. Testing at the ACTF was intended to parallel testing at the PDTS and provide additional experience with solar-only receivers, in contrast to the FSD (hybrid) type.

Some initial testing was done in August 1981 with the standard involute heater, shown in Figure 9-8, to verify operation and the automatic temperature control. The working gas was hydrogen. Testing was resumed in November, with the new receiver body installed. Several changes were made to the receiver. The aperture was opened to a full 40.6 cm (16 in.), which is the maximum possible, and the engine was lowered in its tower frame until the conical heater surface was substantially at the focal plane. In addition, Georgia Tech personnel continued to realign the mirror field for the solar declination, which had not been done since August. With much improved weather, 15 hours of operation was achieved over the weekend. Maximum power was 12 kWe. The best run was made on November 18, after completion of mirror alignment. Maximum power was 18.5 kWe to the grid, with an average of 18 kWe between noon and 1:00 p.m. This can be seen in the accompanying chart, Figure 9-9, of power versus time. The power improvement was achieved as the facility operators learned to optimize the hour-angle setting by observing the heater temperatures. The engine was operating with automatic temperature control, holding the average at about 720°C.

On the weekend of November 21, the engine was operated with the second of the two new heater designs. Maximum power achieved was 16.5 kWe, at about the same insolation level as on November 18. Because the principal goals of the program had been met, the engine was removed from the tower.

In addition to the record electrical power output, three major achievements were realized from these tests:

(1) Solar heat exchangers were tested for the first time under sunlight intensities roughly equal to those from a parabolic dish concentrator.

(2) Two new solar-only heaters were tested successfully in a running engine. Although having somewhat greater dead volume than the standard heater, it did not appear to seriously reduce power or efficiency. No malfunction or leakage occurred.

(3) The 4-95 solarized engine was proved in the solar environment. It performed as designed without requiring maintenance to the basic Stirling cycle.

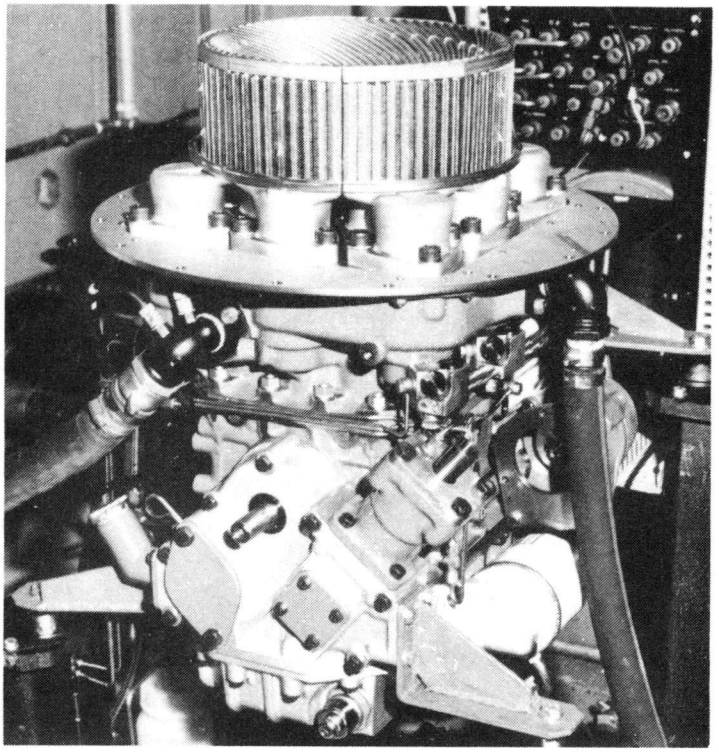

Figure 9-8. 4-95 Standard Involute Heat Exchanger

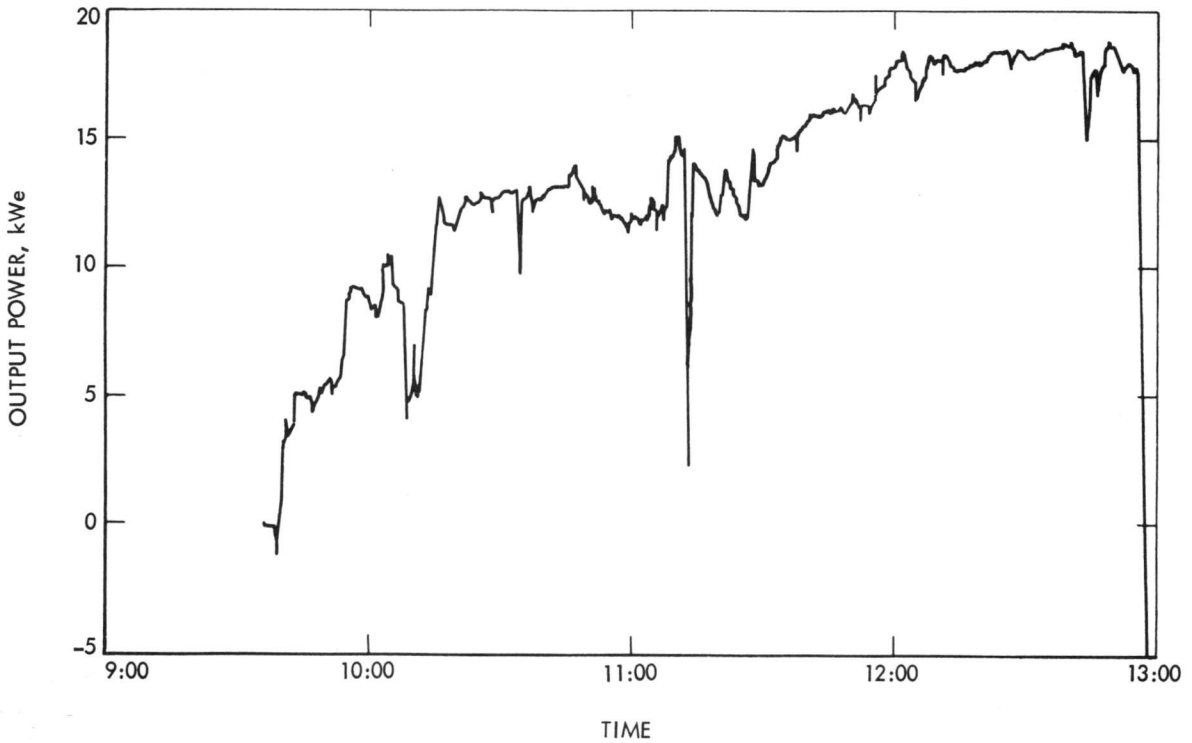

Figure 9-9. Variation of Output Power with Time

2. Testing the Experimental Solar-Only Receivers on the First Dish/Stirling Power Subsystem Module

From January through March 1982, the three experimental solar-only receivers tested at the ACTF were installed and tested on the solar Stirling engine 4-95 No. 21 supplied to JPL by USAB for the first dish/Stirling power subsystem module tests at the Parabolic Dish Test Site, Edwards, California. The power conversion unit was installed on Test Bed Concentrator No. 2 (TBC-2) for these tests. TBC-2 had been optically aligned for the first FSD receiver and hence was not optimally aligned for testing the experimental solar-only receivers. From flux mapping tests of TBC-2, the radiative flux on the receivers was shown to be uniform at about 50 W/cm^2 with no high peaks; however, the flux level outside the diameter (45 cm for ESOR-IIA) of the heater location was fairly high. A large amount of radiative flux of the cavity walls leads to a high wall temperature and losses due to reradiation, conduction, and convection. The receivers were equipped with a number of thermocouples on all four quadrants to indicate the temperatures in (1) the working gas, (2) heater front tubes (backside), (3) heater rear tubes, and (4) cavity wall. A comparison of these heater and cavity wall temperatures for the three receivers were found to be as follows:

	ESOR-I	ESOR-IIA	ESOR-IIB
Cavity Wall Temperature, Maximum, ^oC	1270	1120	1130
Tube Temperature Relative to Working Gas Temperature, ^oC:			
Inner front tube	-10	+ 50	+ 50
Outer front tube	+10	+ 40	+ 90
Upper rear tube	+80		+ 110
Lower rear tube	+30		+ 90

During testing, the measured power output was the alternator electric power output. Figure 9-10 shows the electric power output for the power conversion unit with three different solar-only receivers as the thermal power input to the cavity was varied up to a maximum of 75 kWt at a direct insolation of 1000 W/m^2. In this testing with helium working gas, ESOR-IIA proved best with a maximum electric power output of 21.8 kWe; ESOR-IIB was second with a maximum electric power output of 19.9 kWe; and the standard heater, ESOR-I, had the lowest electric power output (15.8 kWe). An analysis of engine/receiver performance using actual test data in addition to calculations of engine performance results in the best estimation of receiver cavity efficiency. Using this method, the best estimation of receiver cavity efficiency for the different receivers was 55% for ESOR-I, 75% for ESOR-IIB, and 88% for ESOR-IIA.

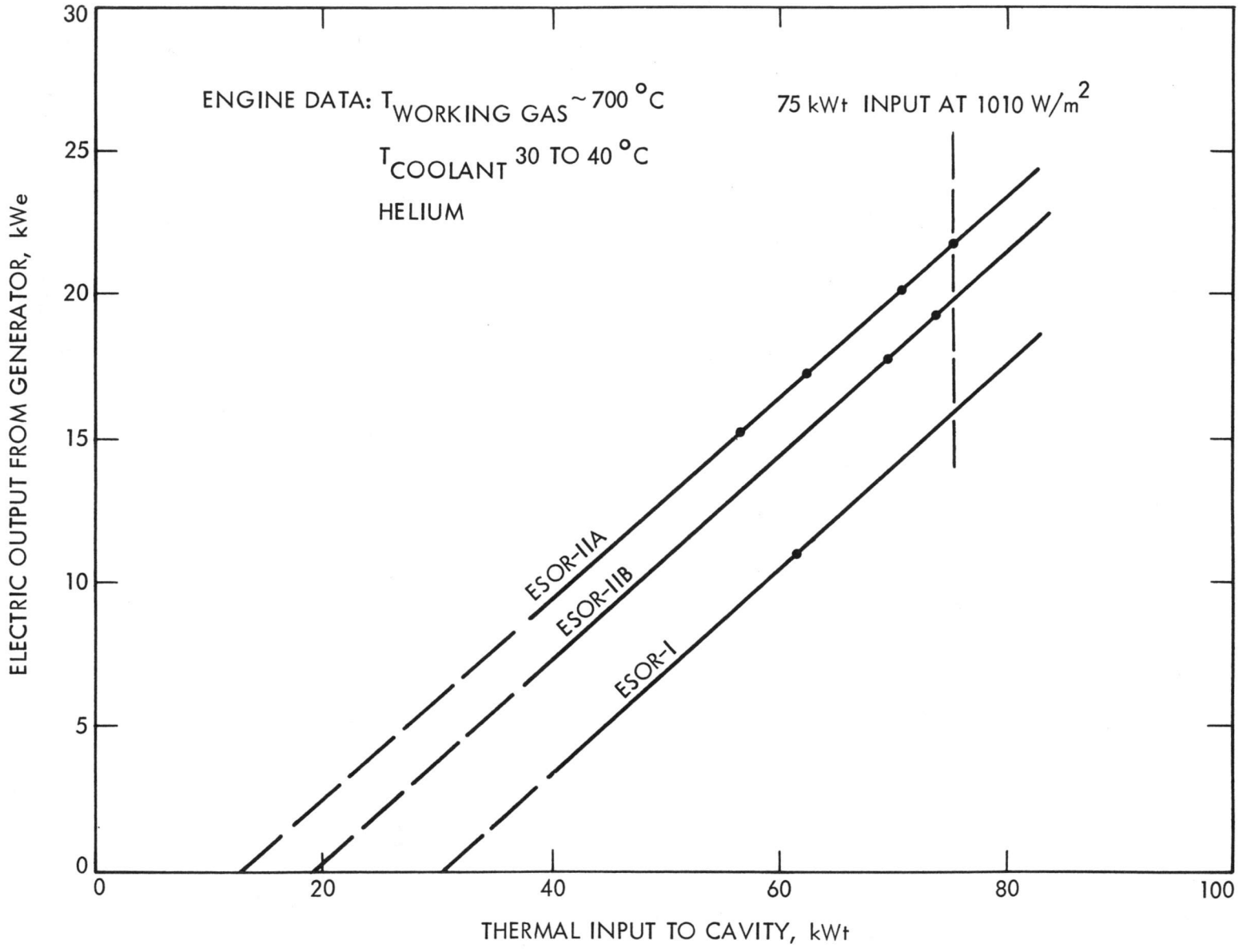

Figure 9-10. Electric Output As a Function of Thermal Input to Cavity for Three Different Experimental Solar-Only Receivers

3. Testing the Improved Dish/Stirling Power Conversion Unit on Test Bed Concentrator No. 2

There have been many facets to the sequence of tests with the USAB-owned and improved dish/Stirling power conversion unit on TBC-2 (Reference 39). Of the several types of tests performed, the most important were the following:

(1) Characterization of receivers.

(2) Full-day performance of a subsystem.

(3) Cavity and aperture window tests.

(4) Special temperature measurements with an infrared camera.

(5) Radiator subassembly tests.

(6) Control subassembly tests.

This test series was no longer concerned with power conversion unit feasibility because that had already been demonstrated. The testing then centered upon improving the performance of the power conversion unit. The concentrator was realigned to improve the radiative flux distribution on the engine/receiver heater. A new receiver aperture cone and receiver cavity were installed with the new USAB Model 4-95 Solar Mk I engine assembly (No. 2). A specially designed USAB mounting frame between TBC-2 and the new PCU allowed the PCU location along the TBC-2 optical axis to be adjusted for optimum performance.

Also, the DOE-owned Model 4-95 Solar Mk I engine (No. 21) was equipped with a new solar control subassembly and a new engine-mounted radiator subassembly. The PCU was then tested on TBC-1 after an optical realignment constraint was removed.

a. Test Bed Concentrator Alignment. TBC-2 was aligned differently than in earlier 1982 tests reported above. In the previous alignment, all 220 reflectors were aimed at one point -- the center point of the FSD receiver assembly aperture. In order to concentrate all radiative power on the receiver heater tubes, most of the reflector facets (so-called B and C facets) were aimed at the center point of the decided aperture; however, the so-called A facets near the center of TBC-2 were aligned to a concentric circle in the aperture plane. The change in the radiative flux distribution from before to after the alignment is illustrated in Figure 9-11. The radiative flux now appears to be doughnut-shaped, with a maximum radiative flux of about 80 W/cm^2 on the receiver tubes. In the 20-cm-diameter focal plane aperture, the maximum radiative flux is now about 800 W/cm^2 where previously the flux was over 1500 W/cm^2. The effect of concentrator alignment on the PCU performance is tabulated in Table 9-1. With the early alignment in March 1982, the DOE-owned PCU generated 19.5 kWe at a conversion peak efficiency[6] of 28.4%; however, in July 1982 an almost identical USAB-

[6]Efficiency numbers do not account for parasitic losses.

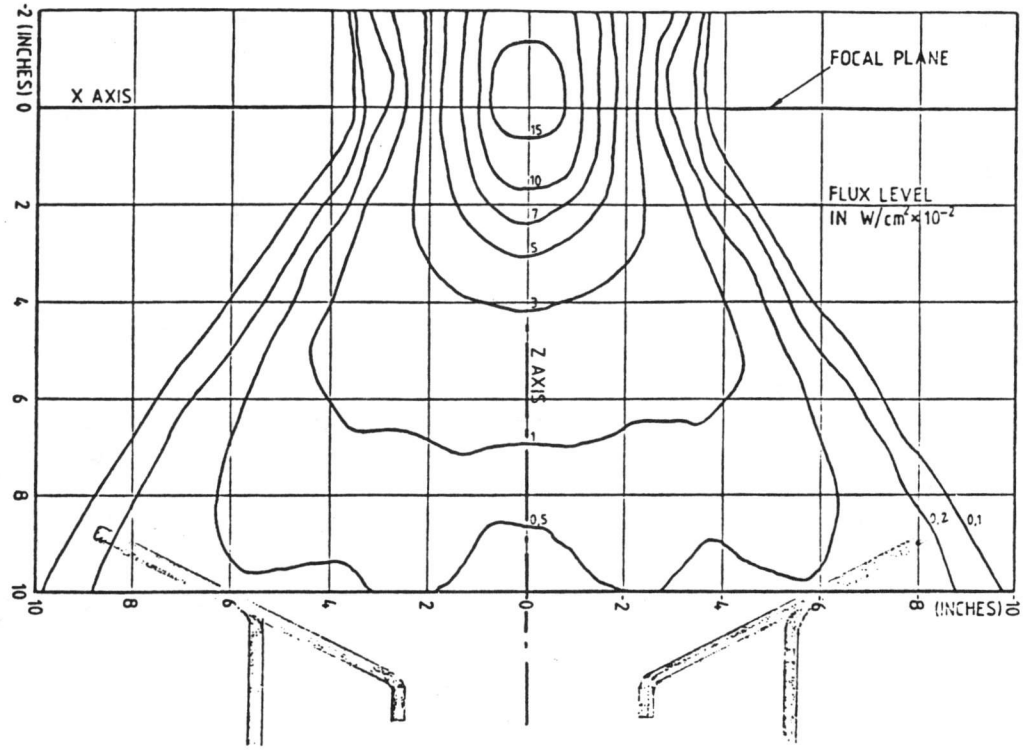

(a) Early Flux Distribution

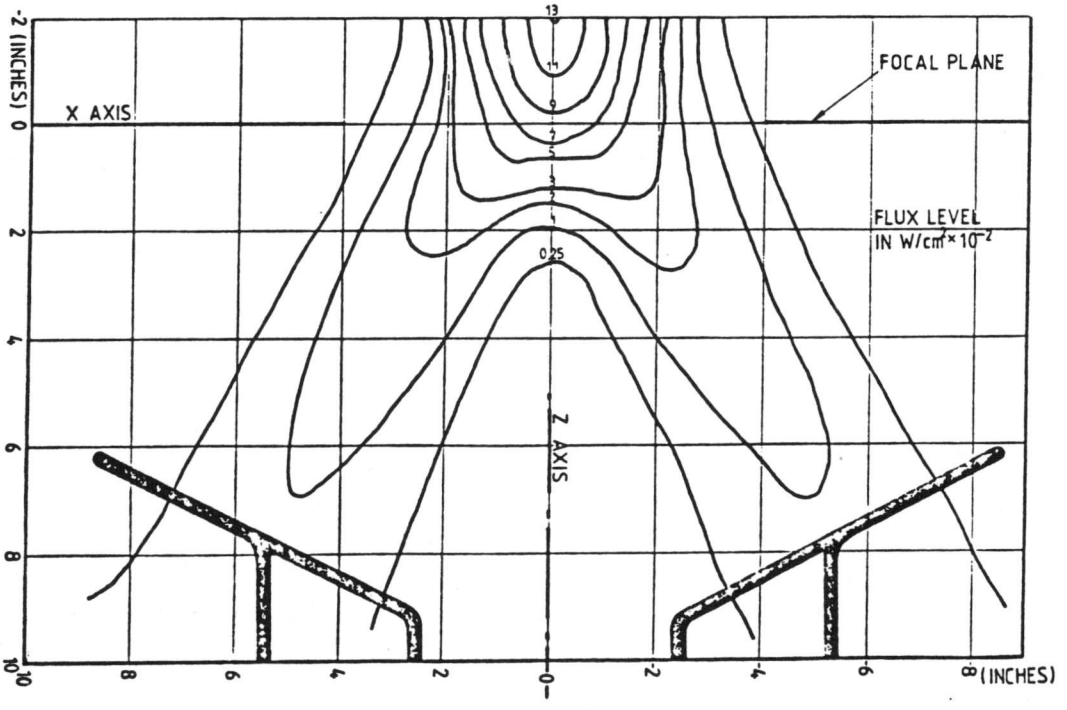

(b) Flux Distribution (August 1982)

Figure 9-11. TBC-2 Flux Maps

Table 9-1. Data Comparison, Different Concentrator Alignments

Receiver Type	Date (1982)	Working Gas	Engine Output, kWe	Max. Pressure, MPa	Gas Temp., °C	Insolation, W/m^2	Input, kWt	Efficiency,[a] %
ESOR-IIA	March	He	19.5	17.3	700	915	68.6	28.4
ESOR-IIB	March	H_2	20.7	15.3	680	980	73.5	28.2
	March	He	19.5	17.0	690	973	73.0	26.7
ESOR-IIA	July	H_2	24.2	19.7	704	960	72.0	33.6
	July	He	20.7	19.4	700	906	67.9	30.5
ESOR-IIB	June	H_2	22.4	17.6	699	898	67.3	33.2
		He	20.6	18.6	691	922	69.2	30.0

[a]Gross PCU efficiency (receiver plus engine plus generator).

owned PCU generated 24.2 kWe at a conversion rate of 33.6% with more thermal input. Concentrator reflector alignment produces a first-order effect on dish/Stirling PCU performance.

b. Effect of Solar Receiver Assembly on PCU Performance. Testing was performed to find the optimal operating conditions for the entire power conversion unit, taking into account a number of different parameters such as working gas temperature, front tube temperatures, cavity temperatures, engine pressure, temperature distribution, power output, and engine location. Testing was conducted at different engine locations in relation to focal point, at different working gas temperatures, at different concentrator configurations, and with different working gases.

Figure 9-12 shows characteristics for the power output at different locations. The optimal heater location for maximum power output is where the heater cage intercepts almost all radiative power in a near uniform flux, and where the tube temperatures are balanced between inner and outer tubes. Cavity wall temperature is kept low at these conditions. The newer model ESOR-III (shown in Figure 9-13) demonstrated higher maximum power output (21.6 kWe) than ESOR-IIA (21.1 kWe) or ESOR-IIB (21.3 kWe) as seen in Figure 9-12. The optical distance of the receiver tube cylinder manifold behind the principal focal plane was 232 mm for ESOR-III, 257 mm for ESOR-IIB, and about 282 mm for ESOR-IIA. Also, ESOR-III has a high ratio between power output and pressure because the tube length has been optimized in comparison to the outer receiver diameter. This means a relatively lower operating pressure for the same output power, and the highest dish/Stirling power subsystem output can be attained with a working gas pressure of no more than 20 MPa.

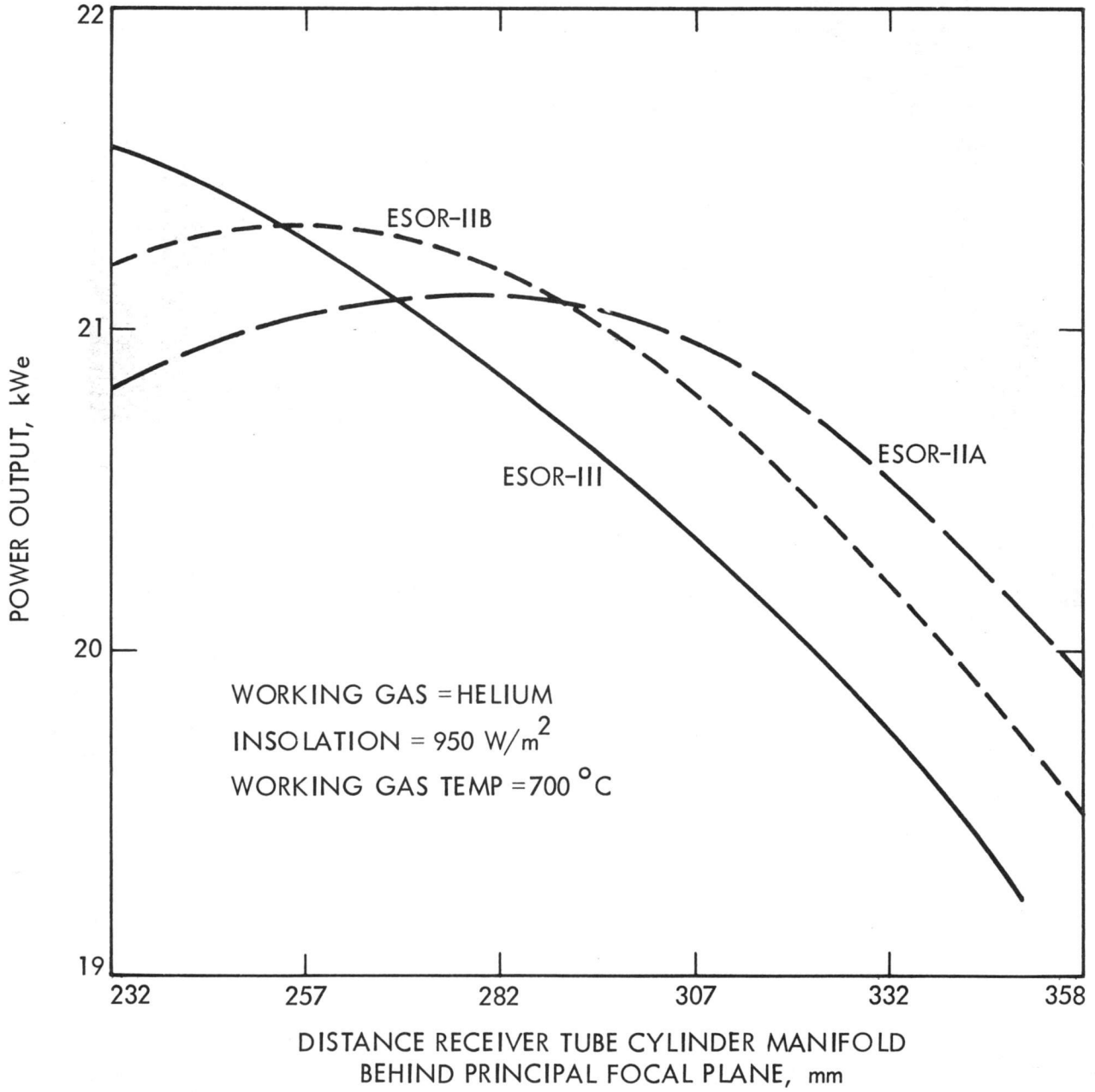

Figure 9-12. Variation of PCU Output Power with Receiver Location

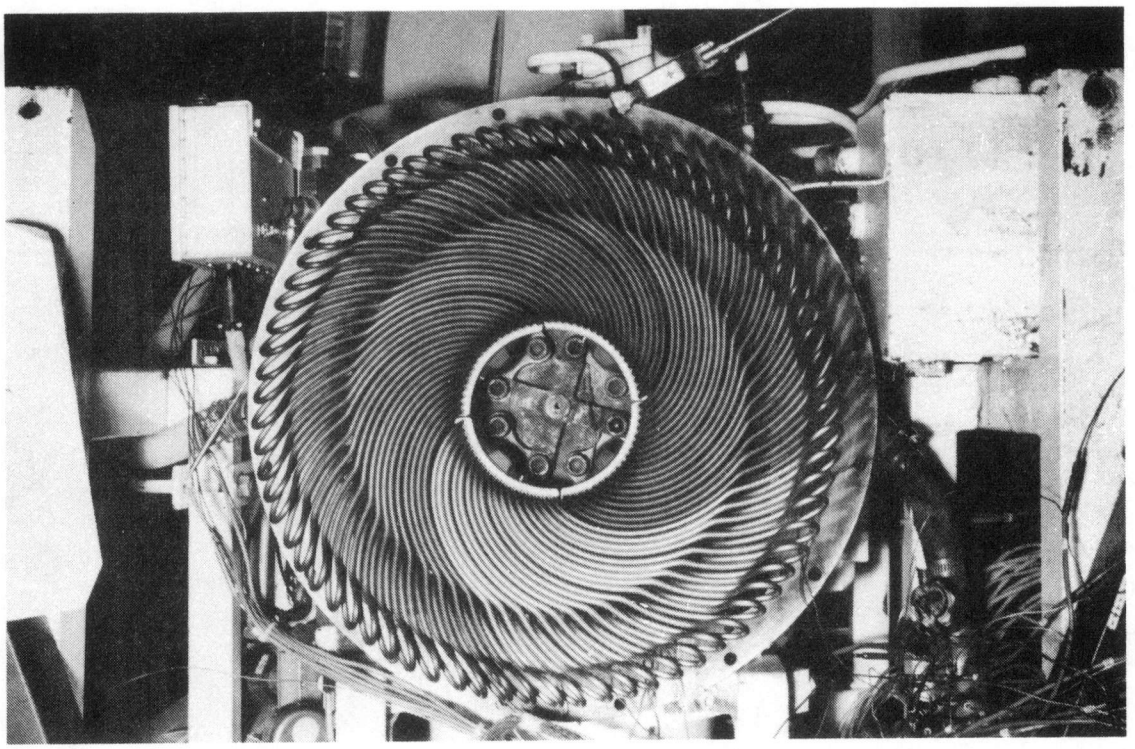

Figure 9-13. ESOR-III

In addition to the solar receiver parametric tests described above, ESOR-IIA was tested without the aperture cone or cavity wells. During testing, an additional heat power loss of about 8 kWt due to reflection, reradiation, and convection was discovered. The additional heat loss varied little with heater temperature or direct insolation level.

A receiver aperture window added to the cavity of ESOR-III actually reduced the electrical power of the subsystem by up to 4% over a receiver with no aperture window and with a working gas temperature of 700°C. Considerably less loss due to the window was found at lower working gas temperatures. Even with the aperture window in place, winds with average speeds of 16 m/s further reduced subsystem electrical power output by up to another 4%. Power loss at high wind speeds was not determined for ESOR-IIA in the absence of an aperture window.

Solar receiver testing ended in January 1984 before ESOR-IV (Figure 9-14) could be evaluated.

c. Receiver Heater Subassembly Temperature Distribution. Different types of temperature measurements were made on the heater subassembly. It is important to evaluate all the different temperatures in the heater subassembly, such as working gas temperature, front tube temperature, rear tube temperature, tube temperature facing the sun as well as the opposite side temperature, temperature variation along the tube, and manifold temperature, especially when the means of heating up the heater involves input mainly on one side of the tube and a varying heat flux over the area.

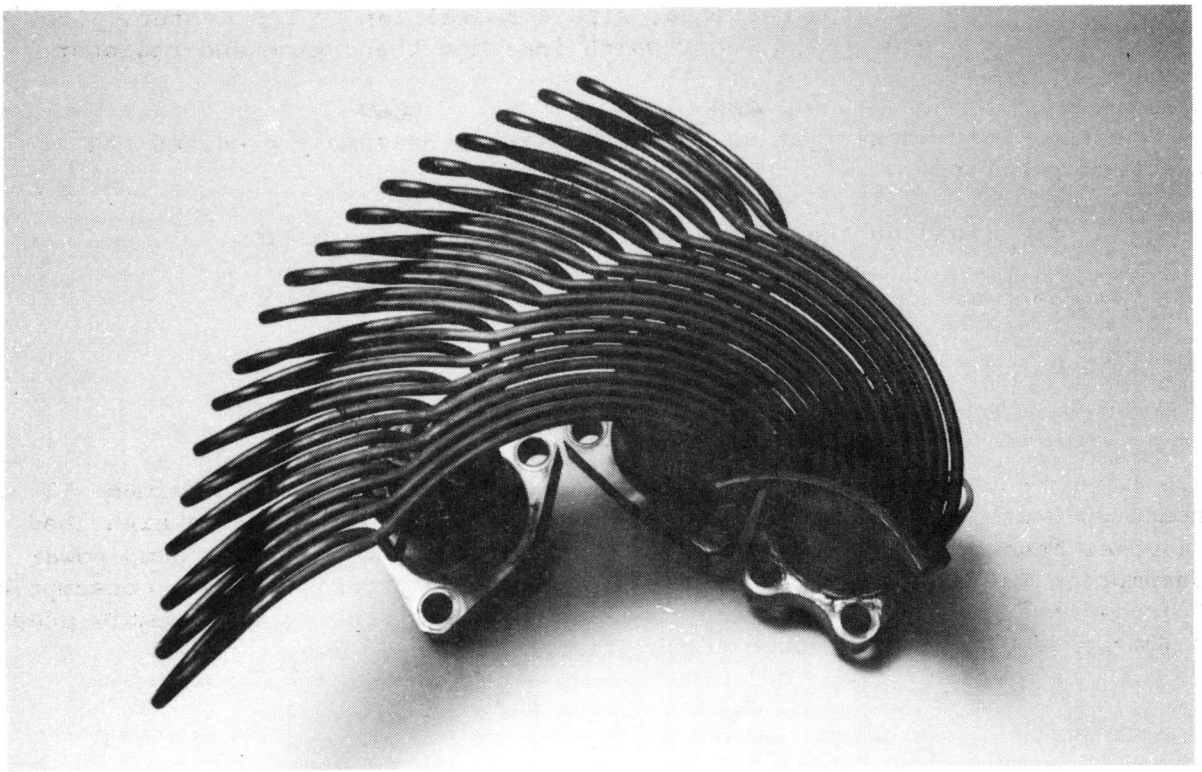

Figure 9-14. ESOR-IV Quadrant, Including Cylinder and Regenerator Housings

Tests were made with placement of a number of thermocouples over the heater and cavity and on both rear and front sides of the tube. To confirm these measurements and also to obtain continuous measurements along the tube -- not only where the thermocouple sleeves were located -- an infrared camera was used. Initial testing was performed with ESOR-IIB in location "3" (282 mm), which was not the location for an optimal system. However, some interesting results were obtained:

(1) The uniform temperature for the different tubes in each quadrant at the same radius showed a uniform internal flow distribution.

(2) The temperature variations between quadrants depended on the internal conditions or flux distribution variations.

(3) The temperature variation along the tube -- warmer tube at the outer diameter -- depended on both internal conditions (gas flow) and external conditions (heat-flux distribution). This variation was as high as 150°C.

(4) No critical hot spots were found on the receiver surface.

d. Engine Cooling Subassembly Tests. The DOE-owned Model 4-95 Solar Mk I engine assembly was installed in TBC-1 equipped with a complete cooling subassembly installed in the focal mount. The cooling subassembly

consisted of four radiator matrices, with a radial fan in the center. Cooling water was pumped through the loop, which included the engine and radiator (Figure 9-15).

Initial functional testing of the cooling subassembly produced the following results:

(1) Full load on the PCU was 22.4 kWe output with helium.

(2) Ambient temperature was 28°C.

(3) Maximum water temperature was 51°C.

(4) Fan power (low) was 790 W.

These results show that the design criteria of reaching a maximum ΔT of around 20°C at full load and full fan power can be achieved. The high load fan power consumption was 1250 W; low load was 790 W. The water pump power consumption was 200 W. This resulted in a maximum parasitic power consumption of around 1.5 kWe for the cooling subassembly. The cooling subassembly used in TBC-2 had a parasitic power consumption of around 4 kWe.

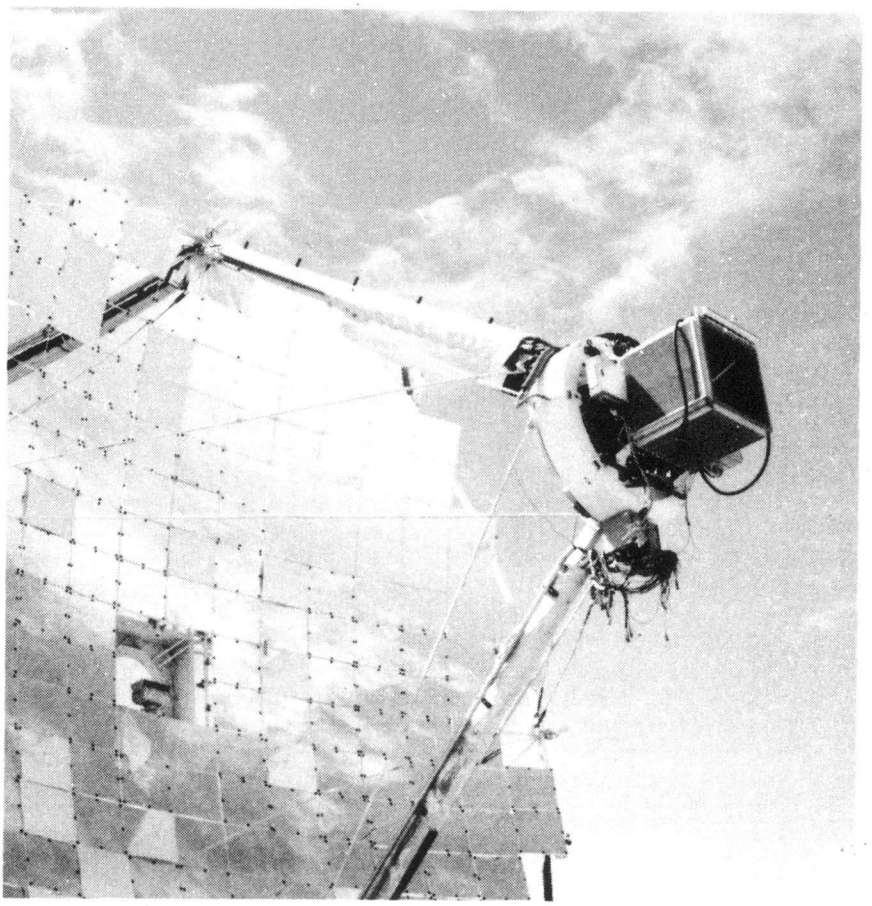

Figure 9-15. Stirling Module with Radiator System

e. Receiver Aperture Cone Material Tests. Parallel to the receiver and cavity testing, initial aperture cone and receiver protection material testings were accomplished. These tests demonstrated what type of material could survive the conditions on and around the aperture when acquiring or detracking the sun. If no shut-off of insolation to the receiver is necessary, a passive cone is sufficient. The material for such a cone must survive heat-flux levels of around 1000 W/cm^2 during short time periods. If a shutter is needed to shut off insolation, it can be located in a less critical area where the flux level is lower, which will make survival easier.

Ceramic board, Nexthel ceramic cloth, and cast silica of different types were initially tested as cone materials. At high insolation levels, only the cast silica survived. Testing conditions were up to 930 W/m^2 insolation levels with 100% concentrator under normal tracking speeds.

As shutter material, a stainless steel gauze was tested with insolation levels up to 900 W/m^2 for 10 min with only minor damage.

Results from initial testing led to the design and fabrication of a complete cast silica cone and one stainless steel gauze shutter for installation and testing.

f. Full-Day Dish/Stirling Power Subsystem Performance. The improved power conversion system showed excellent performance. The module output achieved is the highest so far for any parabolic dish system. The highlights of full-day testing are listed below:

(1) 24-kWe module output.

(2) 28% overall conversion efficiency, solar to net electric.

(3) 13.5 hours of operation with positive power output over one day.

(4) Generation of more than 250 kWe-h over one day.

Figure 9-16 shows the output over a full day with corresponding solar input.

Of special interest is the mean daily efficiency for the system. The Stirling engine has a very high part-load efficiency. For example, one hour after start, system efficiency is very close to daily maximum (Figure 9-17). The mean daily efficiency is around 95% of the maximum.

C. TECHNOLOGY ASSESSMENT

Except for start-up and shutdown, test operation was virtually automatic for both the concentrator and Stirling PCU. The initial three-month series of tests of ESOR-I, IIA, and IIB solar-only receivers were concluded without being able to adequately differentiate the receiver designs. As noted previously, the Stirling engine/generator could not be positioned to place the receiver at the focal point of the dish. Thus, the indicated performance of the receivers in Figures 9-6, 9-7, and 9-10 is not necessarily optimum.

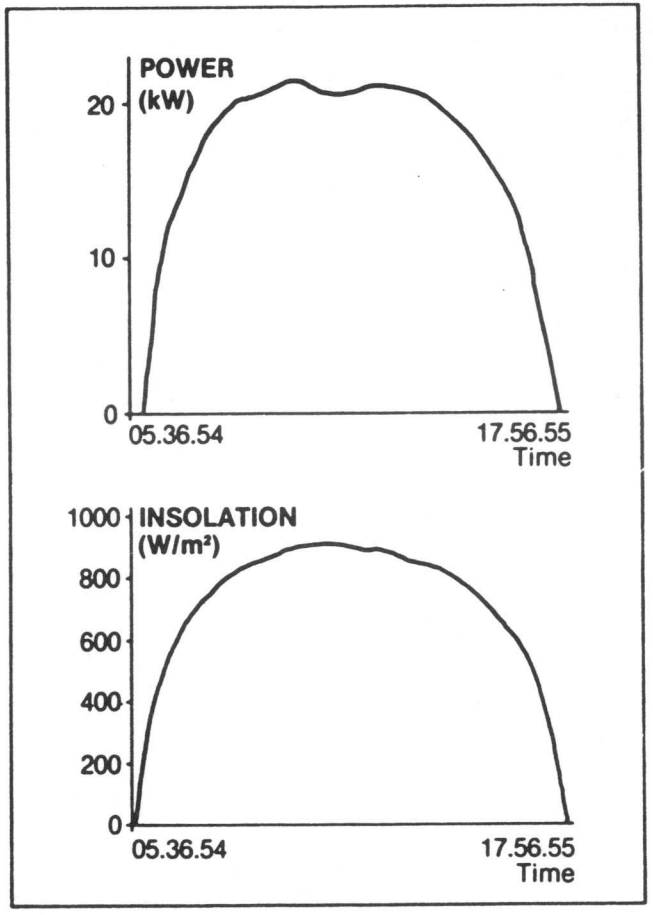

Figure 9-16. Insolation and Power from a Full-Day Test

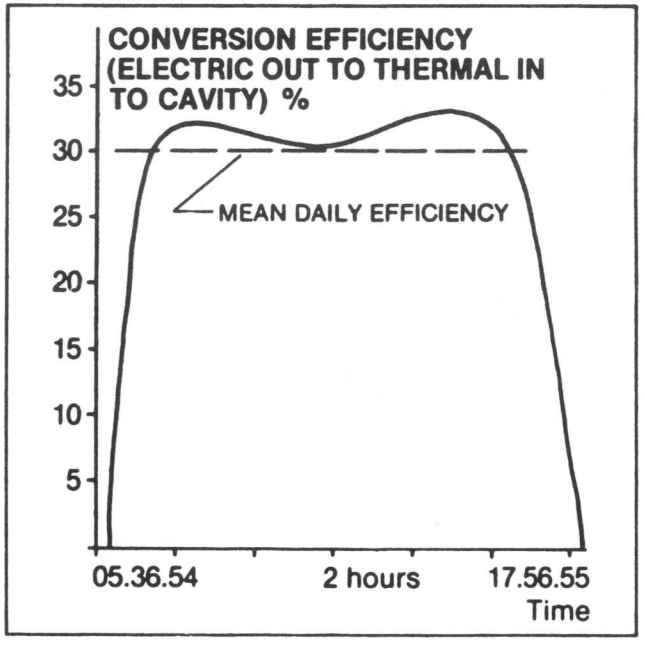

Figure 9-17. Mean Daily Output

Further realignment of concentrator mirrors was then done, and adjustment of receiver position along the Z axis produced the curves of Figure 9-12. Optimization proved to be quite different than previously thought.

Larger temperature differences than in laboratory combustor tests were seen in the solar tests from quadrant to quadrant of the Stirling engine. Some improvement could be obtained by offsetting the concentrator by a small fraction. This was unexpected. The large number of concentrator facets and also the many engine heater tubes were expected to wash out any small heat flux differences. However, it appears that a systematic error was generated because the concentrator facets were also designed in quadrants, which produced flux patterns coinciding with the Stirling engine heater quadrants. A systematic analysis to show how to correct the error is needed.

In the initial series of solar-only tests, a simple algorithm was introduced in the controls to make temperature proportional to working gas pressure (i.e., $T_{wg} = A + B\ P_{wg}$ where T_{wg} and P_{wg} are the temperature and pressure of the working gas, respectively). It could be shown that by this method of control the receiver radiation losses were reduced at partial power, and the system efficiency thereby was increased slightly. This algorithm was eliminated in the second series of tests.

The sunrise-to-sunset testing was done with hydrogen as the working gas with all mirrors uncovered. At peak insolation, test results showed a reduction of conversion efficiency of thermal power into the receiver to electricity generated that was anomalous (Figure 9-17). A careful study of the records has identified a control problem that, at least partially, contributed to this result. Engine control during this series of tests held the temperature constant and varied the hydrogen pressure to control engine power output. Wind fluctuations during test caused power fluctuations that in turn introduced pressure fluctuations. At maximum power, these pressure fluctuations would sometimes exceed the maximum limit setting, thus saturating the controls. The result was to hold pressure lower than optimum and suppress power output. After peak insolation passed, pressure limits slowly dropped out, allowing the power level to increase again.

Engine start-up for testing most often occurred after mid-morning. The high insolation caused a rapid temperature increase when the dish came on sun and the water-cooled plates were opened. If engine cranking did not start quickly, the receiver would overheat and be damaged. Fuse outage at the contactor box and also low engine oil pressure had caused this problem on three occasions. Improved sensing of cranking problems, together with more rapid response to the emergency condition are needed. In addition, a more complete study of all fail-safe requirements would be valuable.

Reliability considerations during testing were somewhat limited. Several changes to the experimental receivers were made; these included changeout of piston rings, seals, and O-rings. Thus, no real lifetime information was gained. However, complexity of the working gas pressurization system was noted as potentially unreliable, and this has been greatly simplified in the Vanguard system. Engine components basically reflect the on-going reliability effort of the Automative Stirling Engine Program. More technical advances will be needed during the next few years to achieve extended life requirements for electric generation systems.

Noise and glint tests were conducted to evaluate possible environmental impacts. Noise was modest -- a maximum of 60 to 65 dBa near the dish -- and of high frequency (mainly above 300 Hz) and thus could be suppressed easily if necessary. There was no noticeable glint while the dish was on sun. Care in selection of stowage positions is recommended to assure desirable reflections while off sun. The receiver cavity produces light emission similar to a sodium vapor light, which is not significant during daylight hours.

In all, much better understanding of solar-Stirling technology was obtained through the testing accomplished. The prototype design of the Vanguard dish/Stirling electric power system was greatly enhanced by the early test program at the PDTS.

SECTION X

TECHNOLOGY TRANSFER

A. REDESIGN AND TESTING THE USAB MODEL 4-95 MK II SOLAR STIRLING ENGINE FOR THE DOE/ADVANCO VANGUARD PROJECT

After the previously described development work with the USAB Model 4-95 engine was completed, the engine was selected by Advanco Corporation and the U.S. Department of Energy for a cooperative agreement project to build a prototype solar parabolic dish/Stirling engine system module. The Stirling engine used in the Vanguard project is the first new-generation engine from USAB called the 4-95 Mk II Solar SE and is the result of a much broader development program at USAB (Reference 40).

A vital part of the USAB solar engine development has been engine testing. Six of USAB's 4-95 engines were designated for solar application development tests. In addition, during the last year tests also have been performed on the JPL-owned USAB engine, the 4-95 No. 21 engine, which was located at the PDTS. Five of USAB's engines were tested in their laboratory in Malmo, Sweden. Two of these engines were used for component development tests (i.e., functional tests, usually of relatively short duration) of redesigned components and subsystems. Three of the engines were used for simulated solar-cycle endurance tests.

The lubrication system, the control system, and the radiator system were first developed and tested on the engines in the laboratory. A special engine stand was designed in order to position the engines as though mounted on a solar concentrator. One of the engines was tested in the USAB yard in order to gain experience in the outside environment. During the last three years, 13,000 hours of solar engine tests have been accumulated in Malmo.

After testing at the USAB facilities, all the subsystems were verification tested at the PDTS, where the sixth of the 4-95 engines had been located. Model 4-95 Mk II Solar SE PCU was delivered to the Vanguard test site at Rancho Mirage, California, at the end of 1983 (Figure 10-1).

B. UNITED STIRLING POWER CONVERSION UNIT INCORPORATED INTO THE McDONNELL DOUGLAS DISH/STIRLING SOLAR ELECTRIC GENERATING SYSTEM

United Stirling AB joined with McDonnell Douglas Corporation to develop, manufacture, and market worldwide the dish/Stirling solar electric generating system. The solar PCU proposed for the system is a USAB Model 4-95 Mk II solar stirling engine. The PCU is mounted upon a McDonnell Douglas concentrator that allows access to the engine by lowering it to ground level. The commercial and private endeavor was made posssible by the USAB experience gained in building 27 Model 4-95 engines and accumulating 41,000 hours of test time with 11,000 hours on a single solar unit. The extensive solar engine development supported by the DOE STT Program and the solar testing conducted by USAB with the Model 4-95 Stirling engine at the JPL Parabolic Dish Test Site has made a significant contribution to the commercialization of the dish/Stirling electric power system.

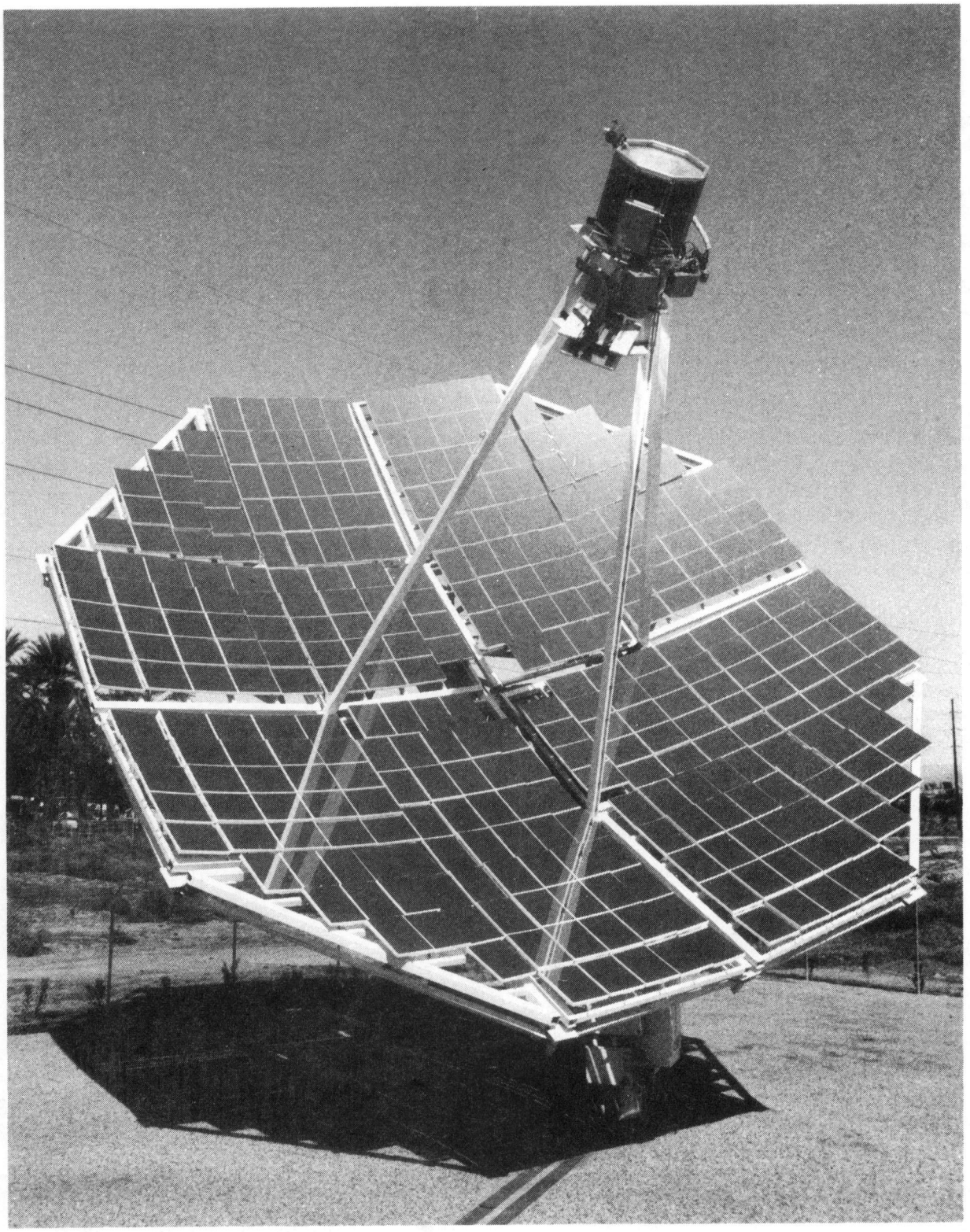

Figure 10-1. Vanguard Dish/Stirling Module

SECTION XI

FUTURE DISH/STIRLING ELECTRIC POWER SUBSYSTEM DEVELOPMENT

A. FUTURE SOLAR CONCENTRATOR UNIT DEVELOPMENT

The first development task was to plan developmental test and evaluation of the present Vanguard solar parabolic dish concentrator unit now installed and operating at the Southern California Edison's Santa Rosa Substation in Rancho Mirage, California. The U.S. Department of Energy Albuquerque Operations Office (DOE/ALO) has pursued the developmental test and evaluation of the Vanguard dish/Stirling electric power system with Advanco Corporation for a test sequence to be performed in FY 1985. The test sequence includes non-destructive quality assurance tests, system reliability tests, and a preventive maintenance demonstration. The Electric Power Research Institute (EPRI) has engaged the Energy Technology Engineering Center (operated for DOE by Rockwell International) to follow the Vanguard test and evaluation, to recommend a number of tests of interest to EPRI members, and to document all test results with an evaluation of the joint DOE/Advanco Vanguard project.

The Innovative Point Focus Solar Concentrator development activities now being pursued by DOE/ALO in conjunction with SNLA and three potential contractors should incorporate the unique requirements of a dish/Stirling solar concentrator unit into the several designs where possible. Of all intended uses of the innovative point focus solar concentrator, heating of the exposed tubular array heat exchanger of the solar-only Stirling power conversion unit is likely to be the most demanding. Not only must the diameter of the tubular array be minimized, but the reflected direct insolation must be uniformly distributed on each tube. These restrictive concentrator design requirements are eliminated for the Stirling power conversion unit equipped with a liquid/vapor-sodium-type solar receiver assembly.

Other solar concentrator unit development activities should be followed closely where possible to evaluate the ability of the concentrators to distribute the reflected direct insolation onto the solar-only Stirling PCU tubular array heat exchanger. An even distribution of reflected direct insolation results in increased electrical power output in addition to less oxidation of the tubes.

In the spirit of promoting effective development of solar concentrator units, environmental loadings due to wind, ice, snow, hail, and earthquakes must be continually evaluated and refined as operational experience is gained. It is important to recognize that the environmental loadings are statistically distributed with a normal or log-normal probability distribution function characterized by mean value, variance, etc. Rather than specifying or referencing specifications and standards for the extremes of these environmental loading probability distribution functions, investigators and designers should be encouraged to seek out the realistic distribution of the particular environmental loading for their application and then incorporate this distribution into a stress/strength approach to designing a desired concentrator reliability rather than using a safety factor approach.

Meteorological instrumentation, instrumented heliostats, and data acquisition equipment at the Solar One solar thermal central receiver pilot plant are acquiring the needed wind environmental data within and surrounding a heliostat field array.

B. FUTURE POWER CONVERSION UNIT DEVELOPMENT

Stirling engines other than the USAB Model 4-95 should be developed and/or modified for solar applications. A new generation of Stirling engines is being developed for a wide variety of non-solar applications and may be easily modified for solar application. It is desirable to evaluate these new engines with respect to meeting the technical and economic goals for future solar Stirling engine ventures. Some of the organizations now developing Stirling engines in the United States and Europe are:

(1) KB United Stirling (Sweden) AB & Co.; Malmo, Sweden.

(2) Mechanical Technology, Inc.; Latham, New York.

(3) Sunpower; Athens, Ohio.

(4) Stirling Thermal Motors; Ann Arbor, Michigan.

(5) ECA; Paris, France.

(6) Energy Research and Generation; Berkeley, California.

(7) University of Washington, Joint Center for Graduate Study; Richland, Washington.

(8) Stirling Power Systems; Ann Arbor, Michigan.

Advanco Corporation and a subcontractor will produce both a preliminary and a detailed design of a hybrid solar receiver. The hybrid solar receiver consists of an assembly of heat exchangers and combustors located within the cylinders and regenerator housings of a USAB Model 4-95 Stirling engine. The hybrid solar receiver will then be fabricated and installed upon the existing USAB Model 4-95 Solar II engine PCU now being tested with the Vanguard dish/Stirling electric power system. The complete system will then be tested and evaluated as a "solar augmented modular gas-fired cogeneration system" for the Gas Research Institute and for the U.S. Department of Energy.

Solar Thermal Technology Program activities in direct support of the dish/Stirling electric power system's overall goals should include an adequate technology base activity in order to be responsive to the program needs and to support private-sector commercial development activities. The Stirling engine's technology base should include such ongoing activities as developing annular regenerators on the cylinder head, eliminating geared crankshafts, synthesizing lubricants for low viscosity, developing pin (roller) bearings, using heat pipe operation, increasing working gas temperature limits, developing ceramic engine hot parts (Reference 41), and developing new components to extend time between overhauls (Reference 42).

SECTION XII

REFERENCES

1. Hodel, Donald Paul, "Guest Editorial," Solar Magazine, pp. 13, May-June, 1984.

2. Fujita, T., et al, Techno-Economic Projections for Advanced Small Solar Thermal Electric Power Plants to Years 1990-2000, JPL Publication 79-25, DOE/JPL-1060-4, November 15, 1978.

3. Fujita, T., El Gabalawi, N., Herrera, G., and Turner, R. H., Projection of Distributed-Collector Solar-Thermal Electric Power Plant Economics to Years 1990-2000, JPL Publication 78-10, DOE/JPL-1060-1, December 1977.

4. Latta, A. F., Bowyer, J. M., Fujita, T., and Richter, P. H., The Effects of Regional Insolation Differences upon Advanced Solar Thermal Electric Power Plant Performance and Energy Costs, JPL Publication 79-39, DOE/JPL-1060-17, Rev. 1, February 1, 1980.

5. Livingston, F. R., "Introduction to Advanced Systems Development," Focus on Solar Technology: A Review of Advanced Solar Thermal Power Systems, JPL Internal Report 5102-96, DOE/JPL-1060-78/5, November 15-17, 1978.

6. Bedard, R., and Bell, D., "A Cellular Glass Substrate Solar Concentrator," Proceedings of the First Semiannual Distributed Receiver System Program Review, January 22-24, 1980, JPL Publication 80-10, DOE/JPL-1060-33, April 15, 1980.

7. Anon., Advanced Solar Concentrator: Executive Summary, Acurex Final Report FR-81-10/AE, March 1981.

8. Anon., Advanced Solar Concentrator: Preliminary and Detailed Design, Acurex Final Report FR-80-16/AE, March 1981.

9. Dennison, E., Optical Characterization of the JPL 25-foot Space Simulator for Measurement of Solar Concentrator Gores, JPL internal communication, June 17, 1981.

10. Livingston, F. R., editor, Advanced Technology Development Semiannual Progress Report, October 1977-March 1978, JPL Publication 78-80, DOE/JPL/1060-3, June 1978.

11. Livingston, F. R., editor, Advanced Subsystems Development Second Semiannual Progress Report, April 1, 1978 to October 1, 1978, JPL Publication 79-24, DOE/JPL 1060-6, November 15, 1978.

12. Livingston, F. R., editor, Advanced Subsystems Development Third Semiannual Progress Report, October 1, 1978 to April 1, 1979, JPL Internal Report 5102-117, DOE/JPL-1060-20, August 15, 1979.

13. Dochat, George R., Design Study of a 15 kW Free-Piston Stirling Engine-Linear Alternator for Dispersed Solar Electric Power Systems, DOE/NASA/0056-79/1, August 1979.

14. Anon., United Stirling (Sweden), Design Study of a Kinematic Stirling Engine for Dispersed Solar Electric Power Systems, DOE/NASA/0056-79/2, 1980.

15. White, M. A., Conceptual Design and Cost Analysis of Hydraulic Output Unit for 15 kW Free-Piston Stirling Engine, DOE/NASA/0212-1, August 1982.

16. Zimmerman, W. F., Robertson, C. S., Ehde, C. L., Divakaruni, S. M., and Stacy, L. E., A Conceptual Design Study on the Application of Liquid Metal Heat Transfer Technology to the Solar Thermal Power Plant, JPL Contract No. 955018, DOE/JPL-1060-28, September 25, 1979.

17. Zimmerman, W. F., "Heat Pipe Receiver with Thermal Energy Storage," Parabolic Dish Solar Thermal Power Annual Program Review Proceedings, JPL Publication 81-44, DOE/JPL-1060-46, May 1, 1981.

18. Divakaruni, S. M., Heat Pipe Design Confirmation Testing, JPL Contract No. 955018, DOE/JPL-1060-27, GEAEP-55, September 25, 1979.

19. Zimmerman, W. F., Divakaruni, S. M., and Won, Y. S., Sodium Heat Pipe Use in Solar Stirling Power Conversion Systems, ASME 80-C2/S06-13, presented at ASME Century 2 Conference, San Francisco, California, August 10-21, 1980.

20. Goldberg, Vernon R., "Test Bed Concentrator (TBC)," Proceedings of the First Semiannual Distributed Receiver System Program Review, January 22-24, 1980, Lubbock, Texas, JPL Publication 80-10, DOE/JPL-1060-33, pp. 35-39, April 15, 1980.

21. Argoud, M. J., "Test Bed Concentrator Mirrors," loc cit, pp. 41-46.

22. Starkey, D. J., "Initial Test Bed Concentrator Characterization," loc cit, pp. 47-51.

23. Owen, W. A., The JPL Flux Mapper, JPL Report No. 5105-148, March 15, 1985.

24. Starkey, D. J., "Characterization of Point Focusing Test Bed Concentrators at JPL," Parabolic Dish Solar Thermal Power Annual Program Review Proceedings, JPL Publication 81-44, DOE/JPL-1060-46, pp. 135-142, May 1, 1981.

25. Miyazono, C., Software Used with the Flux Mapper at the Solar Parabolic Dish Test Site, JPL Publication 84-76, DOE/JPL-1060-78, September 15, 1984.

26. Wen, L., TBC-2 Characterization: Focal Plane Flux Distribution, JPL internal communication, October 15, 1981.

27. Hanseth, E. J., Cold Water Cavity Calorimetry of TBC #2, JPL internal communication, August 13, 1981.

28. Haglund, Richard A., Dish Stirling Solar Receiver Program, Final Report, Fairchild Stratos Division, JPL Contract No. 955400, December 15, 1980.

29. Anon., Modification of P-40 Stirling Engine for Integration with Hybrid Receiver and Parabolic Concentrator in a Solar Thermal Power System, United Stirling (Sweden), June 1980.

30. Percival, W., and Nelving, H. G., "First Phase Testing of Solar Thermal Engine at United Stirling," Parabolic Dish Solar Thermal Power Annual Review Proceedings, JPL Publication 81-44, DOE/JPL-1060-46, pp. 37-44, May 1, 1981.

31. Nelving, H. G., and Percival, W. H., "Modifications and Testing of a 4-95 Stirling Engine for Solar Applications," Parabolic Dish Solar Thermal Power Annual Program Review Proceedings (December 8-10, 1981), JPL Publication 82-66, DOE/JPL-1060-52, pp. 179-189, July 15, 1982.

32. Anon., Dish Stirling Solar Receiver Integration and Test Final Report, Advanco Corporation, JPL Contract No. 955892, November 25, 1982.

33. Bankston, C. P., and Back, L. H., Dish Stirling Solar Receiver Combustion Test Program, JPL Publication 81-23, DOE/JPL-1060-41, August 15, 1981.

34. Selcuk, M. K., and Bowyer, J. M., Dish-Stirling Module Performance As Evaluated from Tests of Various Test Bed Concentrator/Stirling Engine Configurations, JPL Report No. 5105-149, April 15, 1985.

35. Stearns, J. W., and Haglund, R., "High Performance Solar Stirling System," AIAA Paper No. 81-2554, December 1981.

36. Kasprzyk, M., Ceramic Heater Head Development, Final Report No. AFWAL-TR-82-2126, Carborundum Resistant Materials Company, January 1983.

37. Nelving, H. G., Performance Test of 4-95 Solar Stirling Engine with Two Different Solar Only Receivers, United Stirling Report 82-0050, JPL Contract No. 955821, September 7, 1982.

38. Nelving, Hans-Goran, "Testing a 4-95 Solar Stirling Engine in Test Bed Concentrator at Edwards Air Force Base," Proceedings: Fourth Parabolic Dish Solar Thermal Power Program Review (November 30 - December 2, 1982), JPL Publication 83-2, DOE/JPL-1060-58, pp. 55-61, February 1, 1983.

39. Nelving, H. G., Testing of 4-95 Solar Stirling Engine in Concentrator at Edwards Air Force Base During Period May 1982 - July 1983, United Stirling Report No. 83-0033, JPL Contract No. 955821, September 7, 1983.

40. Holgersson, Sten, "United Stirlings' Solar Engine Development: The Background for the Vanguard Engine," Proceedings: Fifth Parabolic Dish Solar Thermal Power Program Annual Review, December 6-8, 1983, JPL Publication 84-13, DOE/JPL-1060-69, pp. 95-101, March 1, 1984.

41. Chiw, W., et al, "A Ceramic Automotive Stirling Engine Conceptual Design," Proceedings of the 21st Automotive Technology Development Contractors' Coordination Meeting, November 1983.

42. Ernst, W. D., "Mod II Engine and Technology Development," IECEC Paper 849127, August 1984.